Alaska Department of Transportation & Public Facilities

Alaska University Transportation Center PacTrans

High-Mast Light Poles Anchor Nut Loosening In Alaska

An Investigation Using Field Monitoring and Finite-Element Analysis

Scott Hamel, P.E., Ph.D.
David Hoisington, M.S.

University of Alaska Anchorage

September 2014

Alaska University Transportation Center
Duckering Building Room 245
P.O. Box 755900
Fairbanks, AK 99775-5900

Alaska Department of Transportation
Research, Development, and Technology Transfer
2301 Peger Road
Fairbanks, AK 99709-5399

INE/ AUTC 14.13

DOT&PF Report No. 4000117

REPORT DOCUMENTATION PAGE

Form approved OMB No.

1. AGENCY USE ONLY (LEAVE BLANK)	2. REPORT DATE	3. REPORT TYPE AND DATES COVERED
DOT&PF Report No. 4000117	September 2014	Final Report (June 2012- October 2013)

4. TITLE AND SUBTITLE
High-Mast Light Poles Anchor Nut Loosening in Alaska
An Investigation of Field Monitoring and Finite-Element Analysis

5. FUNDING NUMBERS
Alaska DOT&PF: T2-12-12
PacTrans 24-739439

6. AUTHOR(S)
Scott Hamel, P.E.,Ph.D.
David Hoisington, M.S.
University of Alaska Anchorage

7. PERFORMING ORGANIZATION NAME(S) AND ADDRESS(ES)
Alaska University Transportation Center
Duckering Building Room 245
P.O. Box 755900
Fairbanks, AK 99775

8. PERFORMING ORGANIZATION REPORT NUMBER
INE/ AUTC 14.3

9. SPONSORING/MONITORING AGENCY NAME(S) AND ADDRESS(ES)

State of Alaska, Alaska Dept. of Transportation and Public Facilities
Research and Technology Transfer
2301 Peger Rd
Fairbanks, AK 99709-5399

Pacific Northwest Transportation Consortium (PacTrans)
USDOT University Transportation Center for Federal Region 10
University of Washington
More Hall 112, Box 352700
Seattle, WA 98195-2700

10. SPONSORING/MONITORING AGENCY REPORT NUMBER
DOT&PF Report No. 4000117

11. SUPPLENMENTARY NOTES

12a. DISTRIBUTION / AVAILABILITY STATEMENT
No restrictions

12b. DISTRIBUTION CODE
N/A

13. ABSTRACT (Maximum 200 words)

High mast lighting poles (HMLPs) are tall, roadside structures effective for lighting large areas of highways and intersections. The Alaska Department of Transportation and Public Facilities (AKDOT&PF) maintains 118 such poles in the greater Anchorage and Fairbanks areas. Some of these HMLPs have experienced anchor nut loosening at their foundation connection and an in-depth review of inspection reports suggests that the foundation type and the number of anchor rods affect loosening.

In this study, two HMLPs were field instrumented and the axial force in their anchor rods was recorded during tightening. Excessively high anchor rod pre-tensions were recorded on the first pole, after which a modified tightening procedure was created and used successfully on the 2nd pole. Finite-element (FE) modeling was conducted to examine the mechanical behavior of the foundation connections and recreate the clamp-load loss.

The monitoring and modeling results indicate that plastic deformation of the anchor rods is the likely cause of clamp-load loss in flange-type connections. Anchor rods in double nut moment connections, high strength rods, and increased flange plate thickness were all shown to reduce clamp-load loss. Recommendations for existing and yet to be installed HMLPs are presented based on these results.

14- KEYWORDS : High Mast Lighting (Pmpvch)

15. NUMBER OF PAGES
155

16. PRICE CODE
N/A

17. SECURITY CLASSIFICATION OF REPORT	18. SECURITY CLASSIFICATION OF THIS PAGE	19. SECURITY CLASSIFICATION OF ABSTRACT	20. LIMITATION OF ABSTRACT
Unclassified Unclassified	Unclassified Unclassified	Unclassified Unclassified	N/A

SI* (MODERN METRIC) CONVERSION FACTORS

APPROXIMATE CONVERSIONS TO SI UNITS

Symbol	When You Know	Multiply By	To Find	Symbol
		LENGTH		
in	inches	25.4	millimeters	mm
ft	feet	0.305	meters	m
yd	yards	0.914	meters	m
mi	miles	1.61	kilometers	km
		AREA		
in^2	square inches	645.2	square millimeters	mm^2
ft^2	square feet	0.093	square meters	m^2
yd^2	square yard	0.836	square meters	m^2
ac	acres	0.405	hectares	ha
mi^2	square miles	2.59	square kilometers	km^2
		VOLUME		
fl oz	fluid ounces	29.57	milliliters	mL
gal	gallons	3.785	liters	L
ft^3	cubic feet	0.028	cubic meters	m^3
yd^3	cubic yards	0.765	cubic meters	m^3
	NOTE: volumes greater than 1000 L shall be shown in m^3			
		MASS		
oz	ounces	28.35	grams	g
lb	pounds	0.454	kilograms	kg
T	short tons (2000 lb)	0.907	megagrams (or "metric ton")	Mg (or "t")
		TEMPERATURE (exact degrees)		
^oF	Fahrenheit	5 (F-32)/9 or (F-32)/1.8	Celsius	^oC
		ILLUMINATION		
fc	foot-candles	10.76	lux	lx
fl	foot-Lamberts	3.426	$candela/m^2$	cd/m^2
		FORCE and PRESSURE or STRESS		
lbf	poundforce	4.45	newtons	N
lbf/in^2	poundforce per square inch	6.89	kilopascals	kPa

APPROXIMATE CONVERSIONS FROM SI UNITS

Symbol	When You Know	Multiply By	To Find	Symbol
		LENGTH		
mm	millimeters	0.039	inches	in
m	meters	3.28	feet	ft
m	meters	1.09	yards	yd
km	kilometers	0.621	miles	mi
		AREA		
mm^2	square millimeters	0.0016	square inches	in^2
m^2	square meters	10.764	square feet	ft^2
m^2	square meters	1.195	square yards	yd^2
ha	hectares	2.47	acres	ac
km^2	square kilometers	0.386	square miles	mi^2
		VOLUME		
mL	milliliters	0.034	fluid ounces	fl oz
L	liters	0.264	gallons	gal
m^3	cubic meters	35.314	cubic feet	ft^3
m^3	cubic meters	1.307	cubic yards	yd^3
		MASS		
g	grams	0.035	ounces	oz
kg	kilograms	2.202	pounds	lb
Mg (or "t")	megagrams (or "metric ton")	1.103	short tons (2000 lb)	T
		TEMPERATURE (exact degrees)		
^oC	Celsius	1.8C+32	Fahrenheit	^oF
		ILLUMINATION		
lx	lux	0.0929	foot-candles	fc
cd/m^2	$candela/m^2$	0.2919	foot-Lamberts	fl
		FORCE and PRESSURE or STRESS		
N	newtons	0.225	poundforce	lbf
kPa	kilopascals	0.145	poundforce per square inch	lbf/in^2

*SI is the symbol for the International System of Units. Appropriate rounding should be made to comply with Section 4 of ASTM E380.
(Revised March 2003)

HIGH-MAST LIGHT POLES ANCHOR NUT LOOSENING IN ALASKA

AN INVESTIGATION USING FIELD MONITORING AND FINITE-ELEMENT ANALYSIS

FINAL PROJECT REPORT

by

Scott Hamel, P.E., Ph.D.
David Hoisington, M.S.
University of Alaska Anchorage

for

Pacific Northwest Transportation Consortium (PacTrans)
USDOT University Transportation Center for Federal Region 10
University of Washington
More Hall 112, Box 352700
Seattle, WA 98195-2700

Table of Contents

List of Figures

List of Tables

Acknowledgments

I would like to recognize and thank David Hoisington, whose tireless work on this project made it possible. I would also like to acknowledge significant contributions from Daniel King and Sava White. Thanks also assisting faculty at UAA including Jeffery Hoffman (Co-PI), John Lund, Todd Peterson, and Anthony Paris.

I would also like to thank all of the personnel at the Alaska Department of Transportation and Public Facilities including Elmer Marx, Charlie Wagner, Angela Parsons, Rod Blohm, and Drew Sielbach, as well as Billy Connor and the staff at AUTC.

THIS PAGE INTENTIONALLY LEFT BLANK

Executive Summary

High mast lighting poles (HMLPs) are cost effective structures for lighting highways and intersections. They are 100 to 250 feet (30m to 76m) tall, hold a variety of lamp configurations. The Alaska Department of Transportation and Public Facilities (AKDOT&PF) maintains 114 such poles in the greater Anchorage area and 4 near Fairbanks. Some of these HMLPs have experienced anchor nut loosening. Anchor rods and their associated nuts are used to secure the HMLP base plate to the pole's foundation. When tight, they allow the rods to transfer load from the pole to the foundation. From 2007-2011, 177 inspections were conducted on 104 poles. Fifty-four of these inspections revealed loose anchor nuts. The need for an investigation to determine the cause of this phenomenon is evident.

An in-depth review of the HMLP foundation inspections revealed that the anchor nut loosening is likely unrelated to manufacturer, lamp configuration, date of installation, rod diameter, or temperature during the time of installation. Inspection data suggest that foundation type and the number of anchor rods did contribute to the fastener loosening.

Two HMLPs were field instrumented and monitored to determine the axial force in the anchor rods both during the initial tightening and over time with the pole in service. The fasteners in each pole were replaced with threaded rods instrumented with axial strain gages that were mounted in a hole at the center of the rod. These rods were installed in the first HMLP using a tightening procedure from existing AASTHO provisions. Based on the results of this installation, the procedure was modified and used to install the rods on the second pole. Field monitoring of the original tightening procedure revealed higher-than-expected axial loads in the anchor rods, in some cases far beyond yield. The modified tightening procedure illustrated that controlling the torque at the snug-tight condition and adjusting the degree of rotation in the turn-

of-the-nut method to account for the grip length/rod diameter ratio greatly increased the accuracy and consistency of the final anchor rod pretension values.

Finite-element (FE) modeling was conducted to examine the mechanical behavior of the foundation connections. FE models of several HMLP foundation configurations were created, including those that were monitored in the field. These 3D models utilized contact interactions, friction between parts, nonlinear material behavior, displacement-based tightening, and force-based loading. In addition to existing configurations, the effects of thickening the base plates, adding stiffeners to the poles, and using high strength anchor rods were analyzed. Significant clamp-load loss due to post-yield effects was recreated in all of the scenarios, including one scenario that exhibited full clamp-load loss in five rods with a single application of the design wind load.

This study concluded that permanent deformation of the anchor rods, caused by application of load beyond its yield strength, is the likely cause of clamp-load loss in the flange-type foundations. It was also found that this clamp-load loss is not affected by pretension magnitude in F1554 Grade 55 rods. FE models indicated that anchor rods in double nut moment connections and high strength rods are less likely to experience clamp-load loss due to permanent deformation. In addition, increasing the thickness of the foundation connection plates significantly reduces clamp-load loss, while the addition of vertical stiffeners to the connection had little effect. It is unclear why HMLPs with the larger cast-in-place concrete foundations are also experiencing clamp-load loss, but it is possibly related to localized yielding in the fasteners due to anchor rod bending.

It is recommended that the anchor rods in flange-type foundations be replaced with F1554 Grade 105 to increase the resistance to permanent deformation, and that the frequency of

inspection for these HMLPs be increased. For future pole installations, it is recommended that flange-type connections be designed with a larger number of 1.50 inch diameter anchor rods that utilize double-nut connections with thicker plates. It is also suggested that the diameter of the pole itself be increased to reduce vibration effects. During the tightening and re-tightening of anchor rods, it is recommended that efforts be made to control the torque at the snug-tight condition and final pretension, particularly if F1554 Grade 105 rods are used. This may be done with Direct Tension Indicating (DTI) washers and a turn-of-the-nut procedure that accounts for steel strength and fastener diameter and grip length.

THIS PAGE INTENTIONALLY LEFT BLANK

Chapter 1 Introduction

High mast lighting poles (HMLPs) are cost effective structures for lighting highways and intersections. They are 100 to 250 feet (30m to 76m) tall, and can hold a variety of lamp configurations. They are commonly used at highway interchanges because a single unit effectively covers more area than the typical, approximately 30 foot (10m) tall, light poles. Because each HMLP covers more area, they can be placed further from the edge of the roadway. The Alaska Department of Transportation and Public Facilities (AKDOT&PF) maintains 104 such poles in the greater Anchorage area (see fig 1.1) and four poles in the vicinity of Fairbanks.

There have been problems with HMLPs in the past, including a collapse of a 140' lighting tower in Iowa in 2003. An investigation by Connor et al. (1) showed that the collapse was due to fatigue cracking at the base of the pole. The study concluded that the fracture surfaces were due to weld discontinuities and improper implementation of fatigue based design. The recommendations included a thicker pole base, a thicker pole base plate, and full penetration welds. The HMLPs that the AKDOT&PF currently uses have base plates with thicknesses of 2.25" (compared to 1.25" thickness of the collapsed Iowa pole), backer plates to increase the effective thickness at the pole's base, and full penetration welds. AKDOT&PF inspections have not revealed any signs of fatigue cracking.

The major issue that has been observed by the AKDOT&PF with HMLPs is anchor nut loosening. Anchor rods and their associated nuts are used to secure the HMLP base plate to the pole's foundation. When they're tight, they allow the rods to

transfer load from the HMLP to the foundation. The anchor nuts have been loosening on many HMLPs regardless of foundation type, pole height, lamp configuration, date of installation, number of anchor rods, rod diameter, or temperature during the time of installation.

Figure 1.1: A High-mast Light Pole on the Glenn Highway in Alaska

Since the issue was discovered in 2007, AKDOT&PF has instituted pole inspections on a 5 year cycle. Any poles that have loose nuts undergo a re-tightening

procedure outlined by the American Association of Highway Transportation Officials (AASHTO). From 2007-2011, 177 inspections were done on 104 poles. Fifty-four of these inspections revealed loose anchor nuts. This program is too costly for the Department to continue indefinitely. The need for solutions for existing and yet to be installed poles is evident.

It has been suggested by Garlich and Koonce (2) that nut loosening is primarily caused by failure to follow proper tightening procedures as outlined by AASHTO. However, proper tightening procedures have been carefully followed and observed during installation and re-tightening, and the phenomenon of loosening persists.

1.1 Objectives

The primary goals of this research project is to reduce the risk of the failure of the anchor bolts of AKDOT&PF's current and future high-mast light poles and to reduce or alleviate the cost of the current HMLP inspection program. The key objectives of this study are to:

- investigate the extent, severity, and cause of the observed loosening of the base plate anchor nuts
- develop recommendations for remediating the problem in current poles
- evaluate and recommend alternative designs for future installations.

These objectives were met through a review of the HMLP inspection results, field data collection during the tightening of two HMLPs, and Finite-element mechanical modeling of HMLP base plate configurations.

THIS PAGE INTENTIONALLY LEFT BLANK

Chapter 2 Literature Review

In order to find solutions to the loosening problem, the mechanics of bolted joint behavior must be studied closely. This section will review literature on previous research on HMLPs, the mechanics of pre-tensioned joints, tightening procedures, wind loading, and Finite-element modeling of pre-tensioned joints.

2.1 Previous Research on High-mast Light Poles

Catastrophic failure of the poles has occurred in several states, including Ohio, Iowa and South Dakota. An investigation including testing and analysis was initiated in Iowa after a failure in 2003 and it was determined that these failures were caused by wind-induced fatigue cracking (see fig 2.1). The remaining high-mast structures were retrofitted and recommendations were made relating to the weld details around the base and base plate thicknesses (1). AKDOT has monitored the research in the other states and has already implemented improved weld details and better weld inspections on the high-mast poles (3).

Figure 2.1: High-mast failure in Iowa

The testing in Iowa included analysis of the effects of some loosened nut configurations *on* the pole strength because it was speculated that this was the cause of the failure. However, it was determined that the insufficient welds had a much larger effect. No mention or speculation as to the cause or prevention of bolt loosening was made because it was assumed by the Iowa investigators that all loosening was the result of improper tightening during construction. Improper tightening has been ruled out as a cause by the Alaska DOT (3). An experimental study conducted in Texas determined the fatigue resistance of the bases of the high-mast poles. It was determined that fatigue life increases with thicker base plates, a larger number of bolts, and by using a full penetration weld (4). These practices have already been adopted in the installation of poles in Alaska.

2.2 Bolted Joint Connections

The purpose of the threaded fasteners at the base of HMLPs is to clamp the pole to its foundation through a bolted joint interface. The clamping force is equal to the compression applied to the joint, which is equal and opposite of the tension load in the fastener group. The initial clamping load at each anchor rod is generally achieved by rotating one of its nuts to induce tension in the rod. This tension is referred to as "pre-tension", because it exists before external load is applied.

While the bolt and joint are subject to equal and opposite forces, they do not undergo equal changes in length (or strain). This is due to the difference in stiffness

between the bolt and the joint. Generally, the bolt will have 1/3rd to 1/5th of the stiffness of the joint, and stretch 3-5 times more than the joint for a given pretension (5) .

2.2.1 Pretension ranges

The Research Council on Structural Connections (RCSC) *Specification for Structural Joints Using High-Strength Bolts* (6) recommends that the minimum pretension in high strength bolts should be equal to 70% of their minimum tensile strength (Also known as "ultimate strength" or "rupture strength"). RCSC also dictates the amount of rotation beyond snug tight recommended to reach this minimum pretension. Non high-strength bolts are outside the scope of this standard because the pretension could cause yielding. For these lower-strength bolts, Garlich (7) recommends pretension between 50%-60% of the minimum tensile strength. Based on research by James (8), this should keep the pre-tension high enough to avoid loosening.

2.2.2 External Tensile Loading

The pre-tensioned bolted joint interface will absorb external force based on the stiffness ratio of the bolt and the joint, and how close the bolt is to yield. Figure 2.2, a graph modified from Bickford (5), shows the effect of initial pre-tension on the behavior of the rods in the connection with respect to the joint clamp load. In this figure, F_p is the pre-tension magnitude and P is the external tensile load applied to the interface. P_{crit} is the external tensile load that completely unloads the compression in the joint, and P_{sh} is the external load that results in the bolt absorbing additional plot-yield load, that is, the initiation of strain-hardening. The "low" pre-tension rod absorbs external load after the

plate is unloaded prior to yielding, while the “high” pre-tension rod yields before the plate is completely unloaded. Figure 2.2 illustrates that prior to yielding of the rod; the joint can absorb an external force equal to F_P, while the rod can absorb a force equal to (F_y - F_p). Summing these terms indicates that prior to rod yielding, the largest force that the bolted joint interface can absorb is F_y, the strength of the rod. Because of this, P_{sh}, the external load required to initiate strain hardening, will always be equal to F_y, the yield strength of the rod, regardless of the initial pre-tension.

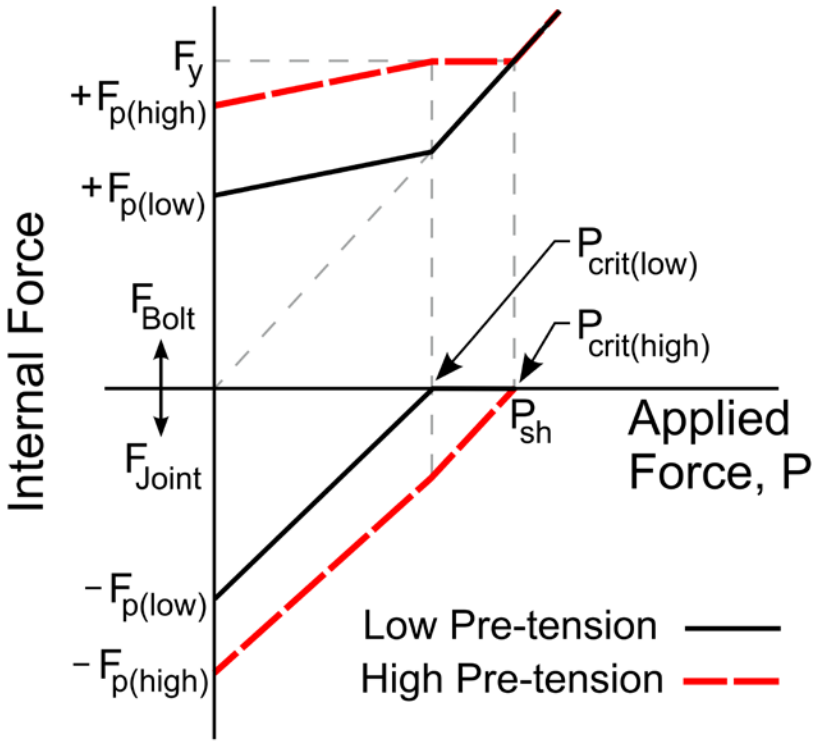

Figure 2.2: Mild steel response to Tensile Load in high and low pretension bolts

Figure 2.2 shows load absorption of a bolted joint where the bolt yields after the plate is unloaded (low pre-tension) and load absorption of a bolted joint where the bolt yields before the plate is unloaded (high pre-tension). The figure shows that prior to bolt yield, the joint can only absorb a force equal to F_p, while the bolt can absorb a force equal to F_y-F_p. Summing the two shows that prior to bolt yield, the bolted joint interface can absorb a force no larger than F_y. Because of this, the value P_{sh} will always be equal to F_y of the bolt, regardless of F_p.

2.2.3 Fatigue Loading

A fatigue load is any load that is repeated many times in succession. Fatigue life describes the number of fatigue loading cycles a bolted joint can sustain before failure and is strongly correlated to the peak stress and mean stress that occurs in each cycle. Fatigue failure eventually occurs when an imperfection initiates a crack that propagates with each cycle until rupture occurs. Because the expected number of wind load cycles is unknown, the AASHTO specification for light poles (9) recommends an infinite fatigue life to avoid fatigue failure. A study by James et al. (8) found that fatigue did not loosen any nuts, even if they were only tightened to 15% of their minimum tensile strength. James also suggests that highly concentrated stresses due to incorrect bolt alignment are more critical than bolt preload when considering fatigue behavior in the elastic range. This is further supported by Bickford (5) as shown in Figure 2.3. Bickford also indicates that the bending stresses can cause localized yielding in bolts if the plates are stiffer than the bolts, which is the case for HMLP foundations. AKDOT&PF is not aware of any

anchor rods that have failed due to rupture, or large cracks that are generally caused fatigue failure.

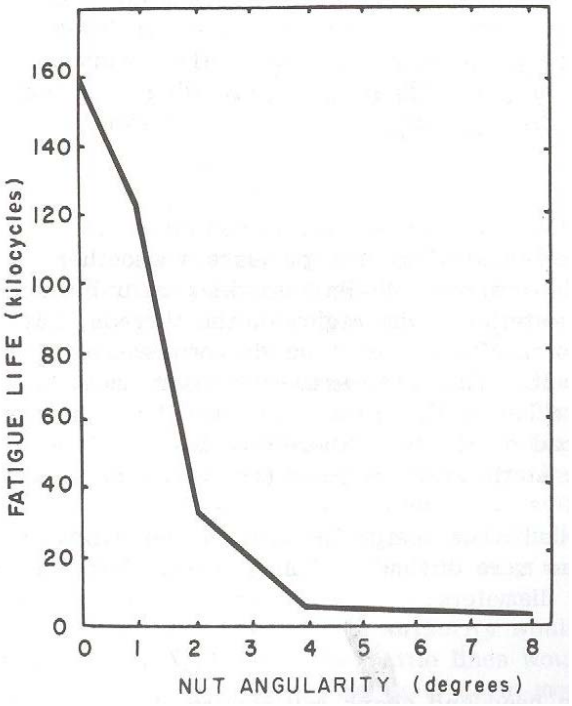

Figure 2.3: Relationship of nut angularity to fatigue life

2.2.4 Post-yield Behavior of Bolted Joints

Nassar & Matin (10) examined clamp-load loss in high strength steel bolts. They showed that the permanent deformation that occurs when a bolt is loaded beyond yield

will result in a loss of clamp load. Figure 2.4, modified from Nassar & Matin shows how a high strength bolt loses clamp load when it is loaded beyond yield.

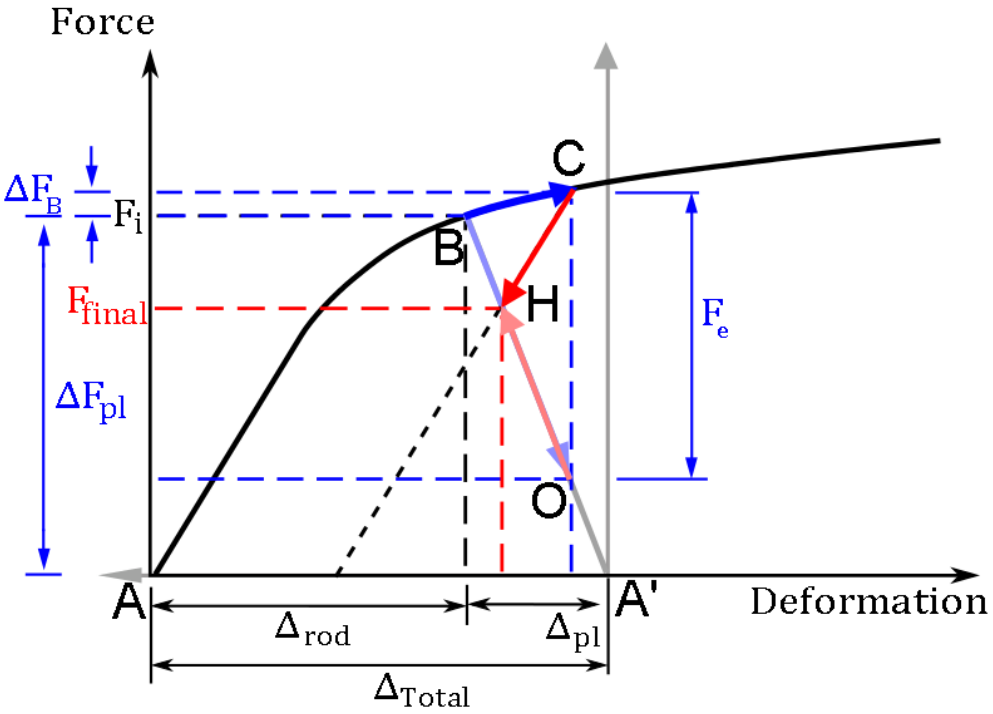

Figure 2.4: Clamp-load loss in High Strength Bolts

Figure 2.4 shows a bolted joint interface, represented by a rod and a plate, being pre-tensioned past yield, undergoing an external wind load, and then having that load removed. The pretension develops in the rod through its stress-strain curve from point A to point B. The plate must absorb an equal and opposite compressive force, travelling from point A' to point B. They both carry the same force magnitude F_i, but have different deformation magnitudes because the plate is stiffer than the rod. When an external tensile load of magnitude F_e is applied, the bolt absorbs a portion of the load equal to ΔF_B, travelling up its stress-strain curve from point B to point C. The plate

absorbs a larger portion of the load equal to ΔF_{pl} because its stiffness is much higher than the bolt's, which is in its post yield region. The plate's compressive force is decreased from point B to point O. When the external load is removed, the plate regains some of its compressive force on a slope equal to its elastic modulus, while the bolt loses some of its tensile force on a slope equal to its elastic modulus. This rebound occurs in both parts until these slopes meet at point H. The bolted joint interface is now at an equilibrium point equal to F_{final}. Due to permanent deformation of the rod, the bolted joint interface has a clamp-load loss equal to F_i-F_{final}. In mild steel bolts, the fundamental behavior is similar. The difference lies in the post yield behavior. Figure 2.5 shows a mild steel rod and plate interface being pre-tensioned past yield, undergoing an external wind load, and then having that load removed.

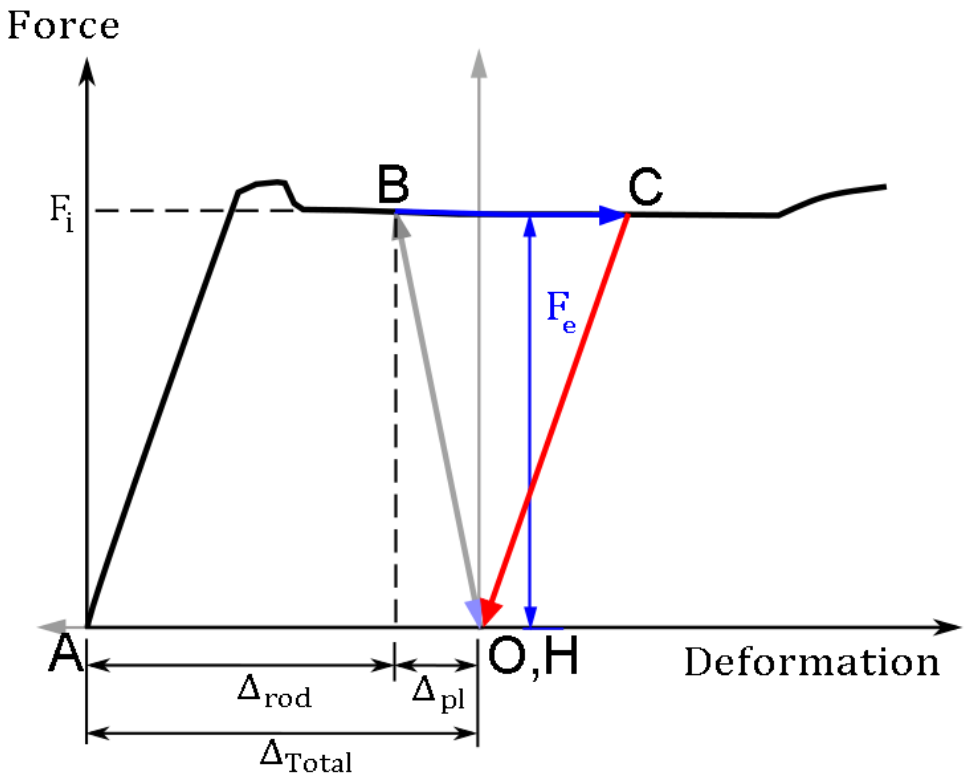

Figure 2.5: Clamp Loss in Mild Steel Bolts

The pretension develops in the rod during tightening through its stress-strain curve from point A to point B. The plate absorbs an equal and opposite compressive force, travelling from point O to point B. When an external tensile load is applied to the pre-tensioned interface, the plate absorbs all of it because the rod's stiffness is zero. If F_e is greater than or equal to F_i, the plate is completely unloaded to point O. During this external load, the rod will stretch depending on the stiffness of the plate and condition of adjacent bolts. When the load is removed, the rod relaxes down a slope equal to its elastic modulus until it meets the plate at point H. In this case, because F_e exceeded F_{ybolt}, the rod was forced to undergo permanent strain large enough to remove

its pretension. Due to this permanent deformation, this bolted joint interface will have no clamp load left after the external load is removed.

2.3 Anchor Rod Tightening

In order to tighten a fastener enough to produce an appropriate pretension, a significant amount of torque must be applied. One method to determine the preload in a bolted joint based on the torque used to tighten the fastener is shown in equation 2.1. 90% of the applied torque is expended in overcoming frictional forces. These same frictional forces keep the fastener from loosening after the fastener has been tightened.

$$T_{in} = F_p\left(\left(\frac{P}{2\pi}\right) + \left(\frac{\mu_t r_t}{cos\beta}\right) + \mu_n r_n\right) \tag{2.1}$$

where:

T_{in} = Torque applied to the fastener (lbf-in)
P = pitch of the threads (in)
F_p = preload created in the fastener (lbf)
μ_r = coefficient of friction between the nut and threads
r_t = effective contact radius of the threads (in)
μ_n = coefficient of friction between the fastener and the surface of the joint
r_n = effective contact radius between the fastener and the surface of the joint (in)

However, the input torque is only known when an instrument is available to measure it. In addition, because friction coefficients determine how much the fastener displaces to create clamp, torque based tightening is not always accurate. Because of this, the "Turn-of-The-Nut Method" was created. Many private and government entities including the Alaska DOT use this method to determine the preload in a tightened bolted joint.

The Turn-of-the-nut method, in conjunction with a tightening procedure, outlines how many steps should be taken, how much the fastener should rotate, and the order in which they are tightened. While there are variations on the number of tightening steps taken, the tightening order remains static. Figure 2.6 shows the tightening order the Alaska DOT utilizes to reduce relaxation during the tightening process. For a 1.5 inch diameter, F_y = 55 ksi bolt, 60 degrees of tightening is expected to produce a pretension equal to 85% of yield. 60-90% of yield is generally accepted as appropriate to prevent the vast majority of loosening (*7*). With a bolted joint carrying this much pretension, how does a fastener receive enough torque to overcome frictional forces and loosen? The system can lose pretension simply due to natural relaxation of the joint, which has been shown to be as high as 5% of yield, depending on the pretension. (*4*) External loading can cause fatigue, large strains, or vibration, which can all promote pretension loss.

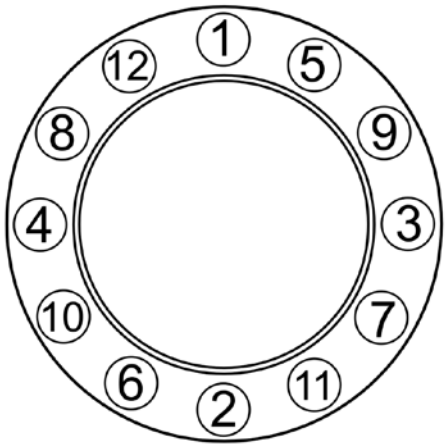

Figure 2.6: 12 Bolt Group Tightening Sequence

2.4 Wind Loading

In the case of HMLPs, wind loading accounts for the vast majority of appreciable external loads. Wind loads manifest themselves in two ways: buffeting, and vortex shedding.

Wind buffeting is simply a gust of wind, either non-steady or higher velocity (35mph+) that exerts a pressure over the entire height of the structure. This will force an external tensile load in the bolts that lie on the windward side of the pole, and a compressive external load on the bolts that lie on the leeward side. Based on the wind speed, the moment exerted onto the foundation can be calculated. Using the moment of inertia of the bolt group, tensile and compressive stresses on each bolt can be found. Doing an approximate moment calculation using bolt group (1.5" diameter, 12 rods) the maximum stress induced on a single bolt by a 120mph wind gust is 24.9ksi.

When wind is less than 35mph, and has less than a 20% change in direction or speed per unit of time (based on the structure's natural frequency), it will force oscillations parallel to the wind direction on tall, cylindrical, cantilevered structures. This is because the wind will create zones of low pressure on two sides of the structure. Figure 2.7 shows a graphical representation of this phenomenon (11). The pole will oscillate at one or more of its natural frequency modes for the duration of vortex shedding. The taper on our poles will provide some resistance against oscillation from vortex shedding because the low pressure zones won't be as uniform. The manufacturer's calculations exclude a vortex shedding analysis because of this taper. However, Giosan (11) specifies excitations for tapered structures, with varying vibration

frequencies along the height of the structure. Thus, the exclusion of a vortex shedding analysis may not be reasonable.

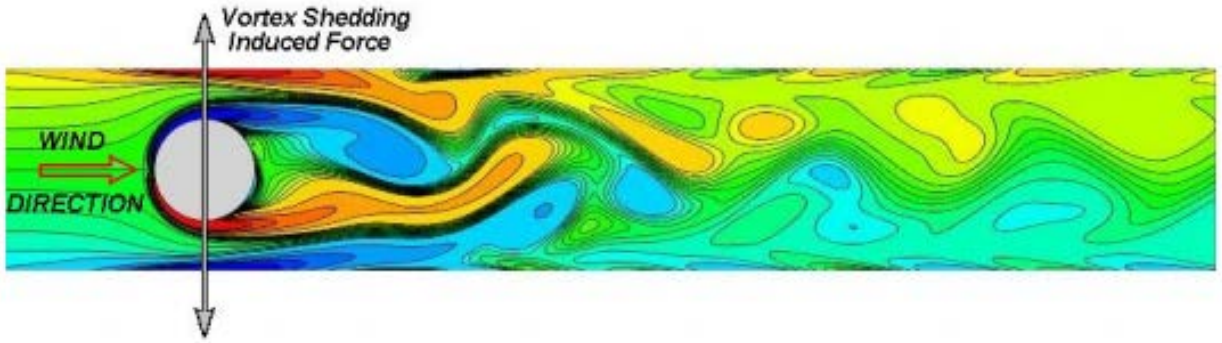

Figure 2.7: Oscillation induced by vortex shedding

2.5 Finite-Element Modeling of Bolted Joints

A finite element model can't perfectly model reality, but techniques can be used to approximate true mechanical behavior. Montgomery (12) discusses different methods that can be used to model a bolted joint interface. The different parts of the interface can be bonded, or represented by surface-surface contact. The plates can be represented by plate elements or 3D solid elements. The bolt can be represented by a line element or 3D solid elements. Accuracy and calculation time are the primary considerations behind choosing a method. Also, the interface must be allowed to separate when pretension is exceeded.

To allow for separation in a typical flange-flange bolted connection, the top flange and bottom flange can't be bonded. Instead, they must be represented by a surface-surface contact interaction that will allow for separation. The nut-top flange

interface and the nut-bottom flange interface are bonded to reduce calculation time. Modelling the bolt and plate as 3D solid elements instead of line and plate elements allows for higher accuracy and a more easily visualized stress distribution. Figure 2.8 shows the cross section of a pre-tensioned bolted joint where all parts are 3D solid elements and flange-flange interaction is represented by surface-surface contact.

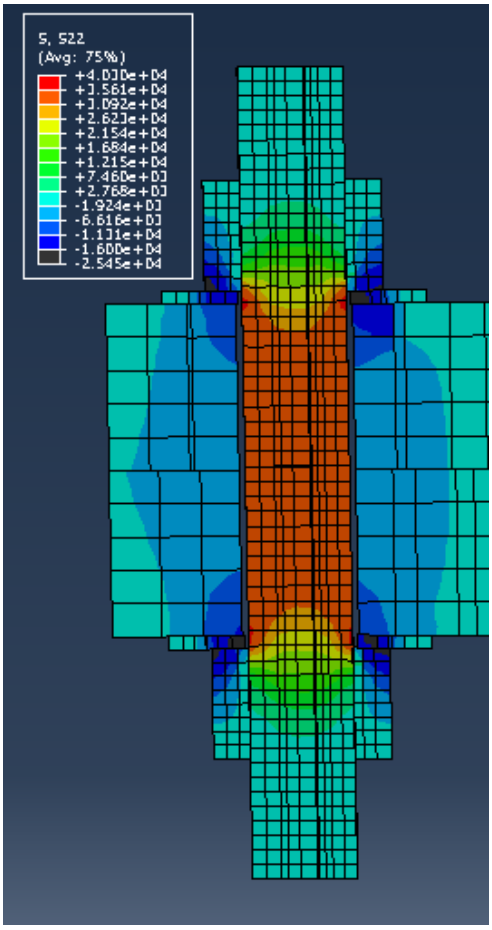

Figure 2.8: Flange-Flange Pretension

Chapter 3 Study Site/Data

This study conducted experimental research on two high-mast light poles in Alaska, both located along the Glenn Highway, north of Anchorage. There are a number of different HMLP foundation types in Alaska, which affected the selection of the poles. The foundation types, selection criteria, and descriptions of the poles are discussed in the following sections.

3.1 HMLP Foundation Types

There are several HMLP foundation designs in service in Alaska. For all types, thick base plates that are welded to the pole are attached to the foundation using F1554 Grade 55 anchor rods. These rods have a diameter of are either 1½ inch (38 mm) or 2 inch (50 mm), and are arranged in groups of 12, 16, or 24. The base plates are attached to a foundation pile in two different ways. In the flange-flange type, a flange plate is welded to the top of steel pile, and then clamped to the HMLP's base plate with a short threaded rod and two nuts, as shown in Figure 3.1a. In the other type, a concrete cap is cast at the top of the pile with long, approximately 90 inch (2.3m), anchor rods cast in that protrude from the top, as illustrated in Figure 3.1c. The base plate of the HMLP is then positioned above the cap with leveling nuts and secured with top nuts on these anchor rods. An additional type of foundation, which is not common in Alaska, but prevalent in other states, utilizes two plates. In this foundation, the pile flange plate is secured with top and bottom nuts, then there is a short section of anchor rod, above which

the base plate sits on leveling nuts and is secured with top nuts. The double-plate type foundation is illustrated in Figure 3.1b.

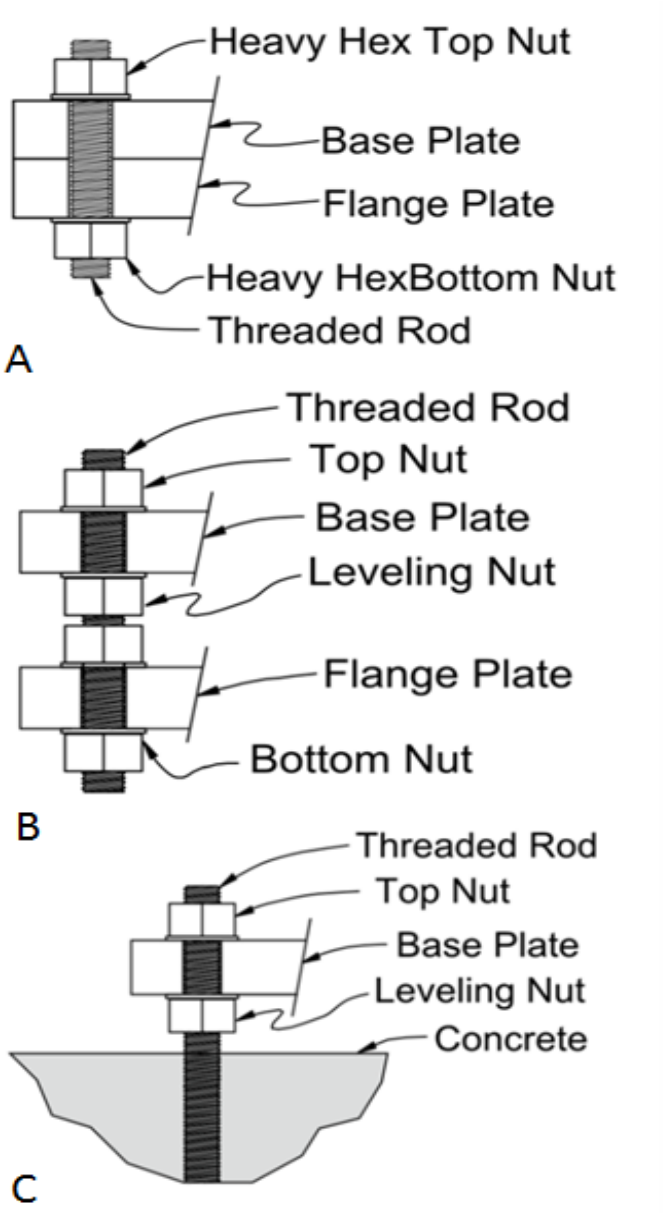

Figure 3.1: HMLP Foundation Types; A: Flange-Flange B: Double Nut C:Cast in Place Concrete

3.2 HMLP at Northbound Weighstation

In order to examine the pretensions in an HMLP bolt group, field testing of an in-service pole during and after the turn-of-the-nut method was necessary. The five year inspection reports from the AKDOT&PF were compiled and reviewed to find a pole that had the following characteristics:

1) The HMLP had a history of nut loosening.
2) The same foundation and bolt group type had a history of loosening in other poles.
3) The HMLP had a flange-flange foundation design.
4) The HMLP has unobstructed location nearby to record wind speed & direction.

For these reasons, the 150 foot (46 m) tall HMLP designated GW1 was chosen. This pole is located in the parking lot of the northbound Weighstation on the Glenn Highway at 61°17'3.98" N, 149° 36'19.44" W. The 43 inch (1092 mm) diameter flange connection consists of twelve 1½ in (38mm) diameter F1554 grade 55 steel threaded rods. These rods clamp the 2.25 in (57 mm) base plate of the HMLP to the 2.25 in (57 mm) flange plate of the driven steel pile. The replacement rods were of the same grade as the existing ones.

3.3 HMLP at Southbound Peter's Creek

The second HMLP selected for instrumentation was chosen to allow a comparison of different foundation configurations. The Glenn Highway-South Peter's Creek #1 (SPC1) is one of ten poles that were installed in 2010 with a modified design intended to

mitigate the anchor nut loosening. This pole is located on southbound side of the Glenn-Highway at the Peter's Creek South exit at 61° 29' 27.53" N, 149° 26' 45.28" W. The pole's foundation, shown in Figure 3.2, contains twenty-four 1½ in (38mm) diameter F1554 grade 55 steel threaded rods that clamp three 2.25 in (57 mm) plates together. These plates are the base plate, welded to the pole, the flange plate, welded to the driven steel pile, and a spacer plate.

Figure 3.2: HMLP foundation connection at Peter's Creek

The ten 2010 Glenn Highway HMLPs had several modifications to the standard HMLP design, including a larger pole diameter at the top and bottom (unmodified pole taper), increase in the number of anchor rods, specified flatness tolerance of the interface-side of the base plates, and the addition of the spacer plate. In addition, the installed

anchor rods were specially manufactured “Smartbolts” with a modified pitch of 8 threads per inch. The Smartbolts contain inserts that allow static measurement of their in situ elongation. After readings were taken in the spring of 2012 of the rod elongations of all 240 Smartbolts (24 anchor rods x 10 poles), it was determined that, while all the rods were in the acceptable range, all of the outlier readings were on the HMLP at Peter’s Creek (SPC1). For this reason, this pole was chosen for strain gage instrumentation.

THIS PAGE INTENTIONALLY LEFT BLANK

Chapter 4 Method

The methodology of this study was to examine the past inspection data and HMLP literature, select and instrument two HMLPs during a tightening procedure, and then utilize this knowledge to examine the poles' behavior using finite-element software.

4.1 Review of the HMLP inspections

As noted in Chapter 1, AKDOT&PF has instituted an inspection program to mitigate the anchor nut loosening problem. This program, which has operated since 2007, visits each pole on a 5 year cycle and conducts a visual inspection of the pole and foundation. The inspection gives each component of the pole a rating between '0' and '4', with a '4' indicating a "Good" condition and a '0' representing "Out of Service". A '1' represents "Critical" performance and requires repair or replacement. Anchor nuts that were loose were given a rating of '1'. A sample inspection report can be found in Appendix C. These inspection reports were compiled and entered into a database in order to identify any patterns in the loosening pattern. Variables that were investigated for effects on nut loosening included number and size of nuts, pole height, number of lamps, location, foundation type, pole manufacturer, among others. Year of erection was not included in this comparison because the erection dates were not available for most of the HMLPs.

4.2 Fastener Monitoring and Testing

To record the anchor rod stresses during the tightening procedure, the resulting pretensions, and the axial force in the rods for several months, the measurement system had to meet the following requirements:

1) Rain and snow contact must be avoided in all exposed electronics
2) Faying surfaces and threads must be free of wires
3) Preload measurements should have an accuracy of +/- 1 kip (4.4 kN)
4) The system should be relatively economical so that it could be replicated for all twelve anchor rods

The best method to meet these requirements was to employ strain gages positioned along the central axis of the anchor rods. A 6 inch (150mm) deep, 0.079 inch (2mm) diameter hole was drilled via Electrical Discharge Machining (EDM) into the middle of each bolt. A strain gauge (Texas Measurements BTM-6C-1LDA Bolt Gages) and strain gauge epoxy (Micro-Measurements M-Bond AE15) with an acceptable minimum temperature of -20°F (-29°C) were inserted in the hole. A finished anchor rod is shown in Figure 4.1. The strain gauge was inserted 5.5 inches (140 mm) into the hole while the epoxy was extruded through a syringe & spinal needle into the hole. The epoxy extrusion continued while slowly pulling the needle out, until the entire volume of the hole was filled with the epoxy. The strain gauge is designed to float in the epoxy, while the epoxy bonds to walls of the hole.

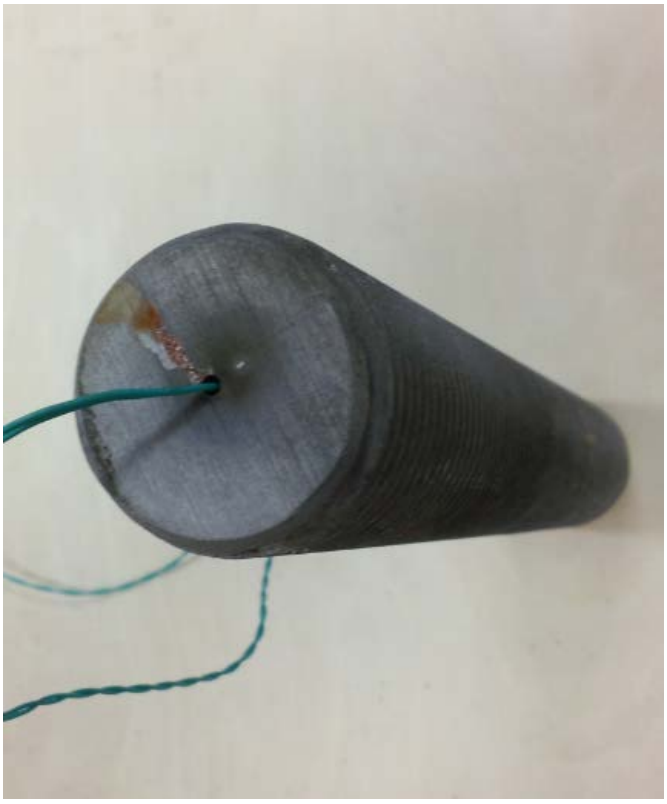

Figure 4.1: Anchor Rod with embedded strain gage

4.2.1 Anchor Rod Strain Gage Calibration

An hydraulic universal testing machine by MTS Systems, Inc. with a 110 kip (500 kN) capacity was used to calibrate the voltage output of the embedded strain gages to a applied axial load on the anchor rods. Custom-built steel adapters, shown in Figure 4.2, were used to mount the anchor rods in the test machine. These adapters were necessary because the anchor rods were too large for the normal grips. In addition, traditional grips do not allow space for the internal strain gage wire that was protruding from one end of the anchor rods.

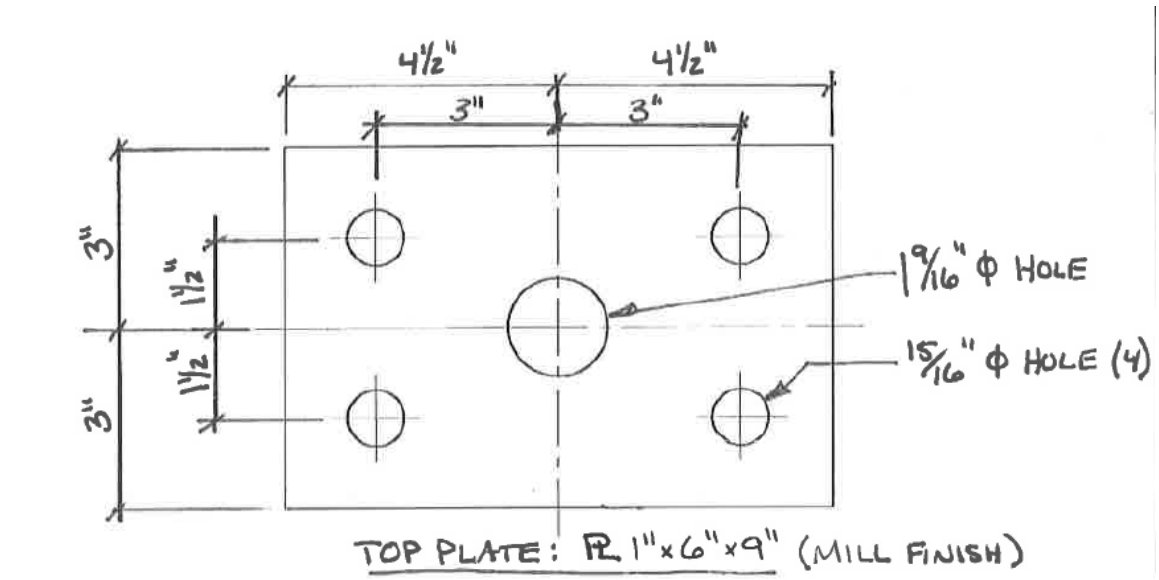

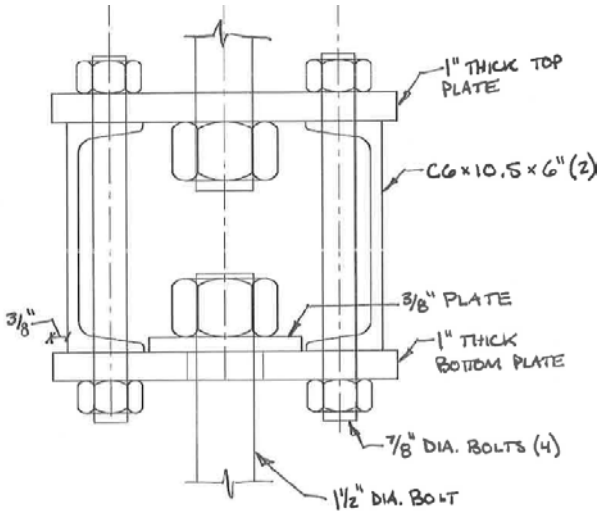

Figure 4.2: Universal Test Machine Adapters for 1.5 inch Anchor Rods

Once mounted in the machine, as shown in Figure 4.3, the load on the anchor rod was increased in a displacement controlled ramp at 0.05 in/min up to approximately 15

kips (67 kN). The strain gauges were connected to a Wheatstone bridge using a ¼ bridge configuration and excited with 10 volts DC. The output voltage was monitored using an NI-9205 cDAQ module. The resulting linear relationship between load and the strain gage output voltage was determined for each anchor rod and subsequently used in the field to calculate the pre-yield axial force applied during tightening.

Figure 4.3: Anchor Rod Calibration in Universal Testing Machine

4.2.2 Anchor Rod Strength Test

In order to determine the constitutive response for Finite-element modeling, evaluate the plastic response of the anchor rod material, and determine the ultimate strength of one anchor rod, a rod was tested to failure according to ASTM E8 (13). This standard specifies that the specimen be machined into the shape of a dogbone. After the internal strain gage was installed and calibrated, the anchor rod was machined to a cylindrical dogbone with a minimum diameter of 0.500 inches and a grip diameter of 0.75 inches. In order to ensure that there was no bending in the specimen, in addition to the internal strain gage, four external strain gages were mounted to the specimen surface, as shown in Figure 4.4. An extensometer was also used to record strains beyond the capacity of the strain gages.

The displacement-controlled test was started at 0.03 inches/minute. At 6.5 minutes (15,000 lbs, approximately 4% strain), partway through strain-hardening, the displacement rate was increased to 0.100 inches/minute. It remained at this rate until fracture. The strain gauges were connected to a Wheatstone bridge using a ¼ bridge configuration and excited with 5 volts DC. The output voltage was monitored using an NI-9205 cDAQ module

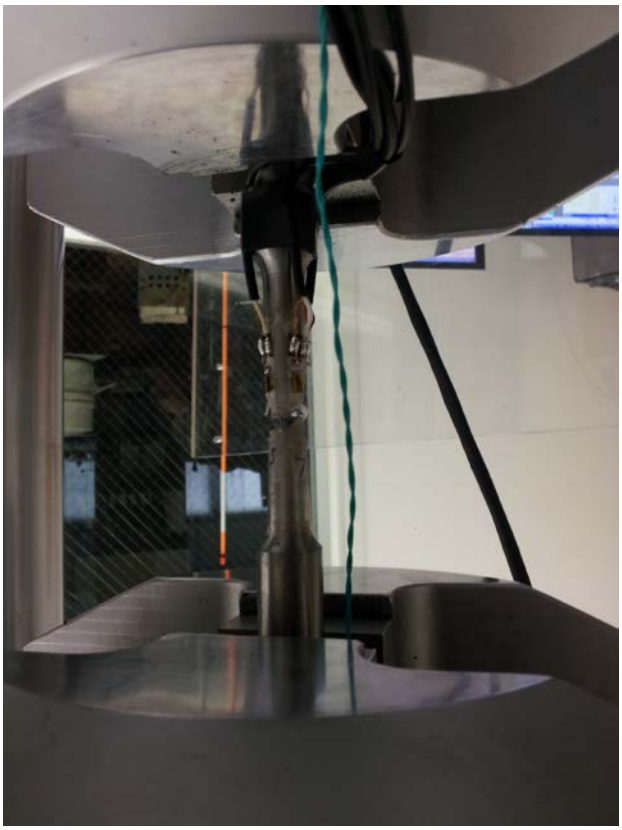

Figure 4.4: Anchor Rod Strength Test

4.2.3 DTI Washer Evaluation

DTI washers are deformable washers that contain pockets of silicon. As the washers are flattened, the pockets of silicon are crushed, and squirt out of the side of the washers. Once all the cells have squirted, a feeler gauge is inserted between the connection plate and pockets of silicon. If the feeler gauge is not allowed to penetrate between the washer and the plate, the washer is carrying a load specified by the manufacturer +-1.5kips.

Direct tension indicator (DTI) washers rated for 54 kips were supplied by Applied Bolting Technology. Prior to installing them in the field, a verification of their rating took place in the lab. Figure 4.5 shows a 1.5 inch threaded rod with an internally embedded strain gage through the center of the test apparatus, which was used to measure the rod tension as torque was applied. Figure 4.6 shows the final test apparatus prior to applying torque to the nuts. Note the box wrench to the left was used as counter torque and the entire assembly is clamped to an I-beam to resist the torsion. Torque was applied using a hydraulic wrench, and controlled using the hydraulic pressure in the system.

Figure 4.5: Direct Tension Indicator (DTI) Washer Calibration

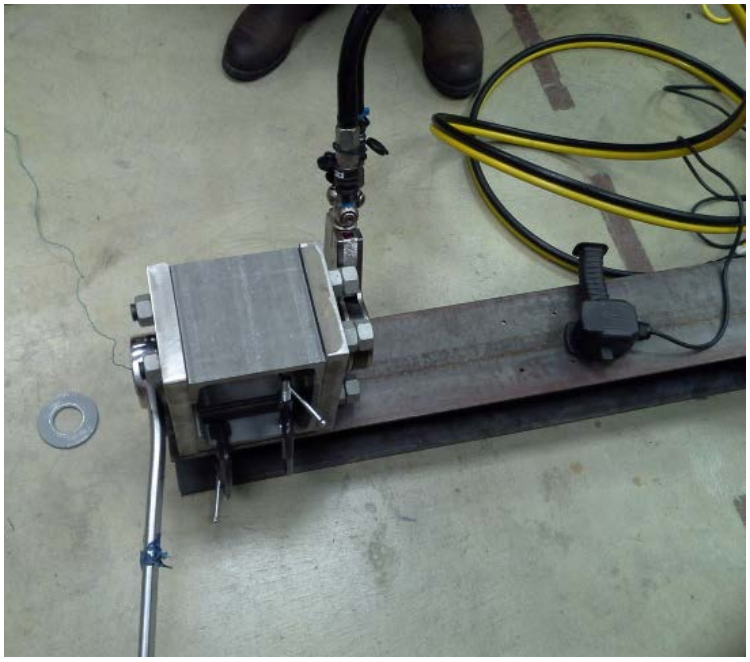

Figure 4.6: Full test assembly ready for torque to be applied

4.3 Field Monitoring of First HMLP (Weighstation)

The anchor rods with internal strain gages were monitored both during tightening, and for some months after. Temperature, wind speed, and wind direction were also measured using a nearby radio tower at the Weighstation building.

4.3.1 Data Acquisition System

The anchor rods installed in the field were monitored using an NI-9205 CompactDAQ module, which was mounted in a cRIO-9111 Chassis attached to a cRIO-9012 Controller, all products of National Instruments. The data acquisition system used a voltage regulator to provide a 5 volt excitation voltage for the strain gages, which were connected using Wheatstone bridges in ¼ bridge configuration. The bridges were

fabricated using 350 ohm resistors and placed connected to the cRIO, which recorded the strain gage output voltages, as well as the air temperature using an EI-1022 thermometer from Labjack Inc. Shielded wires from the anchor rods were connected to the DAQ system via premium RCA connectors. The shielding was not grounded to an outside ground.

Because the pole is located across the parking lot from the weighstation building, and maintenance personel wanted to avoid cables crossing on or over the parking lot, the system required its own source of power. To accommodate this, a 250 Watt solar panel from Lime Solar was mounted to the side of the pole using a 1 5/8" uni-strut frame, as shown in Figure 4.7. A 350 cold-crank amp car battery and solar charge controller (Instapark MPPT30) were placed in a weather-tight NEMA box on the ground near the pole foundation. The data acquisition system was placed in a 2nd NEMA enclosure attached to the pole.

Figure 4.7: Solar Panel Installation at Weighstation

The wind speed and direction was measured using an RM Young Wind Sentry from Cambell Scientific, which was mounted to the top of a radio tower adjacent to the Weighstation structure, as shown in Figure 4.8. At 40 feet tall, the radio tower is above the tree line and approximately 100 feet from the HMLP. A second system consisting of a Labjack U3 data acquisition unit and a laptop computer running Labview was housed inside the weighstation structure and attached to the anemometer. It was powered by the weighstation's grid power.

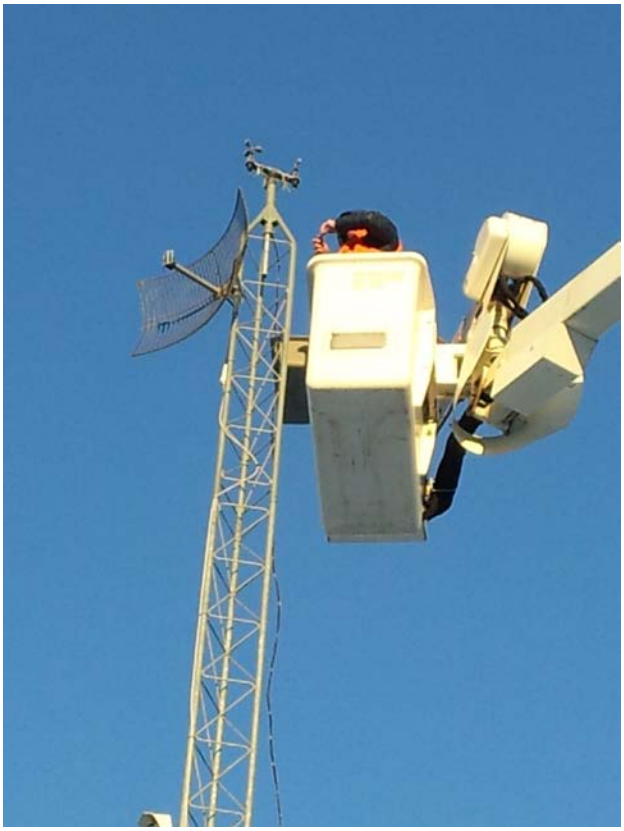

Figure 4.8: Anemometer Installation on Radio Tower at Weighstation

4.3.2 Installation and Tightening

The anchor rods were tightened according to the "turn-of-the-nut-method" in a four stage process using the "star pattern" for a 12 bolt group specified by FHWA. Each existing anchor rod was loosened, replaced with a strain gauged rod, and the new rod was then tightened to the "snug tight" condition. After all the rods were replaced, each nut was turned 20 degrees with a hydraulic wrench. Figure 4.9 shows Rod Blohm (AKDOT bridge crew) rotating one of the anchor nuts 20 degrees.

Figure 4.9: Rod Blohm (AKDOT&PF Bridge Crew) turning an Anchor Nut 20 Degrees

The tightening process was repeated two more times for a total of 60 degrees of rotation as specified by the FHWA Guidelines (7). After one week, as recommended by NCHRP Report 469 (14), the rods were tightened with a verification torque equal to 110% of the installation torque. The installation torque, as defined by the Guidelines (7) is specified as:

$$T_i = 0.12 d_b P_i \tag{4.1}$$

where:

T_i=Installation Torque
d_b=Nominal bolt diameter (inches)
P_i=Installation Pretention (kips), which is calculated using a stress equal to 60% of the minimum tensile strength of Grade 55 rods and the minimum cross-sectional area of the bolt.

The 0.12 coefficient in Equation 4.1 is an approximation that is used to replace the contact diameter constants and friction coefficients. This constant was suggested by Till and Lefke (15). Equation 4.1 utilizes a pretension of 79 kips and resulted in a final torque of 1150 ft-lbs (1.56 kN-m) for the anchor rods in this study. After one week, as per FHWA recommendations, a verification torque of 1300 ft-lbs (1.76 kN-m), which is 110% of the final torque, was applied. These torque values, which were published in the existing AKDOT&PF tightening procedure, were mistakenly based on the nominal cross-sectional area of the rods, 1.76 in^2 (1142 mm^2). The correct usage of equation 4.1, as outlined in NCHRP 469 *(8)*, utilizes the tensile stress area, 1.41 in^2 (906 mm^2), which is calculated from the minimum diameter. This results in a pretension force of 63 kips, and the correct torque values for the final and verification torques are 945 ft-lbs (1.28 kN-m) and 1040 ft-lbs (1.41 kN-m), respectively.

4.3.3 Torque Verification

On May 26, 2014, at the end of the study, the personnel returned to the Weighstation HMLP and re-applied torque to each anchor rod. A wrench was used to keep the bottom nut from turning and the pressure in the hydraulic wrench was increased until movement was detected in the top nut. The hydraulic pressure was translated to an applied torque, which was then converted to an approximate internal force using equation 4.1. This torque was applied to provide an approximate value of the internal force, and to ensure that none of the nuts were loose.

4.4 Field Monitoring of Second HMLP (Peter's Creek)

It was planned that the twelve anchor rods with internal strain gages would be monitored both during tightening, and for some months after. However, as noted below, little data was collected after the initial tightening. Temperature data was also recorded, but wind speed and direction were not measured. It was assumed that data from local weather stations would provide adequate estimates of the wind speed.

4.4.1 Data Acquisition System

The data-acquisition (DAQ) system for this HMLP was built using Labjack U6 units (OEM boards), a Beaglebone Black computer, a USB hub, and custom-built circuits that used linear regulators to manage voltages. An image of the completed unit is shown in Figure 4.10. Power was provided by a 50W solar panel, solar charge controller (MPPT Tracer1210RN), and three 12 Volt, 35 Amp-hour AGM deep cycle batteries (Batteries+). Power calculations demonstrated that the solar panel – battery combination should have more than enough capacity for the system, even in the cold temperatures expected.

Similar to the Weighstation system, the batteries and charge controller were placed in a weather-tight NEMA box on the ground near the pole foundation and the data acquisition system was placed in a 2nd NEMA enclosure attached to the pole. The data acquisition system used a voltage regulator to provide a 5 volt excitation voltage for the strain gages, which were connected using Wheatstone bridges in ¼ bridge configuration. The bridges were fabricated using 350 ohm resistors and placed connected to the cRIO,

which recorded the strain gage output voltages, as well as the air temperature using an EI-1022 thermometer from Labjack Inc.

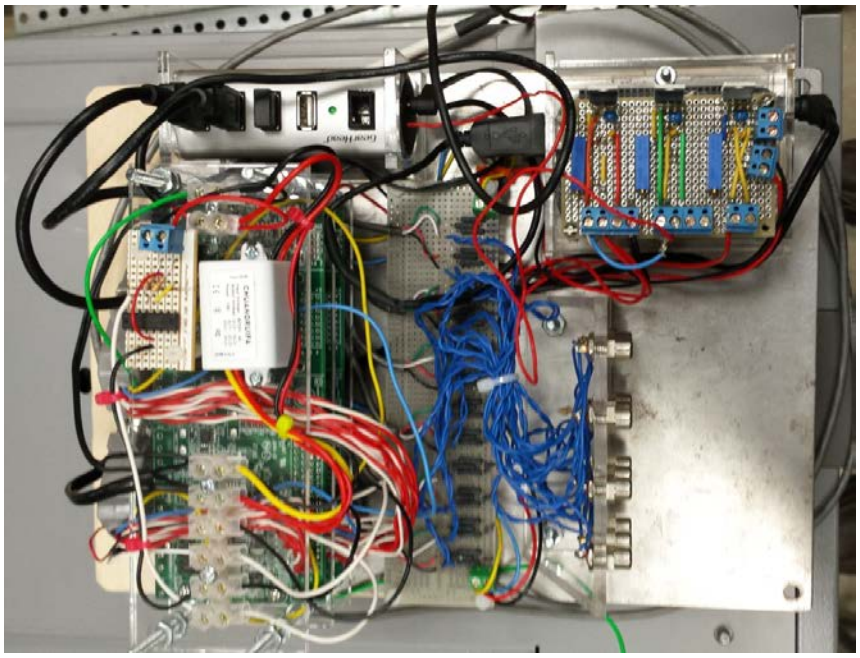

Figure 4.10: Peter's Creek HMLP Custom-Built Data-Acquisition System

Shielded wires from the anchor rods were connected to the DAQ system via standard RCA connectors. Once the system was activated, it was found that there was a large amount of noise, and drifting of the signals, likely due to nearby electromagnetic interference. The system was grounded, using a 4 foot long piece of rebar pounded into the ground, and the strain gage wire shielding was connected to ground. This greatly improved the signals.

Once the tightening procedure was complete, it was found after several weeks that the solar panel didn't generate enough power to keep the system from draining the

batteries. This was solved by creating a digital relay to shut down the USB hub, which also deactivated the Labjack DAQ units. This function significantly reduced power consumption and was successfully used in the laboratory in cold temperatures for several days before the DAQ was returned to the Peter's Creek HMLP. The completed and installed system can be seen in Figure 4.11.

Figure 4.11: Completed Data-acquisition System at Peter's Creek HMLP

The Labjack U6 units were controlled by a custom-written Python script that measured and recorded the voltages in the strain gages. This program was hosted by the Beaglebone computer, which was running Ubuntu, and connected via USB. This system replaced the National Instruments components and Labview programming utilized in the Weighstation system.

4.4.2 Revised Tightening Procedure

The anchor rods at Peter's Creek were tightened in a similar manner to those at the Weighstation. Turn-of-the-nut method was again utilized, along with a 24-bolt star pattern, shown in Figure 4.12. Existing anchor rods were loosened, replaced and tightened to the "snug tight" condition. After all the rods were replaced, each nut was turned 20 degrees with a hydraulic wrench. Due to the increased grip length of the anchor rods, additional 20-degree passes were required for all the rods. The anchor rods were turned a total of 100 degrees in six passes. Figure 4.13 shows Rod Blohm (AKDOT bridge crew) rotating one of the anchor nuts 20 degrees.

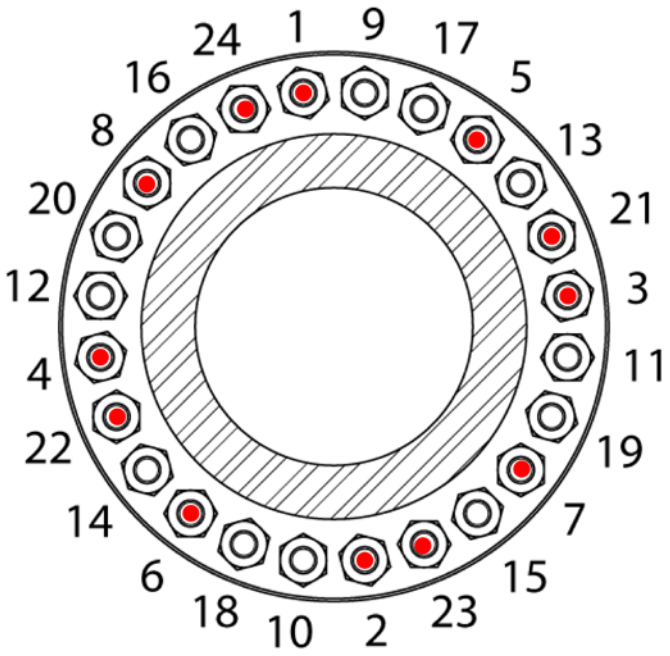

Figure 4.12: Peter's Creek HMLP Tightening Pattern. Red fill indicates rods with strain gages.

As will be shown in Chapter 5, the tightening procedure used at the Weighstation HMLP resulted in large pre-tension scatter. In order to reduce this scatter, several special provisions were adopted. They include the following changes:

Figure 4.13: Installation and Tightening of Anchor Rods at Peter's Creek HMLP

- The inclusion of DTI washers, also known as "squirters". As discussed previously, the DTI washers were calibrated to ensure that they indicated at the correct load. The DTI washers used at Peter's Creek were manufactured to fully indicate at 54 kips. The feeler gauge was not used for this tightening procedure. A photo of the DTI washers with fully extruded orange silicone during installation is shown in Figure 4.14.
- 'Snug Tight' condition includes the use of a torque wrench. Instead of the "full effort of one person on an open-end wrench…", snug tight was taken only as the maximum rotation achieved by a torque wrench outputting 600 ft-lbs of torque.
- A final tightening step was added. After completion of the rotation specified in the procedure, rods that had DTI washers which did not indicate were further

tightened with a hydraulic wrench. The torque on the hydraulic wrench was set to the lowest value required to rotate a nut on a rod whose DTI washer did fully indicate.

4.4.3 Torque Verification

On May 26, 2014, at the end of the study, the personnel returned to the Peter's Creek HMLP and re-applied torque to each anchor rod. A wrench was used to keep the bottom nut from turning and the pressure in the hydraulic wrench was increased until movement was detected in the top nut. The hydraulic pressure was translated to an applied torque, which was then converted to an approximate internal force using equation 4.1.

Figure 4.14: DTI Washers indicating full pre-tension during installation

4.5 Finite-element Modeling

ABAQUS was used for all finite element modeling done in this study. The Newton-Raphson method is used to solve non-linear calculations in ABAQUS implicit, the incremental solver used in this study.

4.5.1 Pole Configurations and Loading

Three different model scenarios were chosen to encompass the majority of HMLPs in service from the three general configurations described above. These are shown in Figure 4.15 and are as follows:

A. Flange-Flange, 12 rods, 46 m (150 feet) height (Weigh-station HMLP)
B. Flange-Spacer-Flange, 24 rods, 47 m (155 feet) height (Peter's Creek HMLP)
C. Double Nut Moment, 12 rods, 46 m (150 feet) height

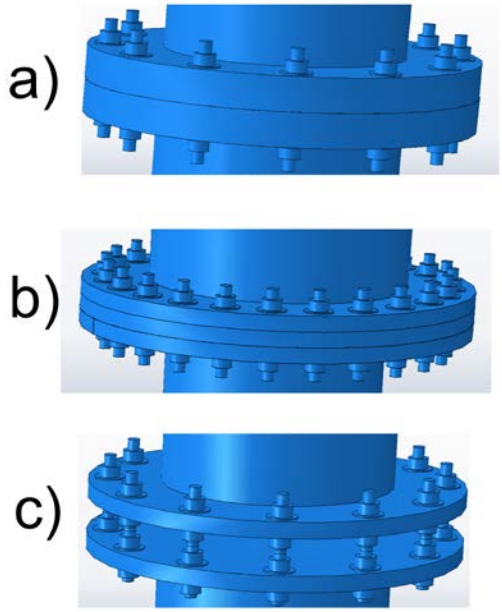

Figure 4.15: modeled HMLP foundation scenarios (a) twelve-rod flange-flange, (b) twenty-four-rod flange-spacer-flange, and (c) twelve-rod double-nut flanges

Configuration B is atypical, and is representative of newly installed poles which utilized design changes to prevent anchor nut updates based on the loosening problem. Configuration C is also atypical in Alaska. A CIP concrete scenario was not included due to the inability to experimentally determine the pretension load in those foundations. High strength rods were used in scenarios A & C to determine their effects. Thicker plates and stiffeners were used in scenario A to determine their effects. The dimensions of the parts for all scenarios are shown in Table 4.1. The dimensions for parts that varied with the scenario are shown in Table 4.2

Table 4.1: HMLP Dimensions for all scenarios

Component	**Dimension (in)**
Inner Nut Diameter	1.41
Outer Nut Diameter	2.4
Inner Washer Diameter	1.5
Outer Washer Diameter	3.5
Rod Diameter	1.41
Pile Diameter	27

Table 4.2: HMLP Dimensions for Specified FE Models

Model Scenario	**Bolt Circle Dia. (in)**	**Plate Dia. (in)**	**Pole Dia. (in)**
A	38	43	26.5
B	42	48	42.0
C	38	43	31.6

In both the flange-flange and the double moment nut scenarios, the bottom of the pile was fixed at a depth of 3.6 m (12 feet). The effective depth-to-maximum-moment

method (16) was used to determine the pile's depth of fixity, L_M, which is defined in equation 4.2. In all scenarios, varying the depth of fixity had little effect on stresses in the plates or rods.

$$L_M = \left(\frac{M_{max}}{P_{max}}\right) - H \tag{4.2}$$

where:

M_{max} is the maximum moment applied to the pile
P_{max} is the maximum lateral force applied to the pile
H is the length of pile above ground.

There are three different load steps that were applied to each model: Pre-tension, Load, and Unload. These were applied sequentially in load steps. To apply pretension, a "bolt load" was applied to each rod. This bolt load is applied between two nuts that are clamping a plate or plates. Selecting "adjust length" for the loading method imposes a stretch in the bolt $\Delta_{B,}$ that mimics the displacement controlled pretension. The magnitude of the length adjustment is selected to reach a pretension equal to 60% of the minimum tensile stress in the rod. To accomplish this, the change in length is set equal to

$$\Delta_B = \frac{\sigma_{60} * A_B * L_g}{E} \tag{4.3}$$

where:

Δ_B = Change of length in bolt
σ_{60} = 60% of the minimum tensile strength of the rod
A_B = Effective tensile area of the rod
L_g = Grip length between nuts
E = Modulus of Elasticity of the rod

Δ_B is equal to 0.20 mm (0.008 inch) in the Scenario A, 0.28 mm (0.011 inch) in the Scenario B, and 0.10 mm (0.004 inch) in both clamp zones in Scenario C. 60% of the rod's minimum tensile stress value was targeted in accordance with existing pretension recommendations by Garlich and Koonce (2). The plate(s) will be flattened by:

$$\Delta_P = \Delta_B * (\frac{K_P}{K_B}) \quad (4.4)$$

where:

Δ_P = Change in thickness of the plate
Δ_B = Change of length in bolt
K_P = Stiffness of the plate
K_B = Stiffness of the rod or bolt

During the "Load" step, external load representing a 160 kph (100 mph) design wind speed is applied to the top pole stub as a moment couple. Unlike the real pole, a 900 mm (36 inch) portion of the pole stub is solid to prevent excessive deformation. The magnitude of this moment couple varies by pole configuration. Scenarios A and C required a design moment of 576 kN-m (6800 kip-in), while the taller, wider pole in Scenario B developed an applied moment of 915 kN-m (8800 kip-in).

The moments used were taken from calculations conducted by the HMLP manufacturer. These calculations were done in accordance with the American Association of State Highway And Transportation Officials' *Standard Specifications for Structural Supports for Highway Signs, Luminaries, and Traffic Signals* (9). They were verified with calculations according to the American Society of Civil Engineers' *Minimum Design Loads for Buildings and Other Structures (7-10)* (17). These verification calculations can be seen in Hoisington (18).

In addition to design wind moments, additional moments of varying magnitudes were applied to cause both small clamp-load loss and complete separation. In each scenario, the "Load" step was followed by an "Unload" step, in which the moment-couple moment is reduced to zero to represent removal of the applied wind.

4.5.2 Model Definitions and Descriptions

The pole, pile, base plate, and flange plate were defined using linear-elastic, isotropic behavior with an elastic modulus, E=200 GPa (29,000 ksi), and a Poisson's ratio $\nu = 0.33$. The F1554 Gr. 55 threaded rods had the same Poisson's ratio, but were defined using the stress-strain relationship shown in Figure 4.16. The figure shows the constitutive behavior of a rod that was determined experimentally using ASTM E8 (13). For model stability, the negative post yield slopes were replaced by slopes of zero. Figure 2.5 shows that separation can occur before the rod reaches the strain hardening zone during external loading. As a result, the exact definition of the strain hardening curve above the yield stress is unimportant in determining clamp-load loss; therefore it is approximated by two lines to reduce computation time.

All FE models used Abaqus element type C3D8R. This is an 8 node brick element with reduced integration and hourglass control. The analysis was conducted using Abaqus implicit. The approximate element size of each mesh was modified until the faces of most elements had a length/width ratio that didn't exceed 1.5 in the rods, washers, plates, and nuts. The sizes of these elements vary with each part. The approximate element size of the rods, washers, and nuts was set to 5.0 mm (0.2 inch).

The approximate element size of all plates was set to 13 mm (0.5 inch), the pole was set to 75 mm (3 inch) and the pile was set to 150 mm (6 inch).

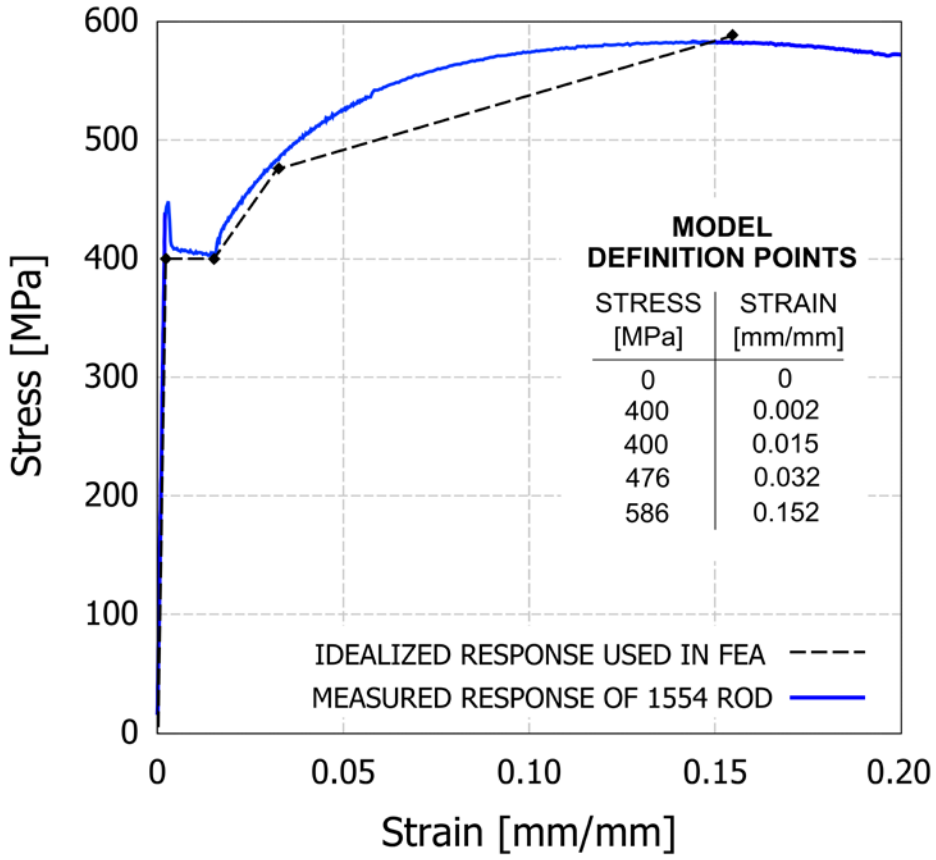

Figure 4.16: Stress-strain relationship used for anchor rods in FE models

Table 4.3 contains the constraint and interaction property definitions for all scenarios. The interactions of following parts were considered surface-surface contact:

- Scenario A : Flange Plate-Base Plate
- Scenario B : Flange Plate-Spacer Plate, Base Plate-Spacer Plate
- Scenario C : Bottom Washer-Flange Plate, & Bottom Washer-Base Plate

All other part interactions were defined as tied.

Table 4.3: Abaqus Interaction Definitions for all Scenarios

Constraints	**Value**
Tie	Surface-Surface
Position Tolerance	Use default
Adjust Slave Surface Initial Position?	Yes
Tie Rotational DOFs if Applicable?	Yes
Contact	Surface-Surface
Sliding	Finite
Slave Adjustment	None
Surface Smoothing	Automatic

Interaction Properties	**Value**
Tangential Behavior	Penalty, μ=0.3
Shear Stress Limit	None
Max. Elastic Slip	0.005 (Fraction of Charac. Surface Dimension)
Normal Behavior	Pressure-Overclosure
Enforcement Method	Default
Contact Stiffness	2.90E+08

The options used to generate the elements in the Finite-Element Modeling scenarios are tabulated in Tables 4.4 – 4.7.

Table 4.4 contains the options used to generate the elements in Scenario A. Table 4.5 contains the options used to generate the elements in Scenario B. Table 4.6 contains the options used to generate the elements in Scenario C. Table 4.7 contains the options used to generate the elements in Scenario D.

Table 4.4: Scenario A Nodes/Element

Instance	Threaded Rod	Base Plate	Flange Plate	Pile
Approximate Size	0.2	0.5	0.5	6
Curvature Control	0.1	0.1	0.1	0.1
Minimum Size (% global size)	0.1	0.1	0.1	0.1
# Nodes (Per Instance)	4047	44022	43080	588
# Nodes (Total)	48564	44022	43080	588
# Elements (Per Instance)	3304	35765	34890	280
# Elements (Total)	39648	35765	34890	280
Instance	Washer	Nut	Pole (Top)	Pole (Bottom)
Approximate Size	0.2	0.2	5	3
Curvature Control	0.1	0.1	0.1	0.1
Minimum Size (% global size)	0.1	0.1	0.1	0.1
# Nodes (Per Instance)	646	1125	520	806
# Nodes (Total)	15504	27000	520	806
# Elements (Per Instance)	283	760	385	432
# Elements (Total)	6792	18240	385	432

Table 4.5: Scenario B Nodes/Elements

Instance	Anchor Rod	Base Plate	Washer
Approximate Size	0.2	0.5	0.2
Curvature Control	0.1	0.1	0.1
Minimum Size (% global size)	0.1	0.1	0.1
# Nodes (Per Instance)	5992	55230	902
# Nodes (Total)	95872	55230	28864
# Elements (Per Instance)	5060	44785	398
# Elements (Total)	80960	44785	12736
Instance	Nut	Pole (Top)	Pole (Bottom)
Approximate Size	0.25	5	3
Curvature Control	0.1	0.1	0.1
Minimum Size (% global size)	0.1	0.1	0.1
# Nodes (Per Instance)	1008	560	988
# Nodes (Total)	32256	560	988
# Elements (Per Instance)	672	399	456
# Elements (Total)	21504	399	456

Table 4.6: Scenario C Nodes/Elements

Instance	Threaded Rod	Base Plate	Flange Plate	Spacer Plate	Pile
Approximate Size	0.2	0.5	0.5	6	6
Curvature Control	0.1	0.1	0.1	0.1	0.1
Minimum Size (% global size)	0.1	0.1	0.1	0.1	0.1
# Nodes (Per Instance)	4690	57546	57546	57546	588
# Nodes (Total)	112560	57546	57546	57546	588
# Elements (Per Instance)	3828	46715	46715	46715	280
# Elements (Total)	91872	46715	46715	46715	280

Instance	Washer	Nut	Pole (Top)	Pole (Bottom)
Approximate Size	0.2	0.25	5	3
Curvature Control	0.1	0.1	0.1	0.1
Minimum Size (% global size)	0.1	0.1	0.1	0.1
# Nodes (Per Instance)	646	574	520	806
# Nodes (Total)	31008	27552	520	806
# Elements (Per Instance)	283	348	385	432
# Elements (Total)	13584	16704	385	432

Table 4.7: Scenario D Nodes/Elements

Instance	Threaded Rod	Base Plate	Flange Plate	Pile
Approximate Size	0.2	0.5	0.5	6
Curvature Control	0.1	0.1	0.1	0.1
Minimum Size (% global size)	0.1	0.1	0.1	0.1
# Nodes (Per Instance)	5390	44022	43080	588
# Nodes (Total)	64680	44022	43080	588
# Elements (Per Instance)	4408	35765	34890	280
# Elements (Total)	52896	35765	34890	280
Instance	Washer	Nut	Pole (Top)	Pole (Bottom)
Approximate Size	0.2	0.25	5	3
Curvature Control	0.1	0.1	0.1	0.1
Minimum Size (% global size)	0.1	0.1	0.1	0.1
# Nodes (Per Instance)	646	574	520	806
# Nodes (Total)	31008	27552	520	806
# Elements (Per Instance)	283	348	385	432
# Elements (Total)	13584	16704	385	432

THIS PAGE INTENTIONALLY LEFT BLANK

Chapter 5 Results

This chapter contains the results of all phases of the study including the examination of previous HMLP inspections, tightening of the anchor rods on the two instrumented poles, and finite-element simulations.

5.1 Review of the HMLP inspections

A number of influence factors were investigated to determine if there were any patterns in the nut loosening as recorded by the 60-month inspections. This was done using Pivot Tables and Pivot Charts in Microsoft Excel. The results of some of the Pivot Table evaluations are shown in Table 5.1. Since many of the poles have only had one inspection, the values presented in the table are all based on the *first* inspection of the HMLP, if more than one has been performed. It is clear that the manufacturer and the number of lamps do not affect the average anchor nut rating, which is the best representation of the poles on which loosening occurred. The average number of loose nuts is also shown in order to supplement the anchor nut ratings and examine possible patterns in single vs. multiple loose nuts. For both the Number of Lamps and the Manufacturer, the average nut ratings are close to the overall value.

The two most obvious influence factors that affect the anchor nut ratings are the number of anchor rods, and the foundation type. Foundations that are made with welded steel flanges (both flange-flange and double nut), all of which have 12 rods, show significantly lower ratings than the 16-rod foundations with Cast-in-Place concrete pile caps. Given the relatively small number of foundations with the lower ratings, its

possible that the observed reduction is a statistical anomaly. However, these observations agree with theoretical conclusions from the FE modeling presented later in this chapter. This is not to say that the loosening is not occurring in the CIP concrete foundations. Anchor nut loosening was found in roughly 30 of the 93 CIP concrete poles, or 32%. In the welded flange poles, anchor nut loosening occurred in 13 of the 15 poles (87%).

Table 5.1: Influence Factor Comparison from AKDOT&PF Inspections

	Number of Towers	Average Anchor Nuts Rating	Average Number of Loose Nuts
Number of Anchor Rods			
12	15	1.40	3.00
16	93	2.96	0.86
Tower Height (ft)			
120	5	2.20	5.80
150	23	2.17	1.00
160	3	3.00	0.67
165	17	3.00	0.41
170	49	3.12	1.02
175	11	2.00	1.27
Number of Lamps			
4	19	2.58	0.73
5	25	2.44	1.76
6	34	2.94	0.62
7	8	3.13	0.13
8	22	2.77	2.05
Foundation Type			
CIP Concrete Cap	93	2.96	0.86
Double Nut	11	1.27	3.81
Flange-Flange	4	1.75	0.75
Manufacturer			
Millerbernd	34	2.82	1.79
Unknown	9	3.00	0.33
Valmont	65	2.66	0.94
Overall	108	2.74	1.16

It appears that the lower-height poles fair worse than their taller brethren, but it should be pointed out that 120-150 foot tall poles have smaller 12 bolt foundations and/or flange plate type connections.

In addition to influence factor observations, it was noticed that for those poles with multiple inspections generally improved over time. That is, those poles who had their anchor rods retightened improved their rating over time, presumably because the anchor rods did not re-loosen. Figure 5.1 shows all of the HMLPs that have had three inspections to date, which as it happens, all have CIP concrete pile cap foundations. Almost all of the poles have had their ratings increase over the three inspections.

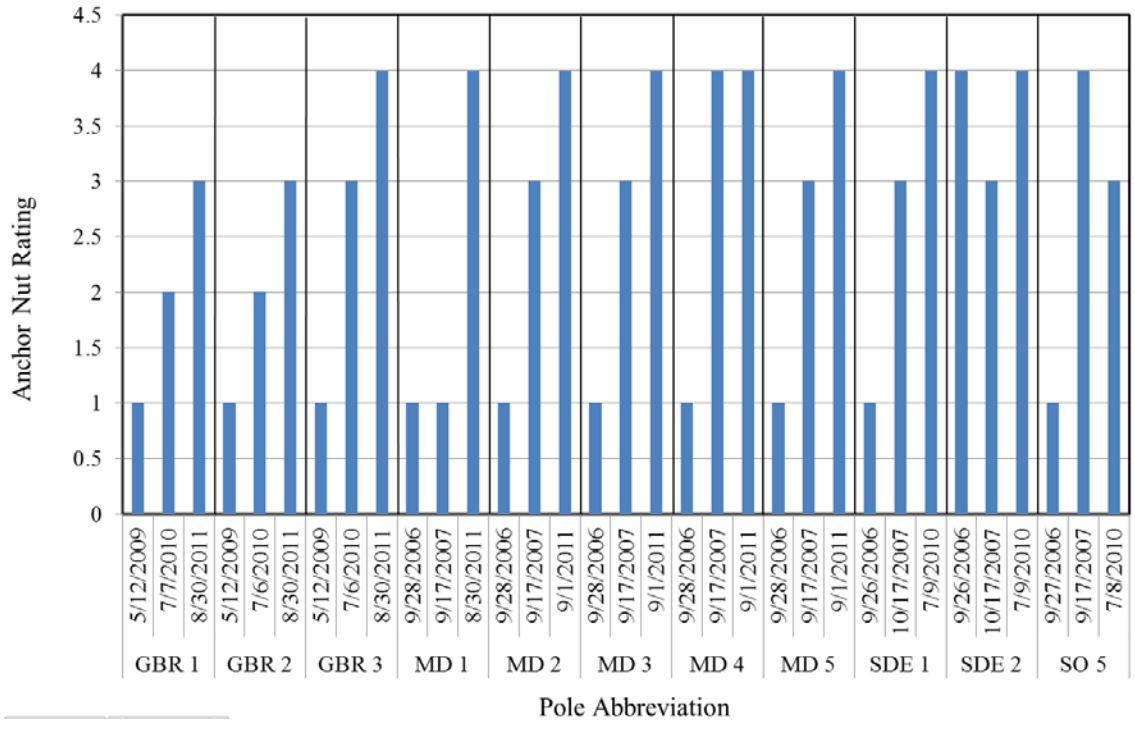

Figure 5.1: Anchor Nut Ratings on CIP Foundations with multiple inspections

It was also observed that often if one nut were loose, others were also. The inspection reports indicate that when a pole had a rod with full clamp-load loss, there was an average of 3.1 such rods on that pole. Of poles with at least 2 loose rods, 56% of the rods were adjacent to at least one other loose rod.

5.2 Fastener Monitoring and Testing

The results of the calibration and testing of the anchor rods with embedded strain gages, and the DTI calibration are presented below.

5.2.1 Anchor Rod Strain Gage Calibration

The results of the calibrations of the anchor rods with strain gages can be seen in Table 5.2 for the Weighstation rods and Table 5.3 for the Peter's Creek rods. The Coefficient of variation for the Calibration was 2.1% for the Weighstation rods and 3.5% for the Peter's Creek Rods. Most of the variation in the Peter's Creek rods was due to the low calibration constant in Bolt 01, which was not ultimately used. Removing Bolt 01, the Coefficient of Variation for the Peter's Creek calibration was 2.2%. The average effective areas were 1.327 in^2 and 1.400 in^2 for Weighstation and Peter's Creek, respectively.

Table 5.2: Calibration Results of Anchor Rods used at Weighstation

Bolt Name	Excitation Voltage (V)	Calibration (Kip/(V/V))	Effective Area (in^2)	Effective Diameter (in)
Bolt 01	6	78369	1.419	1.344
Bolt 02	10	74003	1.340	1.306
Bolt 03	10	77272	1.399	1.335
Bolt 04	10	74872	1.355	1.314
Bolt 05	10	76221	1.380	1.325
Bolt 06	10	78205	1.416	1.343
Bolt 07	10	78073	1.413	1.341
Bolt 08	10	79806	1.445	1.356
Bolt 09	10	77370	1.401	1.335
Bolt 10	10	77694	1.407	1.338
Bolt 11	10	75875	1.374	1.322
Bolt 12	10	75225	1.362	1.317

Table 5.3: Calibration Results of Anchor Rods used at Peter's Creek

Bolt Name	Excitation Voltage (V)	Calibration (Kip/(V/V))	Effective Area (in^2)	Effective Diameter (in)
Bolt 01	10	77420	1.402	1.336
Bolt 02	5	88210	1.597	1.426
Bolt 03	10	86260	1.562	1.410
Bolt 04	5	87520	1.584	1.420
Bolt 05	5	88640	1.605	1.429
Bolt 06	5	81905	1.483	1.374
Bolt 07	10	85330	1.545	1.402
Bolt 08	10	84340	1.527	1.394
Bolt 09	10	85290	1.544	1.402
Bolt 10	10	84950	1.538	1.399
Bolt 11	10	84580	1.531	1.396
Bolt 12	10	87230	1.579	1.418

5.2.2 Anchor Rod Strength Test

The elastic response was measured by four externally applied strain gages, an internal strain gage, and an extensometer. The results are shown in Figure 5.2. The resulting modulus of elasticity ranged from 29,150 to 31,580 ksi with an average of 30,160 ksi. The internal strain gage measured an elastic modulus of 30,180 ksi, which is almost exactly the average. The external strain gages were within +/5% of the average indicating an insignificant amount of bending in the specimen. The result of the full test is shown in Figure 5.3, which clearly shows that this material is a mild steel with a clearly defined yield. Yield was measured at 64.0 ksi, the maximum strength was 84.5 ksi, and the rupture strain was 0.27.

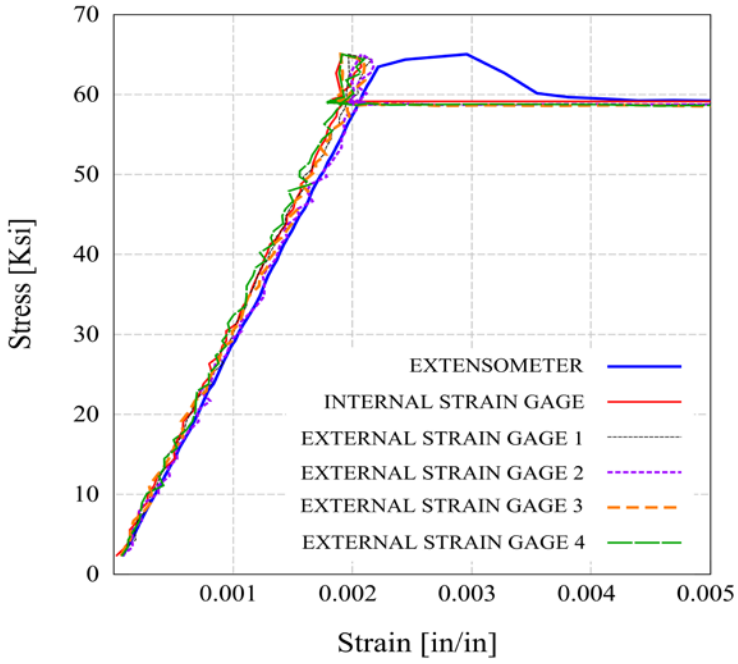

Figure 5.2: Elastic Stress-Strain Response of F1554 Threaded Rod

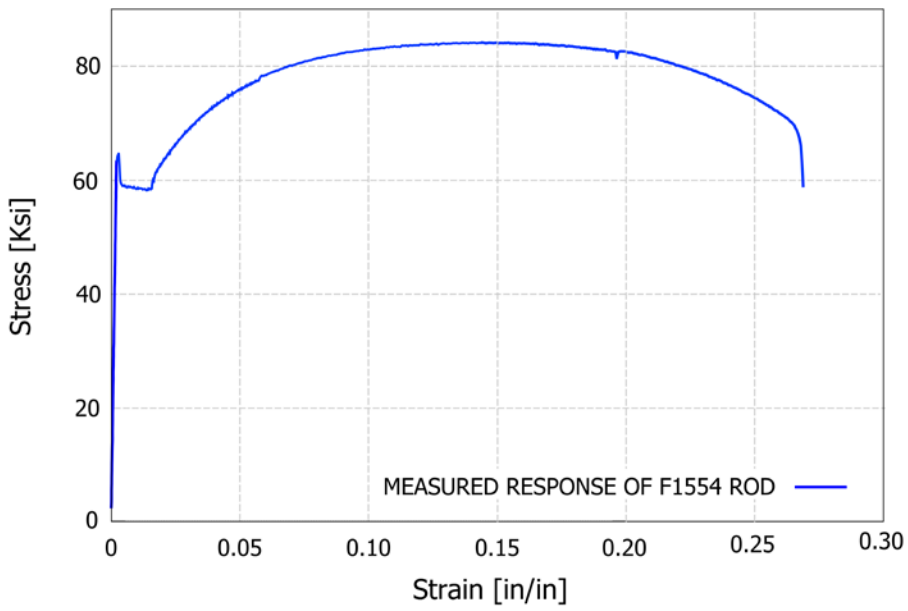

Figure 5.3: Plastic Stress-Strain Response of F1554 Threaded Rod

5.2.3 DTI Washer Calibration

A total of six DTI's were loaded until an indication squirt took place, as observed by the orange beads of silicone on the perimeter of the washer as shown in Figure 5.4. Loads at the time of the indicator squirt ranged from 50 to 55 kips. Results from the strain gages are shown in Figure 5.5, which shows the increasingly slower application of hydraulic pressure to pinpoint the force at which the DTI washers “squirt”.

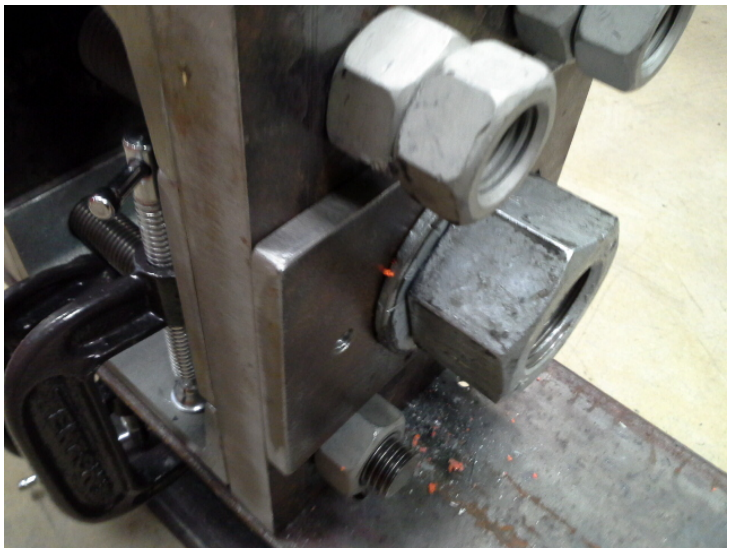

Figure 5.4: View of DTI after indication squirt as noted by the orange bead on the perimeter of the washer

The test assembly was designed to also accommodate 2.0 inch diameter bolts, which meant that the hole was too large for the 1.50 diameter rods and plate washers were initially used to seat the DTI washers. It was observed that the plate washers were inadequate for this purpose, and a ¼ inch thick plate was added with the DTI washers placed directly against that plate, as shown in Figure 5.4. This greatly increased the accuracy of the DTI washers and final runs were within 1 kip of their rating. It should also be noted that the predicted torque at the time of the squirt was considerably lower than predicted by roughly 30 percent and was likely due to the original coefficient of friction assumption.

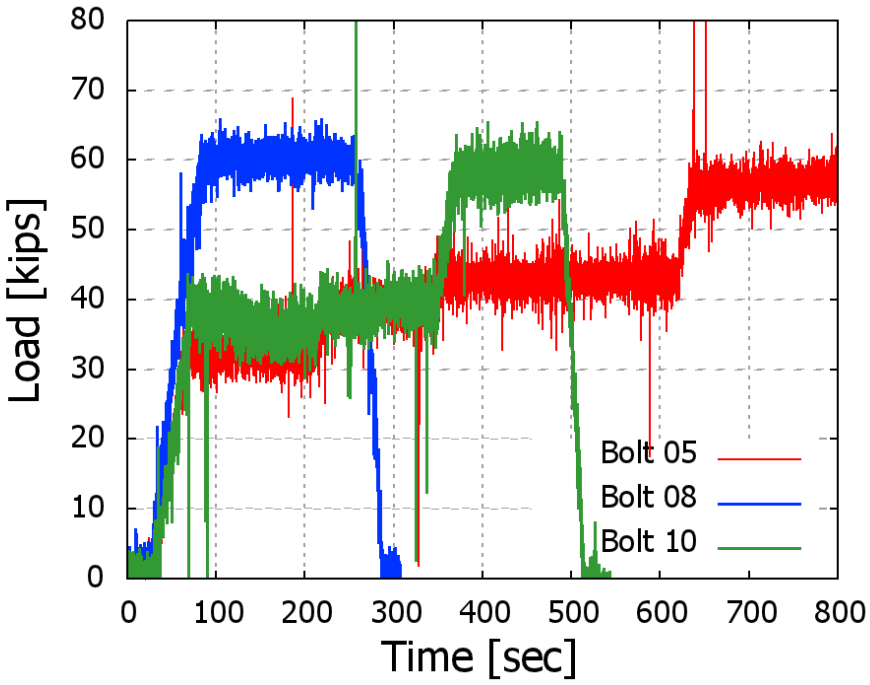

Figure 5.5: Results of DTI Washer Calibration

5.3 Tightening Data from First HMLP (Weighstation)

The installation of the strain-gaged threaded rods was conducted in February of 2013, the ambient air temperature was approximately 25°F (-4°C). The temperature, and the large number of wires, caused the installation to be slower than usual, and took about 3 hours. In some cases, heat was used to unfreeze the existing rods for removal. Four of the twelve rods produced unreliable results either due to electronic hardware components (broken connections) or thermal issues.

The results of the tightening procedure, along with the retightening a week later, can be seen in Figure 5.6. The nominal yield load of 55ksi (379 MPa), based on the tensile stress area is shown. In addition, one bolt was machined to a dogbone specimen

and tested to failure according to ASTM E8. The results of this test are shown in Figure 4.16. The magnitude of the load associated with the measured yield stress from that test of 63 ksi (434 MPa) is shown. It is clear from this figure that at least one anchor rod, #3, exceeded its yield stress during tightening. This matches the experience in the field, where the nut turned with seemingly little resistance when the verification torque was applied. A closer look at rod #3 is shown in Figure 5.7. The rods have a specified yield stress of 55ksi (379 MPa), which combined with a tensile stress area of $1.41in^2$ ($910mm^2$), results in yielding at an axial force of 77kips (343 kN). Rod #3 is around its yield point at the end of the tightening procedure. Upon returning a week later, the rod was tightened with the verification torque, seen in Figure 5.6.

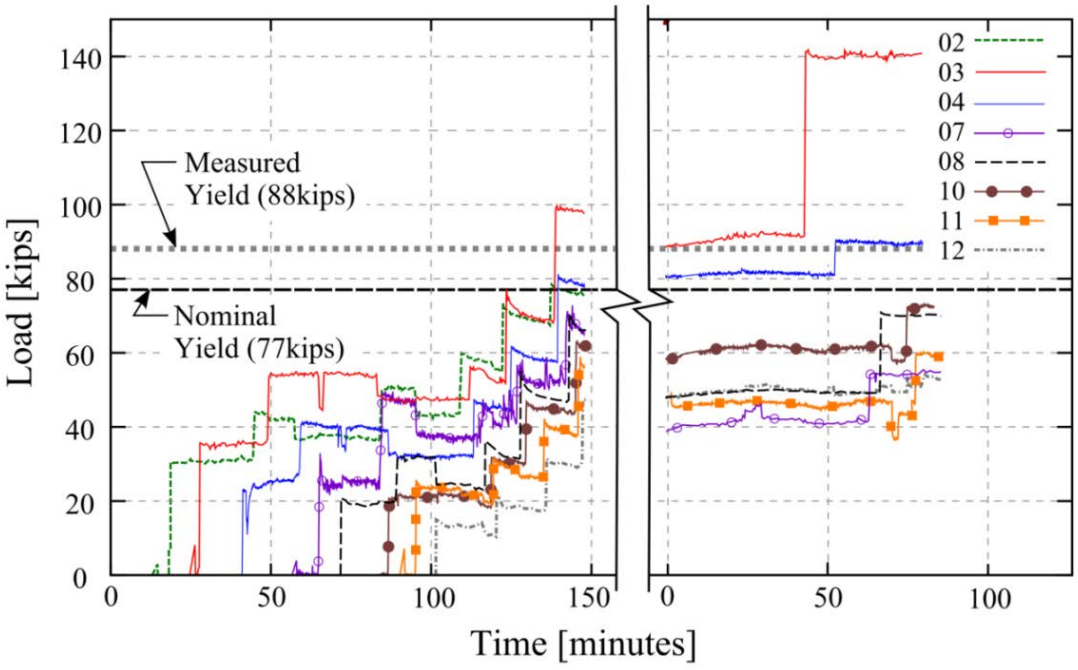

Figure 5.6: Axial Force in Anchor Rods during the Tightening Procedure and Re-tightening

Rod #3 has clearly yielded in this figure. Since the load has been extrapolated from strain based on the elastic modulus of the bolt, any load above the yield stress is inaccurate. It is a reasonable representation of the strain in the bolt as a percentage of the yield strain. In the case of Rod #3, the fastener was stretched about 40% beyond its yield strain.

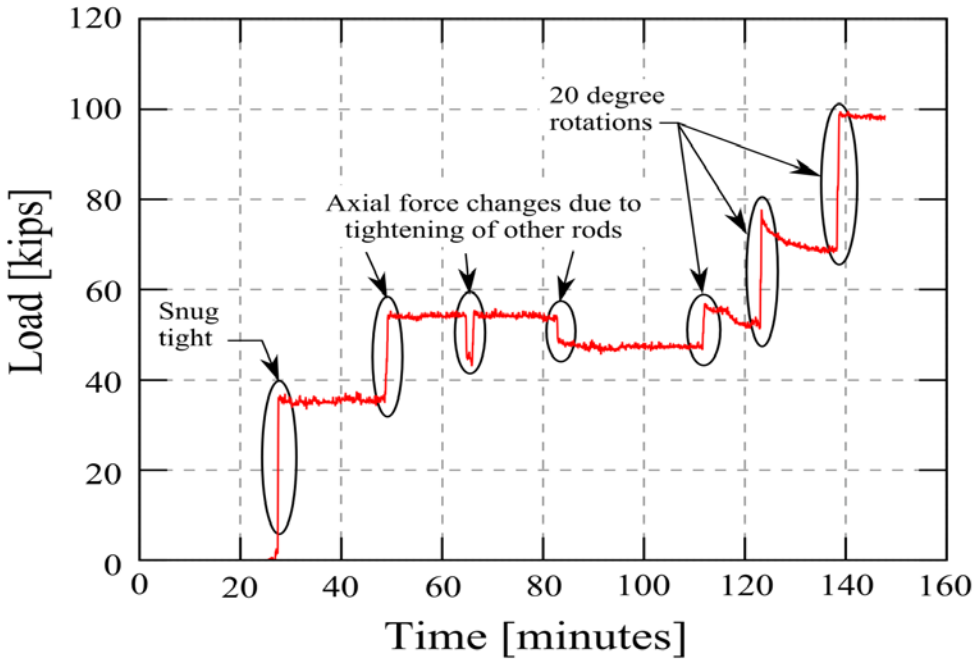

Figure 5.7: Tightening of Anchor Rod #3

As mentioned above, eight of the twelve strain gauges returned complete data during the tightening procedure. Table 5.4 shows the values returned by each strain gauge at the end of each stage of tightening. It also shows the total pretension developed

during the 1/6th of a turn and recorded rotation experienced by each tension nut during re-tightening. Figure 5.6 shows the pretension in each of the 8 strain gauges over time. The break in the data indicates the one week wait before re-tightening with the verification torque.

Using 20-30% of final pretension, which is 60% of minimum tensile strength, as a target for snug tight results in a range of 12-19 kips (57-84 kN) for the rods used in this study. The average force in the rods from the snug-tight procedure was 25 kips (111 kN), and most of the rods were tensioned beyond the recommended range.

Table 5.4: Axial Loads in Anchor Rods as measured by the strain gages (kips)

Bolt #	Snug Tight	20 degrees	40 degrees	60 degrees	Verif. Torque	Pretension turn-of the-nut	Rotation during Verification (deg)
1**	--	--	--	58	--	--	45^{+}
2	31	59	73	76	358*	46	60^{+}
3	36	56	76	99*	141*	63	30^{+}
4	23	47	58	80*	90*	57	8
7	25	41	52	65	55	40	8
8	21	36	53	66	70	45	20
9**	--	--	--	--	--	--	5
10	21	31	44	62	72	41	12
11	25	31	41	57	59	32	10
12	15	21	31	48	53	33	10

*Indicates yielded Anchor Rod
$^{+}$Rotation was halted
** Signal was lost in Rods 1 and 9 due to severed electrical connections

The rods used in this study had a minimum grip length of 4.5 inches (114.3mm), which is 3 times the bolt diameter (d_b). Table 5.4 shows the change in pretension the

rods experience after the nuts have been rotated 1/6th of a turn. In "Guidelines for the Installation, Inspection, Maintenance and Repair of Structural Supports for Highway Signs, Luminaires and Traffic Signals" (7), the FHWA recommends that nuts be rotated 1/6th of a turn for all bolt diameters greater than 1½ inch (38.1mm). The turn-of-the-nut method resulted in an average of 45kips (198 kN) of axial force developed above the snug tight tension. 1½ inch (38.1mm) diameter rods on HMLPs in service in Alaska are as low as $1.5d_b$, and as high as $4.5d_b$. If a nut on a 1½ inch (38.1mm) diameter rod with a grip length of $1.5d_b$, were rotated the same 1/6th of a turn, the rod would develop significantly more preload.

Returning and applying the verification torque used in the turn–of-the-nut method resulted in the yield of four rods, three of which had not yielded prior to re-tightening. Table 5.4 shows the rotations the nuts experienced during this re-tightening. Note that the nut tightening of rods #1, #2, & #3 were stopped after excessive rotation. The rods that were brought close to yield during snug tight and turn-of-the-nut resulted in yielding when re-tightened. The correct verification torque is expected to result in 70 kips (311kN) of pretension, which is equal to 90% of the yield strength.

Isolating changes in the axial force of an individual rod during the tightening sequence demonstrates that the axial load can be affected by adjacent rods in the group. **Figure 5.8** shows anchor rods that affected the axial tension in rod #3.

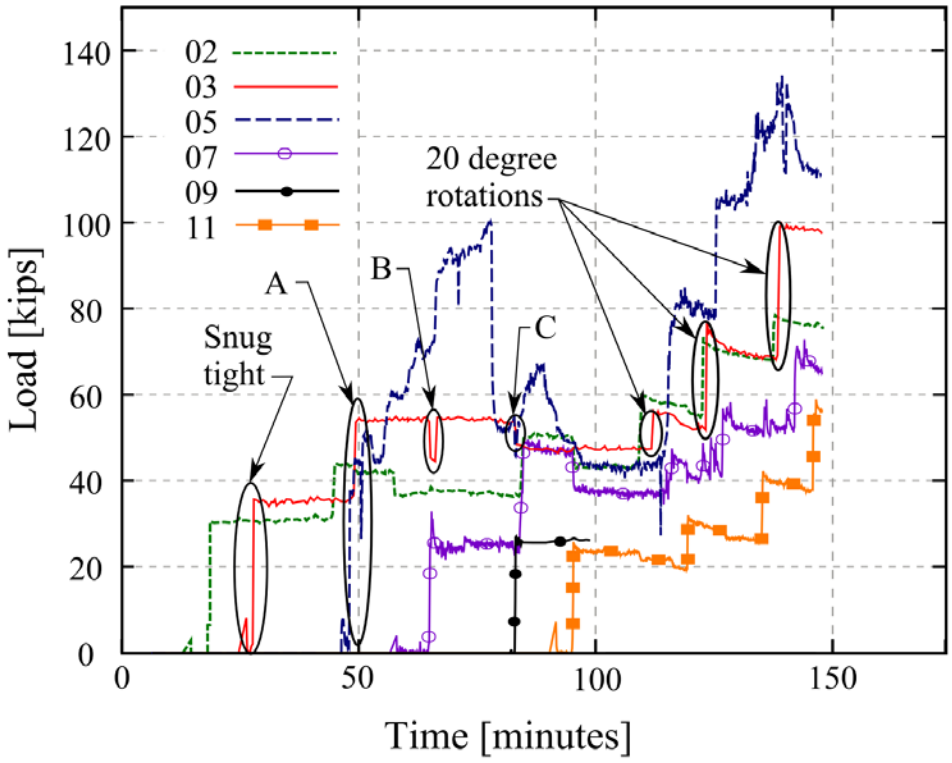

Figure 5.8: Effect of Adjacent Rods in Rod #3 During Tightening

Jump ‘A’ is due to rod #5 being tightened to snug tight. The loss and jump in ‘B’ is due to existing rod #7 being removed (it is adjacent to bolt #3) and then the new rod #7 being tightened to snug tight. The loss in ‘C’ is due to existing rod #9 being loosened and removed. Existing pretension in the original rods likely exceeds snug tight, which when removed affects the surrounding anchor rods. Rods #7 & #9 are adjacent to rod #3, and rods #5 & #11 are two positions away. These four rods are the ones in which a change in pretension is most likely to affect rod #3 and, as shown in the figure, the time at which these rods are brought to snug tight aligns with the pretension changes in rod #3.

As described in Chapter 4, the team returned more than a year after the installation of the anchor rods and re-applied torque to the rods to ensure that none were loose. The results can be seen in Table 5.5.

Table 5.5: Applied Verification Torque at Weighstation HMLP in May 2014

Rod #	Pressure (psi)	Torque (ft-lbs)	Approximate Internal Force (kips)	Initial Force in Feb, 2013 (kips)
1	1300	1102	44	65
5	1200	1017	41	80
9	1300	1102	44	66
3	1250	1060	43	88**
7	1000	848	34	55
11	1200	1017	41	60
2	1250	1060	43	88**
6	1250	1060	43	80
10	1200	1017	41	75
4	1400	1187	48	88**
8	1250	1060	43	70
12	1050	890	36	48

**Yielded

5.4 Tightening Data from Second HMLP (Peter's Creek)

There were twenty-four 1.5 inch diameter rods on this HMLP, 12 of which were strain gauged. Figure 5.9 and Figure 5.10 below show the load monitored in ten of the strain gauges over the duration of the tightening procedure. It can be seen that there was significant noise during 50 and 100 minutes. This was due to process of connecting the cable shielding to ground, which occurred during the snug-tight sequence.

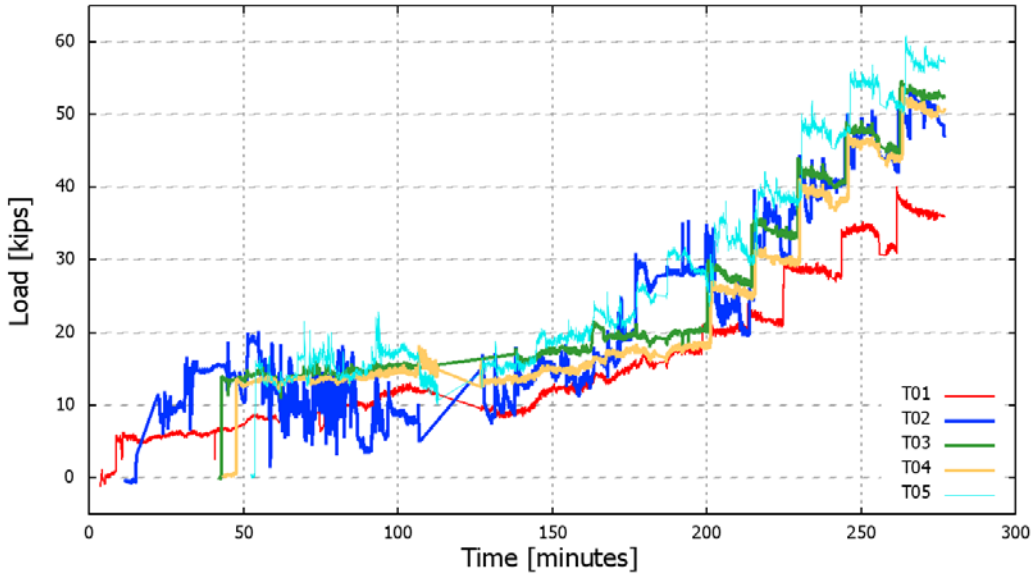

Figure 5.9: Peters Creek Tightening of Strain Gauges (1)

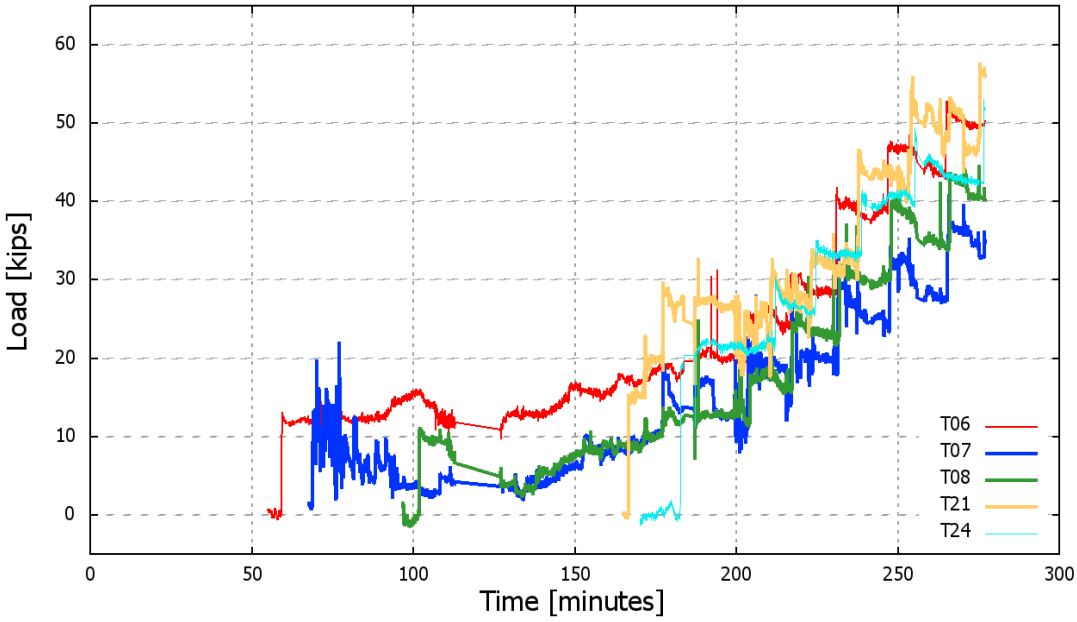

Figure 5.10: Peters Creek Tightening of Strain Gauges(2)

The noise was reduced after grounding the cables, but continued to a lesser degree throughout the tightening. This is due to electromagnetic interference thought to be originating from a nearby transformer. The final pretension values for each strain gauge are summarized in Table 5.6.

The pretension scatter was greatly minimized compared to the Weighstation tightening procedure. This is especially the case in the snug tight condition, which had a standard deviation of only 1.67 kips. The DTI washers performed especially well, even without the feeler gauge. The recorded pretension range of rods with DTI washers that were deemed fully indicated by observation alone was 51-58kips.

Table 5.6: Pretensions in Strain Gage Rods

Bolt #	Snug Tight	20 degrees	40 degrees	60 degrees	80 degrees	100 degrees	Squirt Status
1	12	21	25	30	35	40	+
2	14	24	33	38	43	48	*
3	15	28	35	42	49	54	-
4	15	26	32	40	47	53	-
5	16	30	38	47	53	58	-
6	14	25	30	39	45	51	-
7	--	--	--	25	30	36	*
8	12	18	25	31	36	42	+
21	15	25	32	41	48	54	-
24	17	27	33	39	44	52	-
Avg	14.4	24.9	31.4	37.2	43.0	48.8	
S.D.	1.67	3.62	4.28	6.56	7.18	7.15	

*No DTI indication, torqued until squirt.
+Partial indication, no further torque.

-Full Indication, no further torque.
all measurements considering +/- 2 kips error

As described in Chapter 4, the team returned more than a year after the installation of the anchor rods and re-applied torque to the rods to ensure that none were loose. The results can be seen in Table 5.7.

Table 5.7: Applied Verification Torque at Peter's Creek HMLP in May 2014

Rod #	Pressure (psi)	Torque (ft-lbs)	Approximate Internal Force (kips)	Initial Force in Oct, 2013 (kips)
1	900	763	31	40
2	1700	1442	58	48
3	1250	1060	43	54
4	1300	1102	44	53
5	1450	1230	49	58
6	1450	1230	49	51
7	1550	1315	53	49
8	1350	1145	46	42
9	1000	848	34	
11	1300	1102	44	
12	1450	1230	49	
13	1400	1187	48	
14	1150	975	39	
15	1000	848	34	
16	1250	1060	43	
17	1150	975	39	
18	1200	1017	41	
20	1000	848	34	
21	1250	1060	43	54
22	1400	1187	48	
23	1100	933	37	
24	1200	1017	41	52
10*	650	550	22	
19*	850	720	29	

*Tightened to 850 ft-lbs

5.5 Long-term Monitoring of Anchor Rod Tension

In addition to monitoring axial force during the tightening procedures, strain gauges were used to monitor data over time in both HMLPs. For the weigh-station

HMLP, the same cRIO DAQ used during the tightening procedure was used to record strain gauge voltages until it experienced a catastrophic failure on day 50. The data acquisition system can be seen in Figure 5.11.

Figure 5.11: Weigh Station HMLP cRIO DAQ

The source of this failure is unknown. Figure 5.12 and Figure 5.13 show the data collected from strain gauges. Wind and temperature were being monitored on a nearby radio tower.

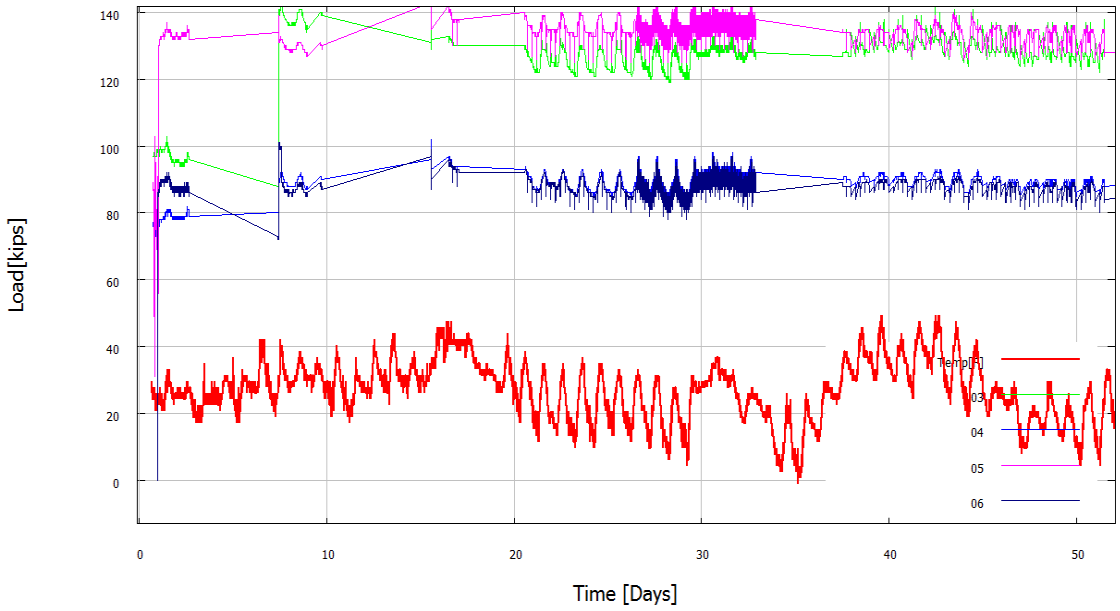

Figure 5.12: Weigh Station cRIO Long Term Data(1)

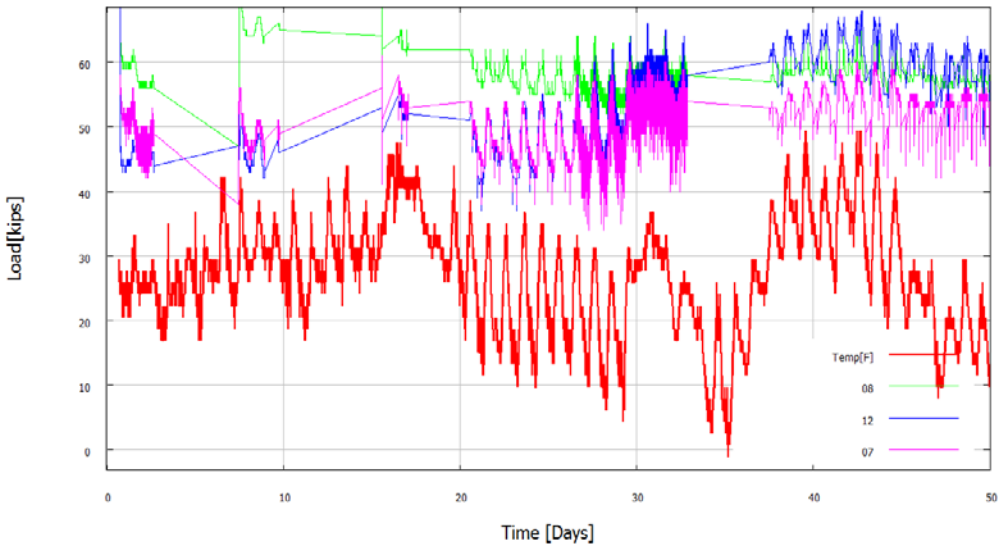

Figure 5.13: Weigh Station cRIO Long Term Data(2)

The change in the axial load in the strain gauges closely matches the change in air temperature over the duration of data collection. No drastic change in axial load was observed after re-tightening on day 7. Note that strain gauges 3-6 indicate yielded rods.

After the failure, a new DAQ was needed. Due to budgetary constraints, a new system was built instead of using an off-the-shelf model. The team elected to use Labjack® modules to monitor voltages which were output to a BeagleBone© miniature computer. A Python program was written that received, displayed, and stored the voltages on the BeagleBone. The system can be seen below in Figure 5.14.

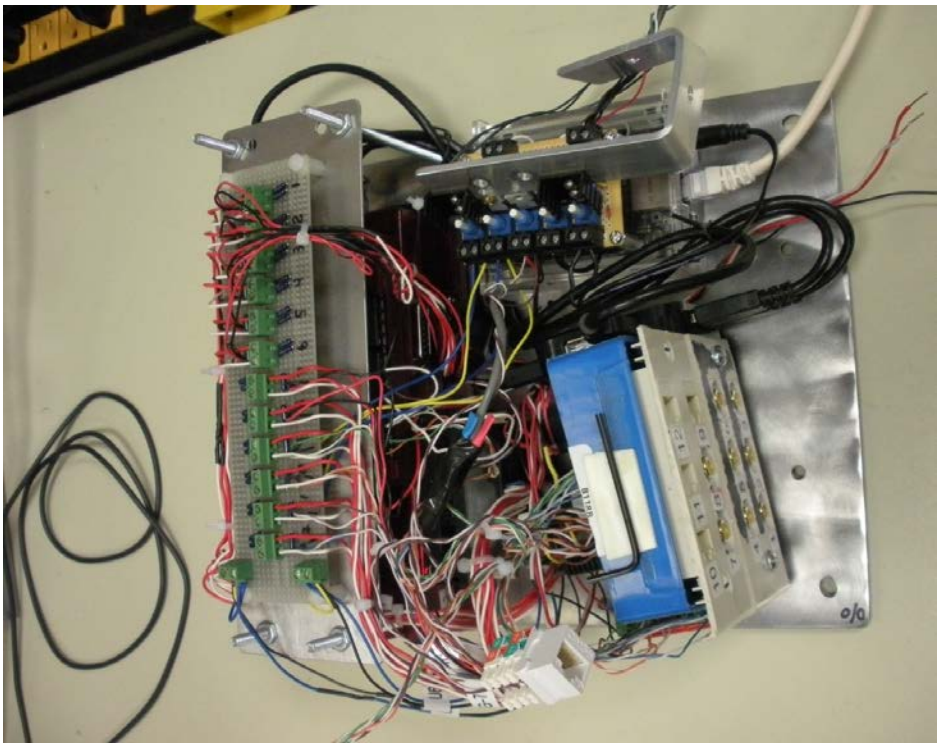

Figure 5.14: Weigh Station Custom Built Data-Acquisition System

This system ran into a few problems. The first of which was overheating. The BeagleBone requires 5V, but was being powered with a 12V battery. Initially, the voltage step-down was executed using a linear regulator. The large amount of heat given off by the regulator combined with a small enclosure and little ventilation resulted in the

BeagleBone quickly powering down. After unsuccessfully trying to dissipate the heat with aluminum and copper heat sinks, the regulators were replaced with a buck converter. The buck converter steps down the 12V into 5V, meaning voltage potential won't be wasted and turn into heat at the BeagleBone's power socket. After a few weeks of running smoothly, another catastrophic failure occurred. A spider was able to get into the box and span a positive and negative terminal, which rendered the BeagleBone inoperable. A new BeagleBone was purchased, and the DAQ was reassembled.

However, the program only ran for 24 hours in the field due to an error. Further development of the Labjack-Beaglebone DAQ system is needed to create a reliable system. Figure 5.15 and Figure 5.16 show the data recorded from the Peter's Creek system.

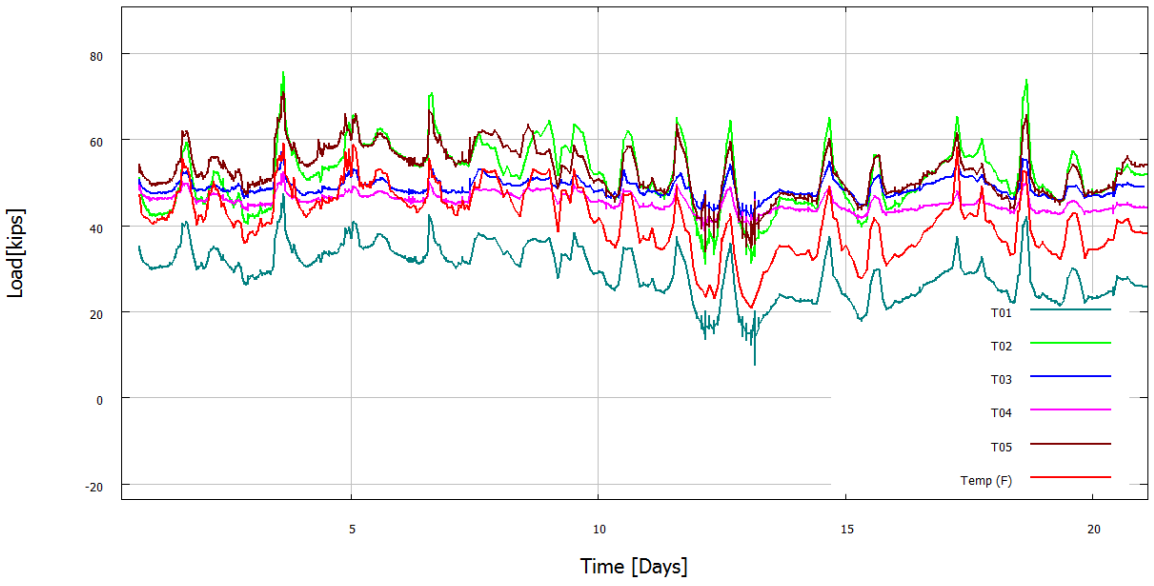

Figure 5.15: Peter's Creek Time Data (1)

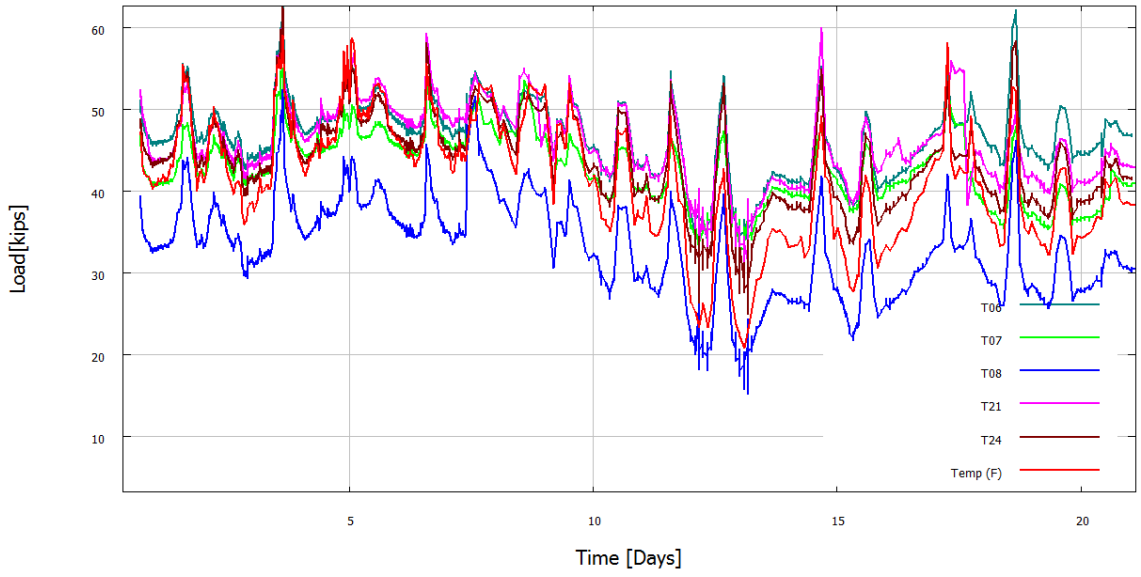

Figure 5.16: Peter's Creek Time Data (2)

5.6 Results of Finite-element Simulations

The clamp-load loss predicted by the FE models due to external wind loading is summarized below. The effect of the design wind moment on all configurations will be discussed, as will the minimum moment required to separate one rod in each scenario, and the minimum moment required to cause significant clamp-load loss equal to 10% of initial pretension. The effect of high strength rods in scenarios A & C will be summarized, as will the effects of stiffeners and thicker plates on scenario A.

5.6.1 Flange-Flange Connections

Scenario A, a flange-flange connection with twelve 38 mm (1.50 inch) diameter rods was loaded by applying a 768 kN-m (6800 kip-in) moment about the z axis of the connection, which simulated a 160 kph (100 mph) wind. The results are shown in Figure 5.17.

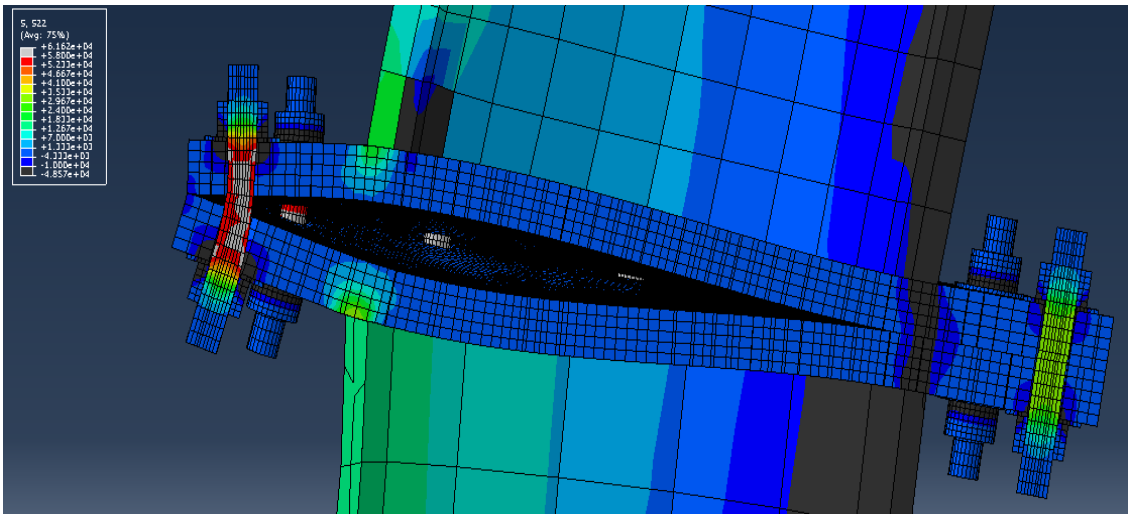

Figure 5.17: Z-axis (vertical) stress results of scenario A: twelve-rod flange-flange subjected to a 6800 k-in (768 kN-m) moment

The figure shows a section cut center parallel to the applied force, with the tension side of the moment on the left, and the compression on the right. Deformation is scaled by a factor of 25. Elements that are darker than the blue color in the middle of the plates are in axial compression. Lighter colored elements are in axial tension. Red elements are carrying stresses approximately equal to yield (58 ksi). Grey elements are carrying axial stresses greater than yield. It was observed that yielding occurs in all seven of the rods that experience tension. They undergo permanent deflection while this moment is applied. Figure 5.18 shows the next step, after the moment is removed.

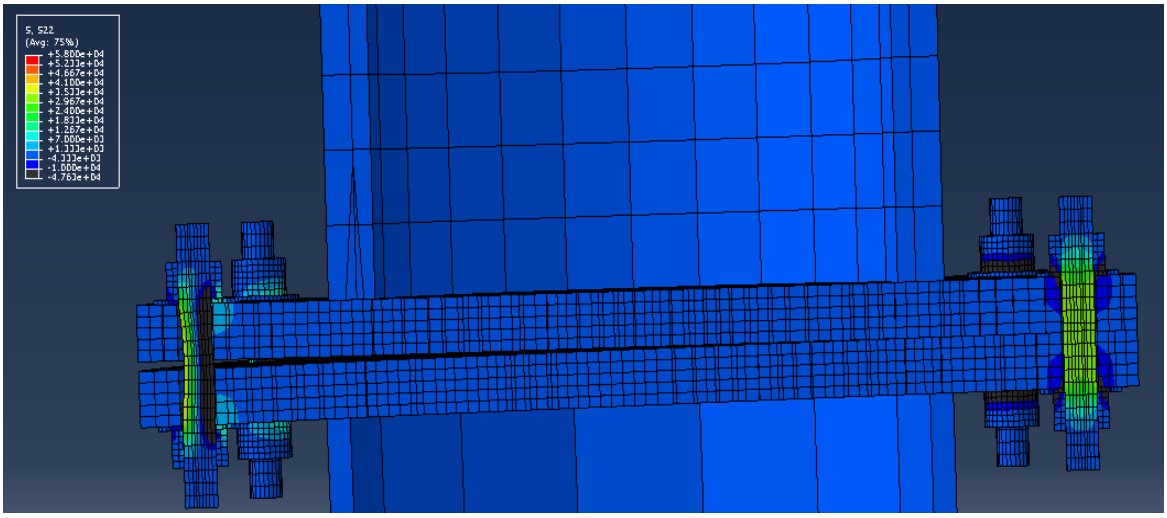

Figure 5.18: Scenario A unload (6800 k-in Moment)

It can be observed that there is no stress in the middle of the leftmost tension rod, there are residual bending stresses of opposite sign on either side of this rod, and there is separation between the two flanges. This separation occurs at five of the tension rods. The permanent deflection the rods undergo during the applied moment exceeds the

stretch that the bolts experience due to pretension in these rods. Because of this, when the moment is removed, the clamp load is zero in these five bolted joint interfaces. This agrees with the discussion above about post-yield behavior of joints, which predicts that joints comprised of mild steel rods will separate if external loads of sufficiently large magnitude are applied. A moment of 6300 k-in (93% of design wind) is required for only one rod to separate in this configuration.

Scenario B, a flange-flange connection with twenty-four 1.50 inch (38 mm) diameter rods was loaded by applying a 8800 kip-in (994 kN-m) moment about the z axis of the connection, which again simulated a 100 mph (160 kph) wind of the wider and taller pole. During the unload step there is no clamp-load loss due to permanent deformation. Since the foundation uses 24 rods, the system has the necessary capacity to absorb the moment without loss of clamp load. To cause separation of one rod, a moment of 11600 k-in (132% of design) is required.

5.6.2 Double Nut Moment Connection

Twelve 1.50 inch (38 mm) rods were utilized in Scenario C, which simulated a double-nut moment connection. This connection was loaded with 6800 kip-in (768 kN-m) moment, which simulated a 100 mph (160 kph) wind. The results can be seen in Figure 5.19.

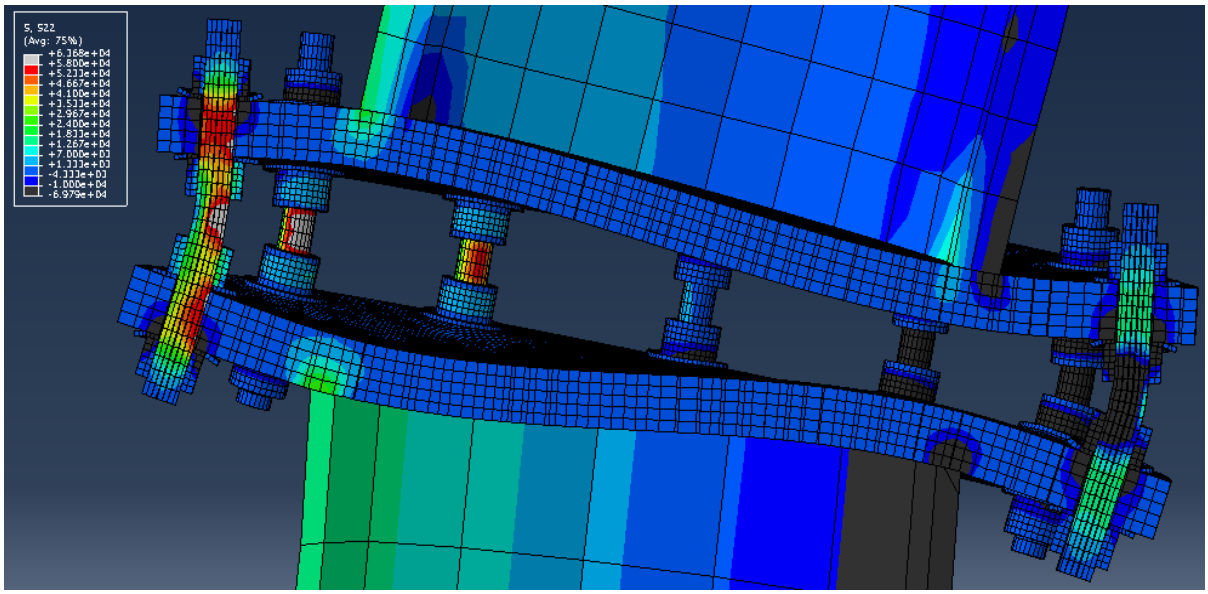

Figure 5.19: Scenario C Load (6800 k-in Moment)

The figure shows a section cut of the model at the center parallel to the applied moment with the tension side on the left, and the compression on the right. Five rods are absorbing the tension component of the moment, while five rods are absorbing the compression component because there is no plate-plate contact. The other two rods carry negligible load because they lie on the plate's neutral axis during the applied moment. The deformation is scaled by a factor of 25. The colors indicate the same stresses as mentioned for scenario A. There is some yielding in the tension rods due to bending, mostly between the two inside nuts. Figure 5.20 shows the step, in which the moment is removed. Because of the yielding, there are residual stresses between the inside nuts at three tension rods and three compression rods. However, because yielding of the rod occurs outside the areas where the rods are being clamped, the system has a much higher

resistance to clamp loss. A moment of 10900 k-in (161% of design) is required for this configuration to separate.

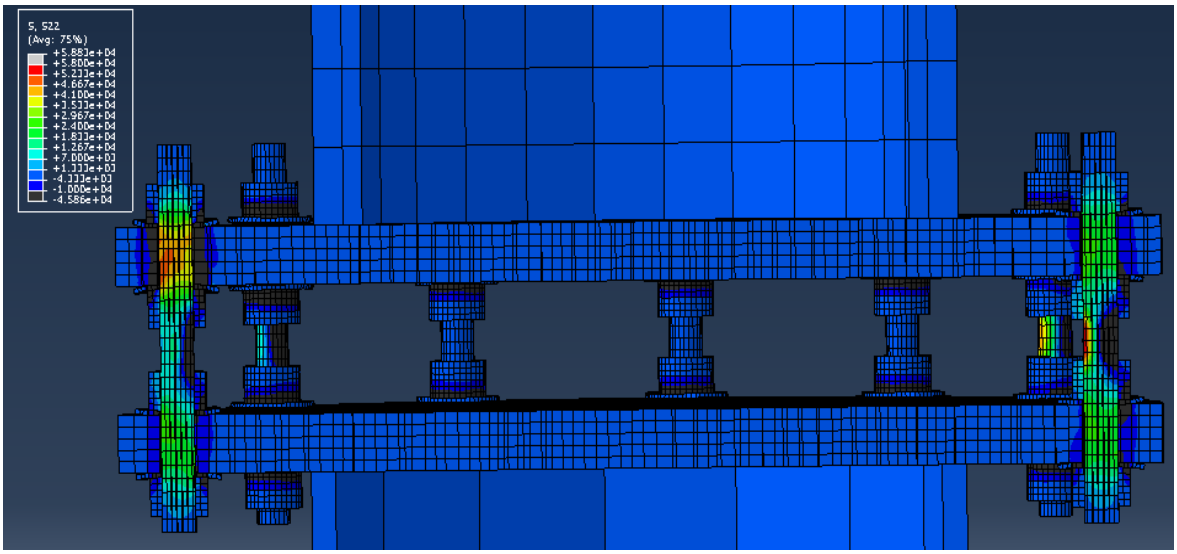

Figure 5.20: Scenario C Unload (6800 k-in Moment)

When an external load of the same magnitude is re-applied and unloaded again, no additional clamp-load loss occurs. Significant localized clamp-load loss (at least 10% of initial clamp load along the centerline of the tension bolt) occurs at the following moments:

- Scenario A: 5100 k-in (75% of design wind)
- Scenario B: 8100 k-in (99% of design wind)
- Scenario C: 9200 k-in (136% of design wind)

5.6.3 Cast-in-Place Concrete Connections

This FE model represents a HMLP configuration that is widely used in Alaska. The sixteen rods are embedded in concrete, which is represented by a rigid solid. The

nuts clamp the base plate of the pole. In Figure 5.21, the anchor rods are pre-tensioned with a Δ_B = 0.008 inches.

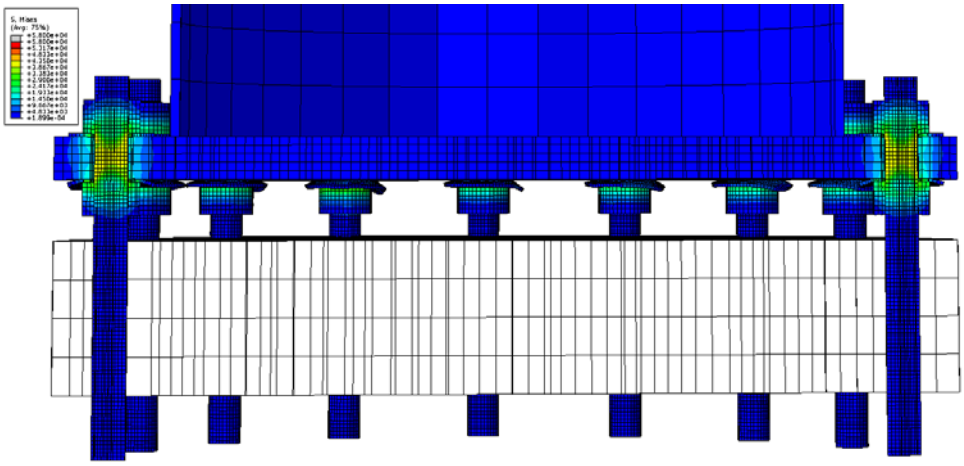

Figure 5.21: CIP Concrete Pretension ($\Delta_B = 0.008$")

Figure 5.22, 110 mph wind is being simulated by applying a 9500 k-in moment to the pole. The model is cut down the middle of the X axis with the tension side of the moment on the left, and the compression on the right. Five rods are absorbing the tension component of the moment, while five rods are absorbing the compression component because there is no plate-plate contact. The deformation is scaled by a factor of 25. In Figure 5.23, the load is removed.

It can be observed that there is not significant clamp loss. In Figure 5.23, a moment of 18000 k-in lowers clamp load below "snug tight" levels.

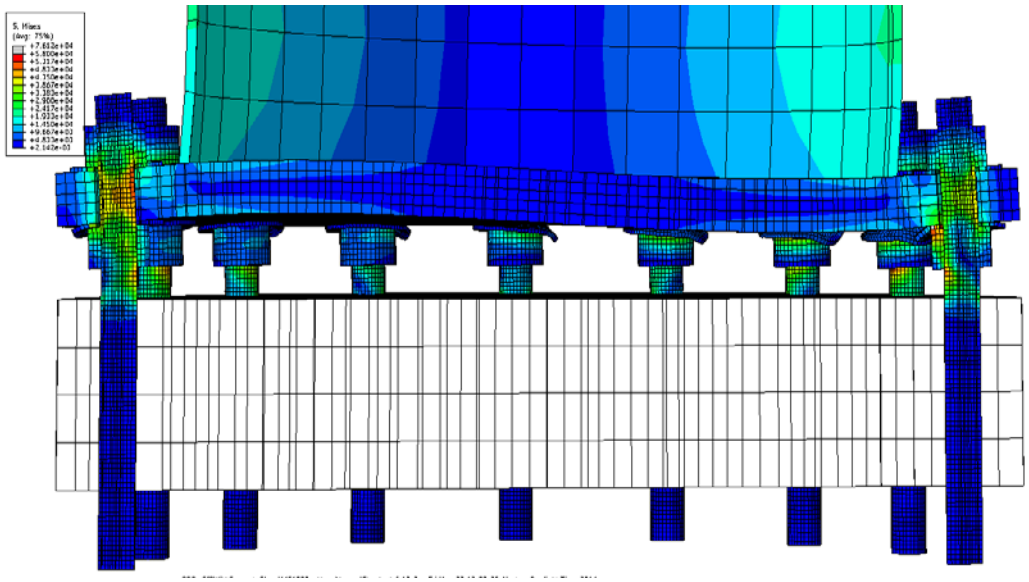

Figure 5.22: CIP Concrete Load (9500 k-in Moment)

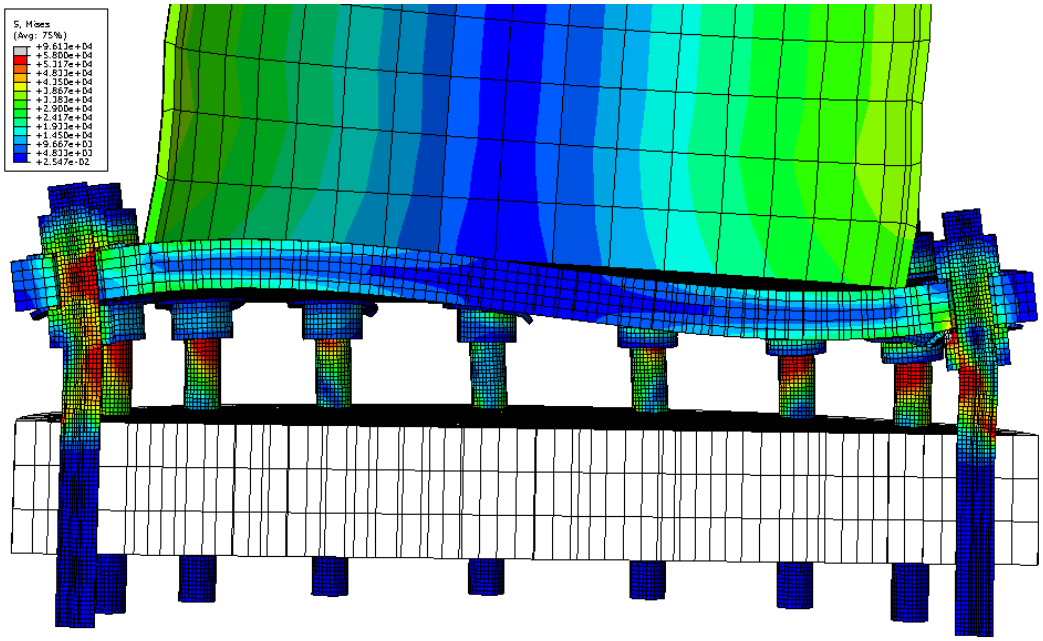

Figure 5.23: CIP Concrete Load (18000 k-in Moment)

The CIP Concrete foundation type separates at 20000 k-in. The design wind moment is equal to 9500 k-in. If the pretension is in the correct range, the FEA model shows that this foundation has a high resistance to clamp-load loss. However, this model is static, and doesn't capture the effects of dynamic loads like vortex shedding. This actual maximum wind load may be much higher than the design wind load. Also, the model's geometry is perfect, and doesn't include variations in the angle of nuts which may be occurring in configurations with very short grip lengths. As seen in Figure 5.23, rods on the compression side of the moment temporarily lose some of their tension during an external wind load. If the pretension in these rods in low enough, the rods will carry no load during the external wind load. If vibration occurs in the nut, it would be free to spin, and traditional loosening may occur. To make sure this bolted-joint interface utilizes its maximum resistance to clamp-load loss due to traditional loosening, pre-tension needs to be kept in an acceptable range.

5.6.4 Effect of Varying Model Parameters

The magnitude of pretension was varied in scenario A by varying the Δ_B value from 0.004 inches to 0.012 inches, and on scenario C by varying Δ_B from 0.002 inches to 0.006 inches. This change in pretension had no effect on the moment required to separate either interface after unloading. This is supported by theoretical considerations in Chapter 2, which indicate that a mild steel bolted joint interface undergoes clamp loss when an external load exceeds F_y of the rods, regardless of pretension.

When high strength rods (F1554 Grade 105) were used instead of the mild steel rods, resistance to separation increased dramatically. In scenario A, the moment required for separation was 11560 k-in, an increase of 183% when compared to the 6300 k-in moment required to separate the mild steel configuration. When high strength rods were used in scenario C, the moment required for separation was 20500 k-in, an increase of 188% when compared to the 10900 k-in moment required to separate the mild steel configuration. Because the bolted joint interface undergoes clamp loss when an external load exceeds F_y of the rods, increasing F_y from 55 ksi to 105 ksi should have this effect. High strength rods weren't used in scenario B because the result would be similar to scenario A, and scenario B already requires 132% of design load to separate.

The effects of both adding stiffeners and increasing the thickness of the plates were analyzed on scenario A. Figure 5.24 shows scenario A with stiffeners attached undergoing the 6800 k-in design load. The maximum distance between the two plates is reduced by 40% when compared to scenario A without stiffeners. However, the clamp-load loss is not significantly mitigated. It can be observed that the majority of elements in the leftmost tension rod are still yielded.

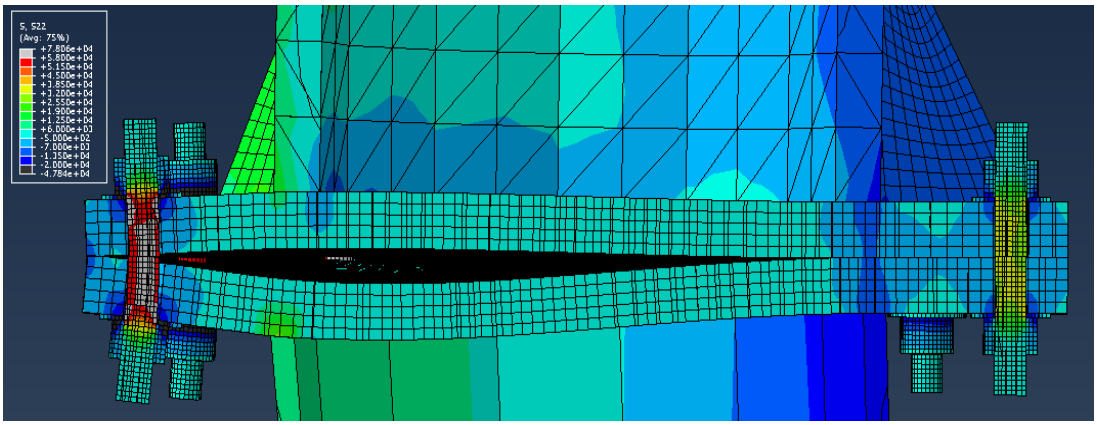

Figure 5.24:Scenario A with Stiffeners Load (6800 k-in)

In Figure 5.25, the base and flange plates are doubled in thickness from 2.25 inches to 4.5 inches. The pretension displacement was increased so that the stress due to pretension was the same as scenario A. In a design wind load, the maximum distance between the two plates is reduced by 80%. The clamp-load loss is reduced to zero. The magnitude of moment required to cause significant clamp loss and the magnitude of moment required to cause separation in one rod can be seen in Table 5.8.

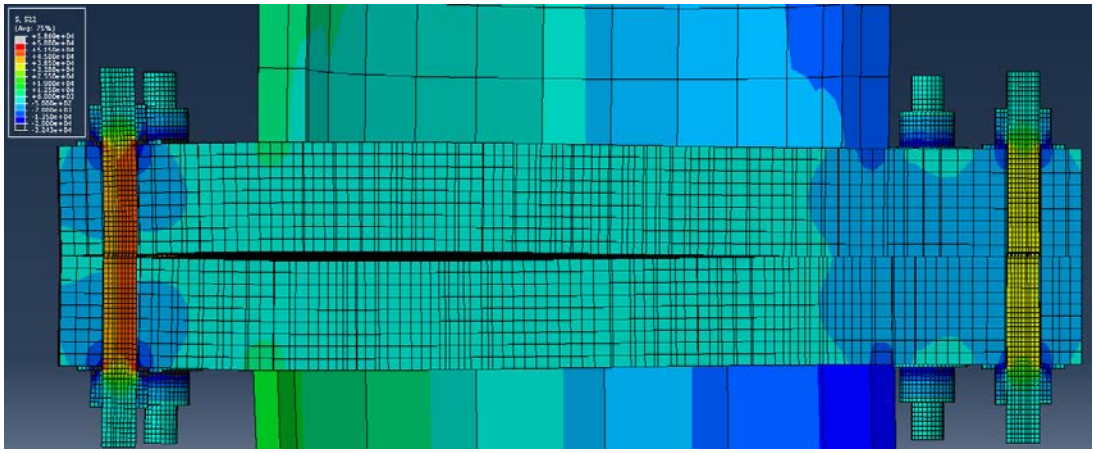

Figure 5.25: Scenario A with 4.5 Inch Thick Plates Load (6800 k-in)

Table 5.8: Minimum Clamp-loss and Separation Moments

Model Scenario	Rod Strength	Design Moment	Clamp-loss Moment		Separation Moment	
		kN-m	kN-m	% of Design	kN-m	% of Design
A	Grade 55	768	576	75	712	93
B	Grade 55	994	915	92	1311	132
C	Grade 55	768	1039	135	1232	160
A	Grade 105	768	1107	144	1299	169
C	Grade 105	768	2056	268	2316	301

Chapter 6 Discussion

This study utilized an FHWA tightening procedure to replace the anchor rods on two flange-flange foundation HMLPs. The axial force of each anchor rod in the HMLPs foundation was monitored during tightening. In addition, finite-element modeling was used to model three HMLP foundation configurations, as well as possible changes to several components of the foundation connection. Discussion is presented below that synergizes the findings of the different activities.

6.1 Anchor Rod Tightening

While it has been shown that the performance of the F1554 Grade 55 anchor rods is not affected by the initial pretension value, it is useful to be able to approximate the losses that occur during tightening, and thus the final preload for a given foundation configuration and degree of nut rotation. This is particularly true if high strength fasteners, such as F1554 Grade 105 rods, are because they do not have a perfectly plastic portion of their stress-strain response. Figure 6.1 shows the resulting axial force at each tightening step for both the Weighstation and Peter's Creek tightening. The chart indicates the average force value with the range of values recorded over the twelve fasteners shown by the error bars. The force imparted on the rods by each 20 degree turn is significantly higher for the Weighstation rods. This is expected, because the nominal grip length (distance between top and bottom nuts) is significantly less for the Weightstation pole (4.5 inches) than the Peter's Creek pole (6.75 inches). However this parameter is not accounted for in the tightening procedure, nor is the yield strength of the

rods, which will also have a significant effect. The existing provisions for top nut rotation beyond snug tight can be seen as a table in appendix E, originally from Garlich & Thorkildsen (7). These provisions are intended for use in use in double-nut moment connections, but have been generalized and used in other configurations.

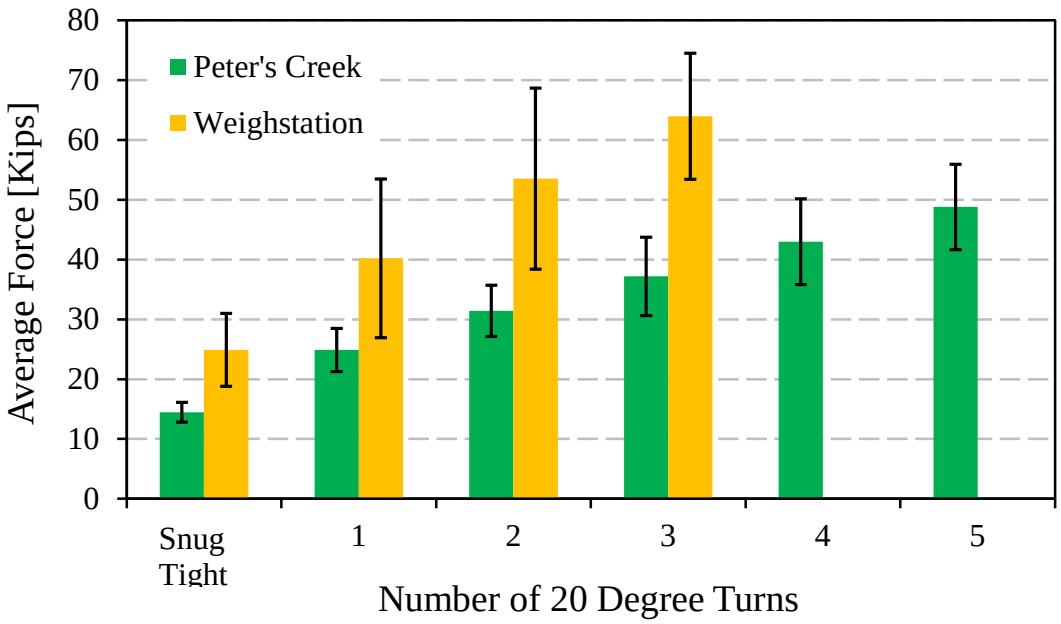

Figure 6.1: Average Axial Forces Developed in Anchor Rods during Tightening

Figure 6.1 also shows that the range of values is much larger for the Weighstation rods. Not shown in this figure, but it was generally true that those rods that started out at the lower end of the scale at the end of snug tight, stayed at the low end throughout the tightening. Because the torque at the snug tight was controlled at Peter's Creek, it led to less scatter in the rods throughout the tightening.

This data can be normalized for the ratio of the fastener's grip length to its diameter (L/d), to show that this is the primary cause of the difference in the average axial deformation and resulting force. The results of this exercise can are shown in Figure 6.2. This figure compares the axial strains multiplied by the L/d ratios for each pole, which are 3 and 4.5 for Weightstation and Peter's Creek, respectively. It is clear from this figure that the 20 degree turns have a similar effect, when adjusted for the L/d ratio.

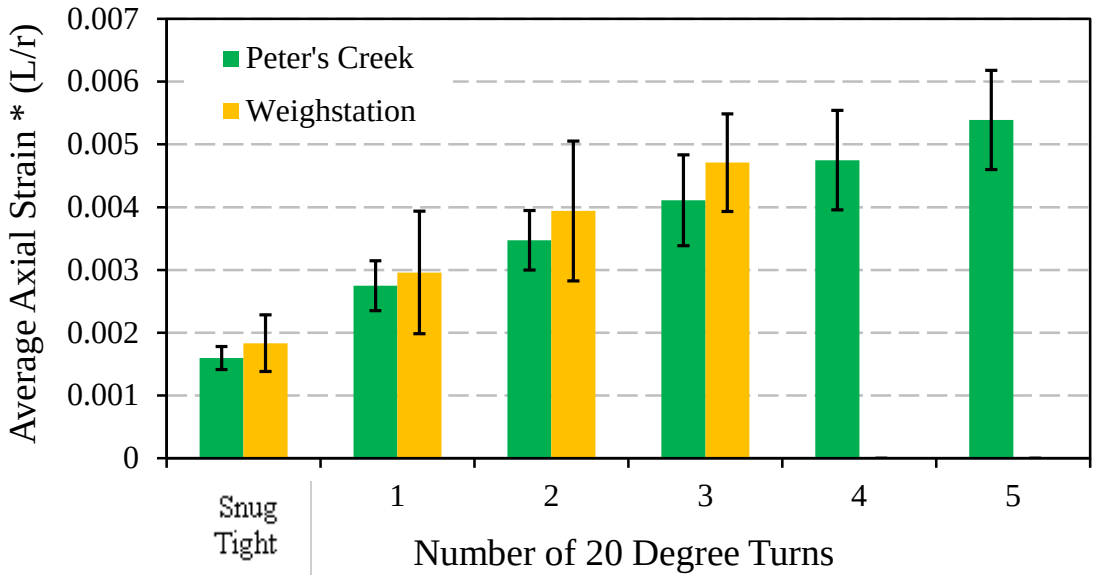

Figure 6.2: Normalized Axial Strain Developed in Anchor Rods during Tightening

The axial strain data can be combined with the FE modeling to determine the magnitude of the losses that occur at each tightening step. Since the axial strain data was recorded during the tightening procedure, the displacement of the anchor rod in the FE model, which is the input for the model, can be adjusted such that the final rod pretention

matches that recorded in the field. This results in the theoretical displacement of the nut to produce the final pretention. The displacement of the nut in the field, relative to the anchor rod, is a function of the thread pitch and amount of rotation, which was also recorded during tightening. Thus, the difference between the theoretical and recorded nut displacements can be evaluated to determine how much of that displacement was "lost". Losses include displacement energy used to flatten high points in the plates, bend the rod to account for our of straightness or nut angularity, and deformation not accounted for the in the computer model, such as bending of the threads.

The results of this calculation are shown in Figure 6.3 for the HMLP at Weighstation and in Figure 6.4 for the HMLP at Peter's Creek. The average losses during the tightening at the Weighstation was $5.6x10^{-3}$ inches (0.14 mm). The average losses during the tightening at the Peter's Creek was $4.2x10^{-3}$ inches (0.11 mm). Presumably, the difference between these values is due to the lower flatness tolerance used to manufacture the plates in the Petere's Creek HMLP.

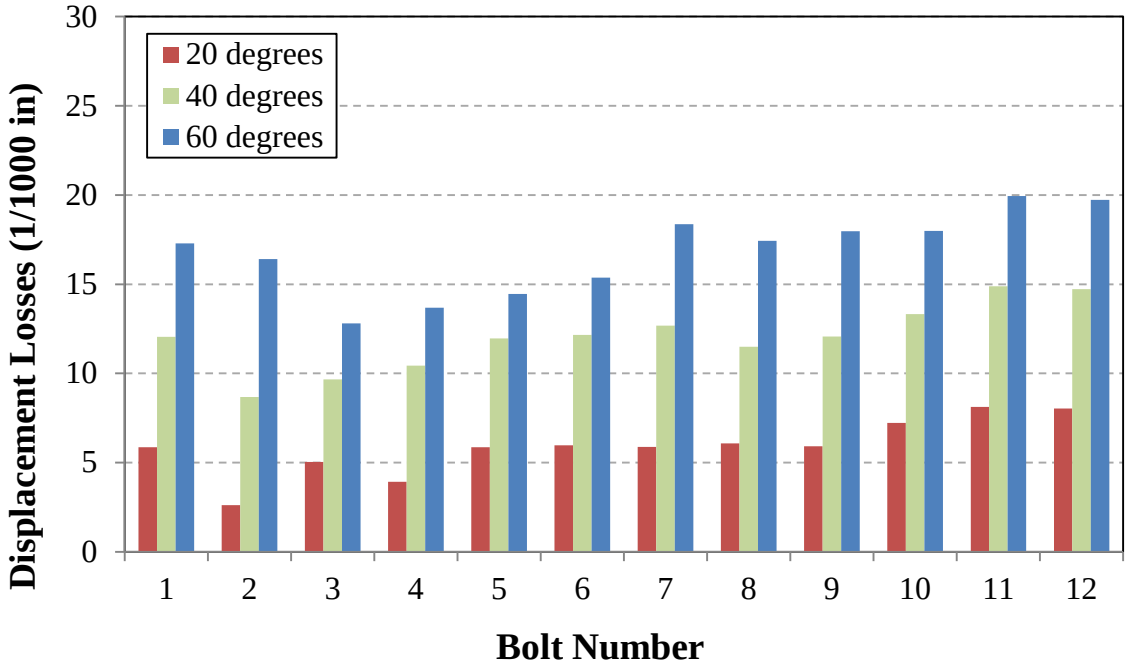

Figure 6.3: Displacement Losses at Weighstation during Tightening

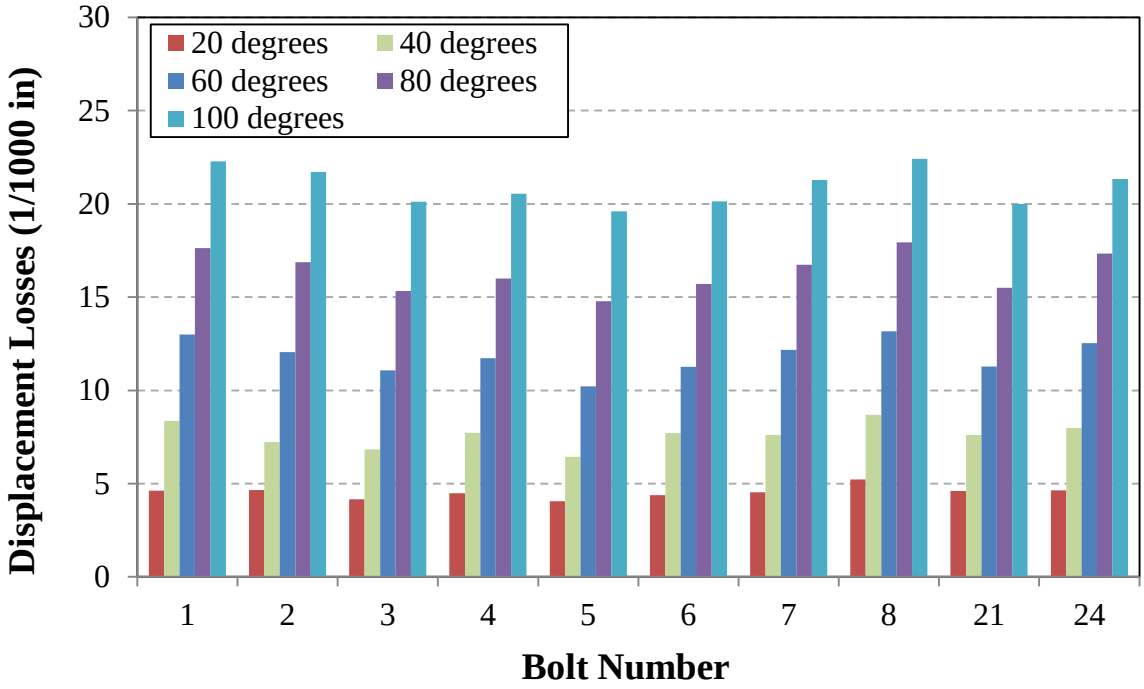

Figure 6.4: Displacement Losses at Peter's Creek during Tightening

6.2 Limitations of Strain Gages

Strain gauges are not the ideal choice to record clamp-load loss due to permanent rod deformation. In the best case scenario, if the DAQ monitoring the strain gauge was recording continuously, it would be capable of capturing an anchor rod's strain during any large wind event. If the wind event exerted an external load of sufficient magnitude to cause separation, the strain would increase, indicating that the rod had deformed. When the external load ceases, the strain decreases, but it would not return to its original value. There would be residual strain due to the permanent deformation of the rod. If the DAQ wasn't recording during the separation load, it would appear as if nothing happened because the pre-load strains and the post-load strains would be similar. Any dissimilarity would likely be indiscernible due to electronic noise and strain gage drift.

The epoxy used to bind the strain gauges to the inside of the rods was sensitive to temperature changes. In addition, the rods themselves act as thermometers, their axial strain increasing as the temperature rises in accordance with steel's coefficient of thermal expansion. It was found that the temperature of each rod around the HMLP varies significantly due to environmental effects, such as angle of the sun, snow cover, and wind speed and direction. As a result, the thermal variations in strain could not be adequately adjusted for using the temperatures recorded a few feet above the fasteners on one side of the pole. In order to accurately account for temperature variations in strain gauges inserted in epoxy cores, the temperature of each anchor rod must be measured, significantly increasing the number of channels needed in the data-acquisition system.

Instead of strain gauges, future research should utilize load cell washers to record axial load of the rods. These devices directly measure the compression load applied by the nut, which directly corresponds to the axial tension in the rod and the applied external load. Their reduced length and full wheatstone bridge would also greatly lessen the effects of thermal strain. Load cell washers are significantly more expensive than strain gages, but they would accurately capture clamp-load loss in the connection.

6.3 Finite-element Modeling and Limitations

A 3D static Finite-element analysis was used in this study. This type of analysis is incapable of producing dynamic effects which may be occurring during the load and unload steps. A dynamic FE analysis may be capable of reproducing traditional loosening, when nuts rotate on the threads of the rod during an external load. A dynamic FE analysis would also be able to determine if separation occurs when loads causing small clamp-load loss are repeated, such as may occur during a dynamic loading.

While possible using the FE solver used in this study, thermal modeling of the HMLP foundation connections was not performed. This type of analysis is complex, requires a special skill set, and time-consuming to set up. It was determined, given that the connections are entirely made of a single material, that the resulting benefits of performing such a model would be minimal.

THIS PAGE INTENTIONALLY LEFT BLANK

Chapter 7 Conclusions and Recommendations

This chapter contains conclusions pertaining to the specific objects of the study, recommendations related to modifying both in-service HMLPs and the design of new ones, and subjects for future research.

7.1 Conclusions

The results of this study do not have a "smoking gun" that point to a clear explanation of the anchor nut loosening, but there is evidence to suggest its causes. The anchor rods are likely "stretching" and not loosening, that is, the nuts are not turning. This is supported by reports of field personnel that recorded the orientation of particular anchor nuts and later returned to discover that the rods had lost their pre-tension without the nuts rotating.

Evidence that suggest stretching is primarily in the inspection review and the results of the Finite-element modeling. Inspections indicate that the flange plate foundations (both double nut and flange-flange type) are far more likely to experience clamp-load loss in the anchor nuts. FE modeling indicates that an applied wind load of approximately 93 mph (3 sec gust, static bluff body) will cause complete clamp-load loss in one anchor rod on a 12-rod foundation. Modeling also predicts that only slightly more force is required (5 rods loosened at 100mph) to remove the clamp load in multiple rods. This is consistent with the inspection reports that show poles are likely to have more than one rod loose, and there is a relatively high probability that loose nuts are adjacent.

Between February and December of 2013, instantaneous wind gusts over 120 mph were recorded by the radio-tower Anemometer in eight separate wind storms at the Weighstation Hightower. The worst of these, in mid-October recorded instantaneous gusts over 160 mph and 3-sec gusts of approximately 100 mph. It is known from weather data that the storm in September of 2012 exceeded these wind speeds.

Stretching of the anchor rods by relatively regular wind speeds is further supported by discussions with engineers from Valmont, manufacturer of the majority of the HMLPs. Valmont indicated that their pole baseplates are not designed for prying action, and that a double-nut style connection is assumed, in which the overturning neutral axis is located at the center of the pole. A flange-flange connection, like that on the Weighstation HMLP, has an overturning neutral axis shifted toward the compression side of the connection, increasing the force on the rods in tension during an applied overturning moment.

Given the evidence presented, it is uncertain why the 16-rod CIP concrete foundations experience clamp-load loss. The causes attributed to the rod stretching in the flange plate foundations require much larger loads to cause clamp-load loss in the CIP foundations. It is speculated that localized yielding due to anchor rod bending, combined with manufacturing tolerance factors (such as low plate flatness that contributes to nut angularity) contribute to the clamp-load loss. This is supported by the improved performance of the anchor rods after re-tightening, as observed over multiple inspections. In addition, personal observations during the September 2012 windstorm suggest that the HMLPs are susceptible to dynamic loading induced by vortex-shedding. It is not known

the magnitude of forces or strains that the anchor rods would be subjected to in this type of loading.

Other conclusions were made throughout the study that do not directly affect the clamp-load loss problem, but are related to the design and installation of HMLP foundations. These include:

- F1554 Grade 55 exhibit ductile behavior.
- Large diameter fasteners with short grip lengths that are snug-tightened with "average workman" procedure likely exceed target pretension.
- Significant displacement losses (difference between theoretical and actual rod stretch for a given nut rotation) occur during tightening, up to 6/1000 of an inch per 20 degrees.
- Clamp-load loss due to permanent rod deformation is not affected by pretension magnitude (in F1554 grade 55 rods).
- The use of direct tensioning indicators (DTI's) reduced pre-tension variation across the fasteners during anchor rod tightening
- The difference between the magnitude of the external load required to separate one rod, and the load required to separate several rods, is relatively small. This is because the rods adjacent to the yielding critical rod are absorbing the force that the critical rod can no longer absorb.
- Rods in double nut moment connections are less likely to experience clamp loss due to permanent deformation.

In addition, several conclusions were made from FE analysis pertaining to proposed design solutions:

- Grade 105 rods are less likely to permanently deform than grade 55 rods.
- The addition of stiffeners to existing 12-rod flange-flange foundations did not significantly increase the resistance to clamp-load loss.

- Doubling the thickness of the flange and base plates in 12-rod flange-flange foundations did significantly increased the resistance to clamp-load loss.

7.2 Recommendations

Following are recommendations pertaining to mitigation of loosening in existing HMLP installations, modification of the design of new HMLPs, and the tightening procedures used in both new installations, and retightening.

7.2.1 Existing HMLP Foundations

Based on both the modeling and inspection review, it is recommended that the frequency of inspections of the 15 HMLPs with flange foundations be increased to once every 24 months. This would increase the safety of those poles, as well as provide data more quickly about whether the loosening phenomenon improves after tightening in flange foundations, as evidence suggests is true for the CIP foundations.

It is recommended that the Grade 55 anchor rods are replaced with F1554 Grade 105 anchor rods in the 15 HMLPs with flange foundations. This relatively low cost action will serve to greatly reduce the potential for stretching of the anchor rods. In addition, during installation of the higher-strength anchor rods, it is recommended that DTI washers are utilized to limit the range of anchor rod pre-tensions. While it was found in this study that anchor rod pretention magnitudes are not critical for the mild steel Grade 55 rods, they are much more critical in high strength rods.

Throughout this study, other mitigation strategies have been suggested, such as increasing the anchor rod grip-lengths by jacking up the poles and inserting a spacer

plate. It was determined that these suggestions were all cost prohibitive and did not provide a certain solution. The one suggestion that might have been economically feasible, the addition of vertical stiffener plates between the base plate and the pole, was shown to be ineffective in the FE model and is not recommended.

7.2.2 Design of New HMLP

This project benefited from the work of Charlie Wagner of the AKDOT&PF who previously studied the issue and initiated several design changes that were implemented on ten poles that were installed in 2011 along the Glenn Highway. The Peter's Creek pole that was instrumented was one of these poles. Many of the following recommendations are a confirmation or repudiation of the changes made for those ten poles.

It is recommended that future designs include an increased number of smaller diameter anchor rods, preferably 1.50 inches in diameter, such as the twenty-four 1.50 inch rods used on the Peter's Creek HMLP. These rods need not have a thread pitch other than the standard UNC thread. It also recommended that the change of the size of the pole be maintained. This includes an increase in the HMLP's diameter at the top of the pole, the base of the pole, and a correspondingly large base plate. This increases the stiffness of the pole and likely reduces the potential for dynamic loading or harmonics.

It is recommended that future designs utilize double-nut flange connections, in which the flange plate and base plate are separated by nuts. These connections more closely align with the design assumptions made by the pole manufacturer. They also

provide an increased resistance to rod stretching because the portions of the rods loaded by external forces are not subjected to pretension. In addition, if a rod were to permanently deform, it would do so primarily outside the clamp zone.

It is also recommended that the thickness of the baseplate and flange plate be increased. It is difficult to give a specific recommendation on the required thickness, because the plate stiffness must be balanced with the economy and constructability of very thick plates. Perhaps 50% thicker than the standard plates is a good target.

Similar to the existing poles, it is recommended that the foundation connection be designed for Grade 55 anchor rods, but F1554 Grade 105 rods be installed, to provide an additional level of safety. Likewise, DTI washers should be used to accurately control the axial pre-tension.

7.2.3 Tightening Procedure

It is recommended that the top nut rotation during tightening (currently specified as 60 degrees) should vary with the yield strength, rod diameter, rod pitch, and grip length of the bolted joint interface. In order to produce more accurate and consistent final axial pretension values, at least two methods of determining pretension, and preferably three, should be used. These methods include, but are not limited to:

- a turn-of-the-nut procedure that correlates nut rotation to axial force
- a hydraulic torque wrench that correlates torque to the final hydraulic pressure, which can be approximately correlated to axial pretension
- Direct Tension Indicating (DTI) washers that signal the target pretension.

In addition, it is recommended that a large torque wrench or a multiplier be utilized to verify the torque at the snug-tight condition.

7.3 Additional Research

There are two areas in particular that require additional research: susceptibility of HMLPs to vortex-shedding induced dynamic loading, and clamp-load loss in 16-rod CIP concrete cap foundations. This study suggested that there are dynamic loads applied to the HMLPs by wind forces, but it is unknown what the magnitude of these loads are, how often they occur, and their effects on the HMLPs and their foundations.

The FE modeling conducted during this study did not provide a clear indication of the causes of loosening in the 16-rod CIP concrete cap foundation HMLPs. Because the 96 inch long anchor rods are embedded in the concrete, field investigations were not conducted on this type of foundation. Further study is required to determine the causes of loosening in these foundations. As noted in Chapter 6, the ideal sensors for this type of study are load-cell washers. While these devices are expensive (roughly $1,000 each), they are reusable, and would be able to measure the axial load in anchor rods that embedded in concrete.

THIS PAGE INTENTIONALLY LEFT BLANK

Chapter 8 References

1. Robert Connor, Ian Hodgson. Field Instrumentation and Testing of High-mast Lighting Towers in the State of Iowa. Ames, Iowa: Iowa Department of Transportation; 2006.

2. Garlich MJ, Koonce JW. Anchor Rod Tightening for Highmast Light Towers and Cantilever Sign Structures. Transportation Research Board 90th Annual Meeting [Internet]. Washington, D.C.: Transportation Research Board; 2011 [cited 2013 Aug 1]. Available from: http://trid.trb.org/view.aspx?id=1092267

3. Elmer Marx. Personal Communication. 2012.

4. Rios CA. Fatigue Performance of Multi-Sided High-Mast Lighting Towers [master's thesis]. [Austin, Texas]: University of Texas; 2007.

5. Bickford JH. An Introduction to the Design and Behavior of Bolted Joints. CRC Press; 1995. 998 p.

6. Research Council on Structural Connections. Specification for Structural Joints Using High-Strength Bolts. Chicago, Il: AISC; 2009.

7. Garlich MJ, Thorkildsen ER. Guidelines for the Installation, Inspection, Maintenance and Repair of Structural Supports for Highway Signs, Luminaires, and Traffic Signals. Washington, D.C.: Federal Highway Administration; 2005 Mar. Report No.: FHWA NHI 05-036.

8. James RW, Keating PB, Bolton RW, Benson FC, Bray DE, Abraham RC, et al. Tightening Procedures for Large-Diameter Anchor Bolts [Internet]. College Station, TX: Texas Transportation Institute, Texas A&M University System; 1997 [cited 2013 Aug 1]. Report No.: 1472-1F. Available from: http://144.171.11.39/view.aspx?id=472325

9. American Association of State Highway and Transportation Officials. Standard Specifications for Structural Supports for Highway Signs, Luminaires, and Traffic Signals. AASHTO; 2011. 290 p.

10. Nassar SA, Matin PH. Clamp Load Loss due to Fastener Elongation Beyond its Elastic Limit. J Pressure Vessel Technol. 2005 Aug 5;128(3):379–87.

11. Giosan I. Vortex shedding induced loads on free standing structures. Structural Vortex Shedding Response Estimation Methodology and Finite Element Simulation.

12. Montgomery J. Methods for modeling bolts in the bolted joint. ANSYS user's conference [Internet]. 2002 [cited 2014 Sep 2]. Available from: http://ainastran.org/staticassets/ANSYS/staticassets/resourcelibrary/confpaper/2002-Int-ANSYS-Conf-38.PDF

13. ASTM-E8. Standard Test Methods for Tension Testing of Metallic Materials [Internet]. West Conshohocken, PA: ASTM International; 2013 [cited 2014 Mar 29]. Report No.: ASTM E8. Available from: http://www.astm.org/Standards/E8.htm

14. Dexter RJ, Ricker MJ. Fatigue-Resistant Design of Cantilever Signal, Sign, and Light Supports. Washington, D.C.: Transportation Research Board; 2002. Report No.: NCHRP 469.

15. Till RD, Lefke NA. The Relationship Between Torque, Tension, and Nut Rotation of Large Diameter Anchor Bolts. Lansing, MI: Michigan Dept. of Transportation; 1994 Oct. Report No.: R-1330.

16. Chai YH, Hutchinson TC. Flexural strength and ductility of extended pile-shafts. II: Experimental study. Journal of Structural Engineering. 2002;128(5):595–602.

17. American Society of Civil Engineers, Structural Engineering Institute. Minimum Design Loads for Buildings and Other Structures, ASCE 7-10. ASCE Publications; 2010. 608 p.

18. Hoisington DB. Investigation of Anchor Nut Loosening in High-mast Light Poles using Field Monitoring and Finite-element Analysis [Masters of Science]. [Anchorage, AK]: University of Alaska Anchorage; 2014.

Chapter 9 Appendices

THIS PAGE INTENTIONALLY LEFT BLANK

Appendix A Weighstation Tightening Procedure

The following procedure shall be used for the WS1 High-mast Light Pole (Weight Station NB) during installation of strain-gaged bolts. This was taken from the HT Special Provisions contract dated 6/14/2010. It has been modified slightly to account for the strain gage wires and accelerometers. The rod assembly type used on this HMLP is type B. Figure A.1 shows the order in which type B rod assemblies are to be tightened. Figure A.2 shows the type B configuration, which is a flange-flange connection.

A. General. For ALL High Tower nut retightening use the following procedures:

- Tighten nuts only on days when the ground wind speed is less than 15 mph.
- Once the tightening procedure is started, tighten all Rod Assemblies without pause or delay.
- Field numbered Rod Assemblies may NOT match the "Tightening Sequence" shown.
- DO NOT use vise grips, channel locks, adjustable end or pipe wrenches.
- Use the appropriately sized hydraulic wrench system. Submit hydraulic wrench system information to the Engineer for review and acceptance. Include a pressure-torque curve.
- Place a smooth beveled washer in contact with the sloped surface, when the outer edge of the assembly has a slope greater than 1:20.

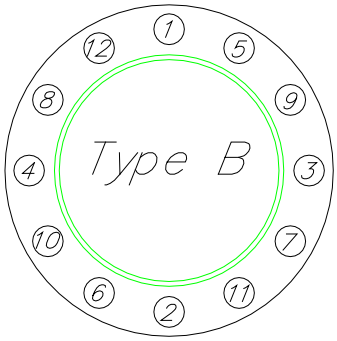

Figure A.1: Type ‘B’ Tightening Sequence

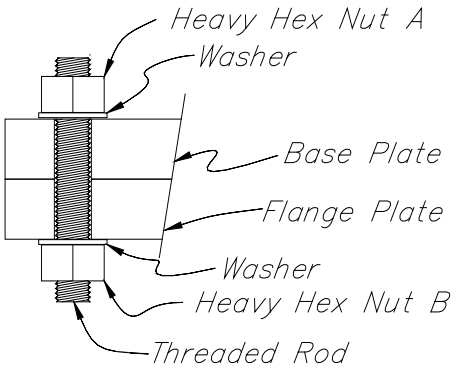

Figure A.2: Type ‘B’ Rod Assembly

B. For ‘Type B’ foundation, bolt replacement and nut tightening use the following procedure:

1) Clean exposed threads on <u>all</u> existing bolt assemblies.

2) Tighten all nuts “Snug tight”.

a. Wherever mentioned, “Snug tight” is defined as 600 ft-lbs of torque. Use a hydraulic torque wrench to bring nuts to snug tight torque. Consult manufacturer documentation to determine delivery pressure required to achieve specified torque. -or-

b. If torque wrench cannot be used, “Snug tight” is the full effort of one person on an open-end wrench close to the end with a length equal to 14 times the rod diameter but not less than 18 inches.

3) Bolt assembly replacement and nut retightening begins with Rod Assembly labeled #1 in the “Type ‘B’ Tightening Sequence” above and continues sequentially until all bolts are replaced and new Rod Assemblies are tightened. **Remove only one bolt assembly at a time.**

   a. Remove existing bolt assembly and discard. DO NOT reuse existing bolts, washers or nuts.

   b. Clean plate bearing areas immediately before tightening.

   c. Install threaded rod, washer and ‘A’ nut.

   d. Install washer and ‘B’ nut

   e. Snug tight both nuts. Ensure that a minimum of three threads stick through at each ‘A’ nut and ‘B’ nut.

4) Repeat step 3 until all Bolt Assemblies are sequentially replaced and all Rod Assembly nuts are snug tight.

5) Initial Turn of the Nut.

   a. Beginning with Rod Assembly labeled #1 in the Type ‘B’ Tightening Sequence,

   b. Mark nut ‘A’, base plate, flange plate, nut ‘B’ and threaded rod with a permanent felt tipped pen or crayon as a reference for determining the relative rotation of the nut and threaded rod during the tightening.

   c. Rotate nut ‘A’ 20 degrees. **Prevent nut ‘B’ and threaded rod from moving whenever turning nut ‘A’.**

6) Repeat step 5 above until all 12 ‘A’ nuts are sequentially tightened 20 degrees.

a. After all Rod Assemblies are tightened 20 degrees, re-check snug tightness of the ‘B’ nuts. If nut ‘B’ or threaded rod moves then, loosen ‘A’ nut, snug tight both nuts and repeat step 5 on that Rod Assembly.

7) Intermediate Turn of the Nut.

   a. Continue tightening ‘A’ nuts beginning with Rod Assembly labeled #1 in the Type ‘B’ Tightening Sequence,

   b. Rotate nut ‘A’ an additional 20 degrees for a total rotation of 40 degrees.

8) Repeat step 7 above until all 12 ‘A’ nuts are sequentially tightened 40 degrees.

   a. After all Rod Assemblies are tightened to 40 degrees, re-check snug tightness of all ‘B’ nuts. If nut ‘B’ or threaded rod moves then, loosen ‘A’ nut, snug tight both nuts and repeat steps 5 and 7 on that Rod Assembly.

9) Final Turn of the Nut.

   a. Complete tightening ‘A’ nuts beginning with the Rod Assembly labeled #1 in the Type ‘B’ Tightening Sequence,

   b. Rotate nut ‘A’ an additional 20 degrees for a total rotation of 60 degrees.

   c. Do not over torque. If the delivered torque reaches 2,500 ft-lbs without achieving the required turn of the nut then on that Rod Assembly:

      (1) Remove nut ‘B’ nut then, loosen nut ‘A’,

      (2) Clean and re-lubricate all contact surfaces,

      (3) Snug tight nuts ‘A’ and ‘B’.

      (4) Mark nuts, base plate, flange plate, threaded rod and rotate nut ‘A’ 60 degrees.

      (5) If required rotation is not achieved at 2,500 ft-lb torque then, notify the Engineer and proceed with Final Turn of the Nut on remaining ‘A’ nuts.

10) Repeat step 9 above until final tightening is sequentially completed on all 12 Rod Assemblies.

11) After all Rod Assemblies are tightened to 60 degrees, re-check snug tightness of all ‘B’ nuts. If nut ‘B’ or the rod moves during snug tight check then loosen ‘A’ nut, snug tight both nuts and repeat steps 5, 7 and 9 on that Rod Assembly.

12) A minimum of 1 week and a maximum of 2 weeks after re-tightening apply a 1,300 ft-lb torque to ‘A’ nuts and check snug tightness of ‘B’ nuts. If any nut or threaded rod moves, mark the nut and notify the Engineer.

THIS PAGE INTENTIONALLY LEFT BLANK

Appendix B Peter's Creek Tightening Procedure

Last Modified 10/04/2013

The following procedure shall be used for High-mast Light Pole #1 at Peter's Creek (GSPC1) during installation of strain-gaged bolts. This was taken from the HT Special Provisions contract dated 6/14/2010. It has been modified slightly to account for the strain gage wires. It has been updated based on the results of the rod tightening at the Glenn Highway Weigh Station in February 2013.

A. General. For ALL High Tower nut retightening use the following procedures:

- Tighten nuts only on days when the ground wind speed is less than 15 mph.
- Once the tightening procedure is started, tighten all Rod Assemblies without pause or delay.
- Field numbered Rod Assemblies may NOT match the "Tightening Sequence" shown.
- DO NOT use vise grips, channel locks, adjustable end or pipe wrenches.
- Use the appropriately sized hydraulic wrench system. Submit hydraulic wrench system information to the Engineer for review and acceptance. Include a pressure-torque curve.
- Place a smooth beveled washer in contact with the sloped surface, when the outer edge of the assembly has a slope greater than 1:20.

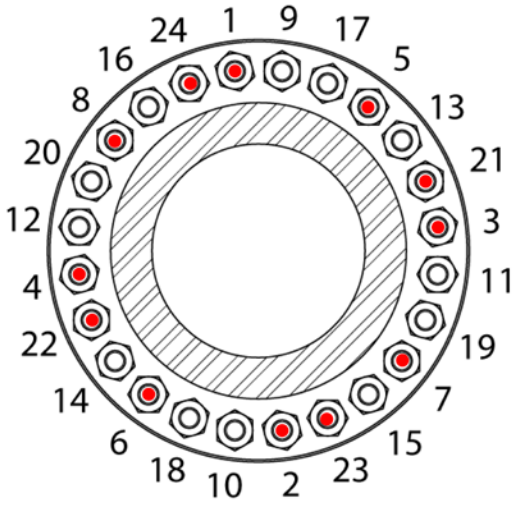

Figure B.1: Tightening Sequence

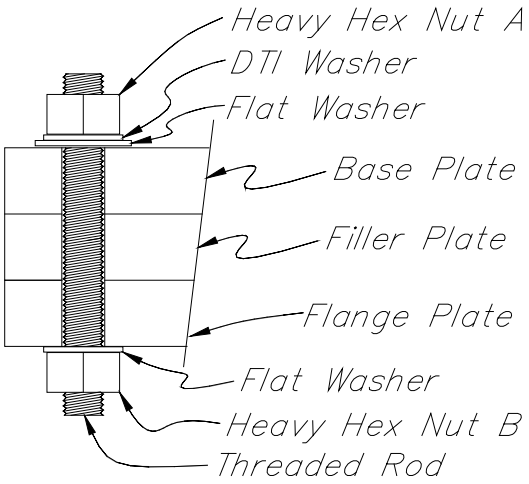

Figure B.2: Rod Assembly

C. For 24-bolt rod replacement and nut tightening use the following procedure:

1) Clean exposed threads on <u>all</u> existing bolt assemblies.

2) Tighten all nuts “Snug tight”. “Snug tight” is defined as 600 ft-lbs of torque. Either a Torque multiplier or a hydraulic torque wrench may be used to bring nuts to snug tight torque. Consult manufacturer documentation to determine delivery pressure required to achieve specified torque for the hydraulic wrench.

3) Bolt assembly replacement and nut retightening begins with Rod Assembly labeled #1 in Figure B.1 and continues sequentially until <u>all</u> bolts are replaced and new Rod Assemblies are tightened. **Remove only one bolt assembly at a time.** Rods that

have an embedded axial strain gage (SG Rod) shall be installed in locations 1, 2, 3, 4, 5, 6, 7, 8, 21, 22, 23, 24, as shown in Figure B.1.

f. Remove existing bolt assembly and discard. DO NOT reuse existing bolts, washers or nuts.

g. Clean plate bearing areas immediately before tightening.

h. Install threaded rod, washer and 'A' nut.

i. Install washer and 'B' nut

j. Snug tight both nuts. Ensure that a minimum of three threads stick through at each 'A' nut and 'B' nut.

8) Repeat step 3 until <u>all</u> Rod Assemblies are sequentially replaced and all Rod Assembly nuts are snug tight.

9) Initial Turn of the Nut.

d. Beginning with Rod Assembly labeled #1 in Figure B.1 Tightening Sequence,

e. Mark nut 'A', base plate, flange plate, nut 'B' and threaded rod with a permanent felt tipped pen or crayon as a reference for determining the relative rotation of the nut and threaded rod during the tightening.

f. Rotate nut 'A' 30 degrees. **Prevent nut 'B' and threaded rod from moving whenever turning nut 'A'.**

10) Repeat step 5 above until <u>all</u> 24 'A' nuts are sequentially tightened 30 degrees.

b. After all Rod Assemblies are tightened 30 degrees, re-check snug tightness of the 'B' nuts. If nut 'B' or threaded rod moves then, loosen 'A' nut, snug tight both nuts and repeat step 5 on that Rod Assembly.

7) Final Turn of the Nut.

d. Complete tightening 'A' nuts beginning with the Rod Assembly labeled #1 in Figure B.1,

e. Rotate nut 'A' as follows:

I. For SG Rods, stop rotation if any of the following conditions occur:

(6) DTI washers display full volume of orange silicone

(7) Strain gage instrumentation indicate 68 kips of axial force (70% of nominal yield)

(8) Nut A rotates an additional 30 degrees for a total rotation of 60 degrees

(9) Delivered torque reaches 2,500 ft-lbs

II. For rods without strain gage instrumentation, stop rotation if any of the following conditions occur:

(1) DTI washers display full volume of orange silicone

(2) Nut A rotates an additional 30 degrees for a total rotation of 60 degrees

(3) Delivered torque reaches 2,500 ft-lbs

f. Record the final applied torque for each Rod Assembly

g. If the delivered torque reaches 2,500 ft-lbs without achieving the required turn of the nut, the required axial force, or full indication from the DTI washers, then on that Rod Assembly:

(1) Remove nut 'B' nut then, loosen nut 'A',

(2) Clean and re-lubricate all contact surfaces,

(3) Snug tight nuts 'A' and 'B'.

(4) Mark nuts, base plate, flange plate, threaded rod and rotate nut 'A' 60 degrees.

(5) If required rotation is not achieved at 2,500 ft-lb torque then, notify the Engineer and proceed with Final Turn of the Nut on remaining 'A' nuts.

8) Repeat step 7 above until final tightening is sequentially completed on all 24 Rod Assemblies.

9) After all Rod Assemblies are tightened to their final rotation, re-check snug tightness of all 'B' nuts. If nut 'B' or the rod moves during snug tight check then loosen 'A' nut, snug tight both nuts and repeat steps 5, 6 and 7 on that Rod Assembly.

10) Utilizing the recorded final applied torque for each Rod Assembly, apply a Verification Torque to 'A' nut on each Rod Assembly in the sequence shown in Figure B.1.

11) A minimum of 1 week and a maximum of 2 weeks after tightening, re-apply the Verification Torque to 'A' nuts and check snug tightness of 'B' nuts. If any nut or threaded rod moves, mark the nut and notify the Engineer.

Appendix C Sample HMLP Inspection Report

HIGH TOWER STRUCTURAL INSPECTION REPORT

ALASKA DEPARTMENT OF TRANSPORTATION & PUBLIC FACILITIES
BRIDGE DESIGN & INSPECTION SECTION
3132 Channel Drive, Box 112500, Juneau, AK 99811-2500

GENERAL INFORMATION

Date Inspected	**19-Sep-2007**	*Wind Speed*	**Calm**
Weather	**Overcast**	*Inspector*	**M Higgs**
Temperature	**54 F**	*Assistant*	**D Sielbach**

IDENTIFICATION AND DESCRIPTION

Mast Number	**GW1**	*Structure Name*	**HIGHMAST**
Highway	**GLENN**	*Intersection*	**WEIGH STA**
Offset	**95 ft S**	*Quadrant*	**S**
Frequency	**60 Months**	*Rod Material Type*	**A325**
Erection Date	**unknown**	*Number Lamps*	**4**
Structure Height	**150 ft**	*Number Anchor Rods*	**12**
Stiffeners Present	**none**	*Number Pole Sections*	**5**
Anchor Rod Size	**1.5-in dia.**	*Anchor Nut Size*	**2.625 in**

Longitude:	**149 deg**	**36 min**	**19 sec**	*Latitude:*	**61 deg**	**17 min**	**4 sec**

COMMENTS

NONE

FOUNDATION TYPE DESCRIPTIONS

Foundation
Driven pile w/base plate

CRITICAL CONTACT INFORMATION

NAME	*Work Phone*	*Cell Phone*
Ed Caress	338-1436	440-8461

HIGHTOWER CONDITION RATING DESCRIPTION

RATING	CONDITION	DESCRIPTION
0	OUT OF SERVICE	**Removed from Service.**
1	CRITICAL	Unreliable level of performance: **Repair, Replace or Remove.** i.e.: Heavy Corrosion, Major Section Loss of Base Material or Reinforcing Steel, Flexure or Shear Cracks, Loose or Missing Anchor Bolts. *Contact Maintenance Immediately*.
2	POOR	Significantly reduced level of performance: **Repair or Replace.** i.e.: Moderate Corrosive Section Loss of Base Material or Reinforcing Steel, Weld Crack Suspect, Minor Cracks, Large cracks or spalls in concrete members, Anchor Bolts tight.
3	FAIR	Satisfactory level of performance: **Minor Repair.** i.e.: Structure Sound, Minor Rust w/o Section Loss of Base Material, Minor Cracks or Spalls in concrete members, Anchor Bolts tight.
4	GOOD	High level of performance: **No Repairs.** i.e.: No notable deficiencies, Light Rust of Base Material, Hairline Cracks in concrete members, Anchor Bolts tight.

HIGH MAST TOWER STRUCTURAL INSPECTION REPORT

Mast Number	**GW1**	*Structure Name*	**HIGHMAST**
Highway	**GLENN**	*Intersection*	**WEIGH STA**

DEFICIENCIES LIST

ELEMENT	*RATING*		*COMMENTS*
OVERALL	S.01	1	SEE ANCHOR NUTS
FOUNDATION	S.02	4	2 5/8-in Welded Flange Cap to Base Plate
ANCHOR RODS (or Bolts)	S.03	4	12 bolts (A325)
BASE PLATE	S.04	4	2 1/2-in thick
WELDS (Base & Seams)	S.05	4	Seam welds aligned
ANCHOR NUTS (& Washers)	S.06	1	Loose bolt #10 in 2007, bolt(s) with no lock nut(s)
SERVICE OPENING	S.07	4	Located on W side of pole, 7/16-in bolt, bent on door
STIFFENERS	S.08	4	N/A
COATING	S.09	3	Paint marks, Weld tabs
ALIGNMENT	S.10	4	Not leaning
POLE	S.11	4	None

HIGH MAST TOWER STRUCTURAL INSPECTION REPORT

Mast Number	**GW1**	*Structure Name*	**HIGHMAST**
Highway	**GLENN**	*Intersection*	**WEIGH STA**

RECOMMENDED MAINTENANCE, REPAIR & REHABILITATION

Element	***Recommendation / Repair / Replacement***
Anchor Nuts	Retighten loose tension nut(s) per attached procedure
Welds	Due to loose bolt(s) NDE base weld
Mast Number marked on pole above Hand hole opening (see photos).	
Anchor rods & nut locations marked & numbered clockwise starting at Hand hole opening.	

COMPLETION STATUS

Element	***Correction Complete***	***Date Complete***
Anchor Nuts		
Welds		

POLE THICKNESS READINGS (locations referenced clockwise starting from handhold)

Above Bolt 1		Above Bolt 4		Above Bolt 7		Above Bolt 10	
AT BASE	ABV BASE	AT BASE	ABV BASE	AT BASE	ABV BASE	AT BASE	ABV BASE
0.312	0.312	0.315	0.312	0.319	0.311	0.318	0.313

Number	GW1	Structure	Glenn Hwy-Weigh Sta	Date	09/19/07
Roll No.	5	Inspectors	Higgs / Sielbach	Frame	173

Coating above Rod 5

Number	GW1	Structure	Glenn Hwy-Weigh Sta	Date	09/19/07
Roll No.	5	Inspectors	Higgs / Sielbach	Frame	174

Coating above Rod 9

Number	GW1	Structure	Glenn Hwy-Weigh Sta	Date	09/19/07
Roll No.	5	Inspectors	Higgs / Sielbach	Frame	175

Coating above Rod 13

Number	GW1	Structure	Glenn Hwy-Weigh Sta	Date	09/19/07
Roll No.	5	Inspectors	Higgs / Sielbach	Frame	176

Coating above Rod 1

Number	GW1	Structure	Glenn Hwy-Weigh Sta	Date	09/19/07
Roll No.	5	Inspectors	Higgs / Sielbach	Frame	177

Backside of Foundation

Number	GW1	Structure	Glenn Hwy-Weigh Sta	Date	09/19/07
Roll No.	5	Inspectors	Higgs / Sielbach	Frame	178

Frontside of Foundation

Number	GW1	Structure	Glenn Hwy-Weigh Sta	Date	09/19/07
Roll No.	5	Inspectors	Higgs / Sielbach	Frame	179

NONE

Number	GW1	Structure	Glenn Hwy-Weigh Sta	Date	09/19/07
Roll No.	5	Inspectors	Higgs / Sielbach	Frame	180

NONE

GLENN / WEIGH STATION

THIS PAGE INTENTIONALLY LEFT BLANK

Appendix D Strain Gaging Procedure

Required Equipment:

- M-Bond AE 10 strain gage epoxy (resin, curing agent)
- 2mm diameter hole 6” deep, which has a volume of 0.5cc
- 5.5” long spinal needle

1) Uncoil at least 6” of strain gage wire. Mark 5.5” distance from the bottom of the strain gage on the wire. (0.5” minimum clearance from the bottom) Insert uncoiled strain gage into hole until the mark is flush with the opening.
2) Remove resin and curing agent from refrigerator, let warm at room temperature for 30 minutes. Fill dropper to “10” mark with curing agent. Insert into bottle of resin. Mix for 3 minutes (not 5). Glass jar bottom should be hot to the touch. If bottom is not hot, mix for 2 more minutes (5 total).
3) Once epoxy is mixed fully, its workability for this procedure is 10-15 minutes.
4) Remove plunger from syringe/needle. Funnel 2.0cc mixed resin/curing agent into the syringe. (Syringes used had 3.0cc max volume, leave at least 1.0cc of volume left for plunger.)
5) Slide needle into hole along wall opposite of strain gage. Take care not to puncture the strain gage wire. Needle should not contact the bottom of the hole, it should be at least 0.5” from the bottom. To push epoxy into the hole, apply enough force onto the plunger that its bottom is in constant contact with the epoxy mixture. Once 0.30cc of mixture has been freed from the syringe, pull the needle up so that the bottom sits 1” below the surface of the hole. Continue inserting epoxy until epoxy can be visibly seen extruding from the hole’s surface onto the flat of the bolt. Once this is done, repeat this procedure for the remaining bolts.

THIS PAGE INTENTIONALLY LEFT BLANK

Appendix E FHWA Recommended Turn-of-the-Nut Rotation Table

Table E.1 contains the FHWA recommended Turn-of-the-Nut rotation for mild steel bolts in double-nut-moment connection HMLP configurations.

Table E.1: FHWA Recommended Turn-of-the-Nut Rotation

TABLE 8

Nut Rotation for Turn-Of-Nut Pretensioning

Anchor Rod Diameter, in*.	Nut Rotation from Snug-Tight Condition a, b, c	
	F1554 Grade 36	F1554 Grades 55 and 105 A615 and A706 Grade 60
<1 1/2	1/6 Turn	1/3 Turn
>1 1/2	1/12 Turn	1/6 Turn

a. Nut rotation is relative to anchor rod. The tolerance is plus 20 degrees.
b. Applicable only to double-nut-moment joints.
c. Beveled washer should be used if: a) the nut is not in firm contact with the base plate; or b) the outer face of the base plate is sloped more than 1:40.

THIS PAGE INTENTIONALLY LEFT BLANK

Appendix F ASCE 7-10 Deign Wind Calculation

The design wind moments applied to HMLPs were based off of 100 mph wind velocities in each configuration. They were calculated using the requirements in section 29.5, Design Wind Loads on Other Structures in *Minimum Design Loads for Buildings and Other Structures* (17). They are determined by the following equation:

$$F = q_z G C_f A_f \tag{F.1}$$

where

$q_z = Velocity\ Pressure\ \left(\frac{lb}{ft^2}\right) = 0.00256 K_z K_{zt} K_d V^2$
K_z = Velocity Pressure Exposure Coefficient (Exposure C Assumed)
K_{zt} = Topographic Factor = 1.0
K_d = Wind Directionality Factor = 0.95
V = Basic Wind Speed = 100 mph
G = Gust-Effect Factor =0.85

Giosan (11) showed HMLPs have first mode natural frequencies between 0.88-1.20Hz. Section 26.9 of *Minimum Design Loads* (17) allows for a G of 0.85 when a tall slender structure has a natural period of 1 second or less. Since the natural period is very close to 1 second, G is taken as 0.85.

C_f = Force Coefficient
A_f = Cross Sectional Area

Table F.1 shows the calculation for the total moment applied to the pole in scenarios A & C.

Table F.1: ASCE 7-10 Moment Calculation Scenarios A & C

HMLP A & C	Min Height (ft)	Max Height (ft)	Avg. Pole Diameter (in)	Af (ft^2)	Kz	qz (lb/ft^2)	F (lb)	Moment (k*in)
Section 1	0	5	26.15	16.30	0.85	20.67	200.49	6.01
Section 2	5	10	25.45	15.86	0.85	20.67	195.12	29.27
Section 3	10	15	24.75	15.43	0.85	20.67	189.76	51.23
Section 4	15	20	24.05	14.99	0.90	21.89	195.23	76.14
Section 5	20	25	23.35	14.55	0.94	22.86	197.98	100.97
Section 6	25	30	22.65	14.12	0.98	23.83	200.21	126.13
Section 7	30	35	21.95	13.68	0.98	23.83	194.03	145.52
Section 8	35	40	21.25	13.25	1.04	25.29	199.34	173.42
Section 9	40	45	20.55	12.81	1.04	25.29	192.77	190.84
Section 10	45	50	19.85	12.37	1.09	26.51	195.16	216.63
Section 11	50	55	19.15	11.94	1.09	26.51	188.28	231.58
Section 12	55	60	18.45	11.50	1.13	27.48	188.05	253.87
Section 13	60	65	17.75	11.06	1.13	27.48	180.92	265.95
Section 14	65	70	17.05	10.63	1.17	28.45	179.93	286.09
Section 15	70	75	16.35	10.19	1.17	28.45	172.55	295.05
Section 16	75	80	15.65	9.76	1.21	29.43	170.80	312.57
Section 17	80	85	14.95	9.32	1.21	29.43	163.16	318.17
Section 18	85	90	14.25	8.88	1.24	30.16	159.38	329.92
Section 19	90	95	13.55	8.45	1.24	30.16	151.55	331.90
Section 20	95	100	12.85	8.01	1.26	30.64	146.04	337.35
Section 21	100	105	12.15	7.57	1.26	30.64	138.09	335.55
Section 22	105	110	11.45	7.14	1.26	30.64	130.13	331.83
Section 23	110	115	10.75	6.70	1.26	30.64	122.17	326.20
Section 24	115	120	10.05	6.26	1.31	31.86	118.75	331.32
Section 25	120	125	9.35	5.83	1.31	31.86	110.48	321.50
Section 26	125	130	8.65	5.39	1.31	31.86	102.21	309.69
Section 27	130	135	7.95	4.96	1.31	31.86	93.94	295.90
Section 28	135	140	7.25	4.52	1.36	33.08	88.94	290.82
Section 29	140	145	6.55	4.08	1.36	33.08	80.35	272.38
Section 30	145	150	5.85	3.65	1.36	33.08	71.76	251.88
Sum							4717.56	7145.71

The total moment calculated using this method is equal to 7145 k-in. This is similar to the manufacturer's moment calculation of 6765 k-in. Table F.2 shows the calculation for the total moment applied to the pole used in scenario B.

Table F.2: ASCE 7-10 Moment Calculation Scenario B

HMLP B	Min Height (ft)	Max Height (ft)	Avg. Pole Diameter (in)	Af (ft^2)	Kz	qz (lb/ft^2)	F (lb)	Moment (k*in)
Section 1	0	5	31.25	17.79	0.85	20.67	218.76	6.56
Section 2	5	10	30.55	17.39	0.85	20.67	213.86	32.08
Section 3	10	15	29.85	16.99	0.85	20.67	208.96	56.42
Section 4	15	20	29.15	16.59	0.90	21.89	216.06	84.26
Section 5	20	25	28.45	16.19	0.94	22.86	220.24	112.32
Section 6	25	30	27.75	15.79	0.98	23.83	223.97	141.10
Section 7	30	35	27.05	15.39	0.98	23.83	218.32	163.74
Section 8	35	40	26.35	15.00	1.04	25.29	225.69	196.35
Section 9	40	45	25.65	14.60	1.04	25.29	219.69	217.49
Section 10	45	50	24.95	14.20	1.09	26.51	223.97	248.61
Section 11	50	55	24.25	13.80	1.09	26.51	217.69	267.75
Section 12	55	60	23.55	13.40	1.13	27.48	219.16	295.87
Section 13	60	65	22.85	13.00	1.13	27.48	212.65	312.59
Section 14	65	70	22.15	12.61	1.17	28.45	213.43	339.35
Section 15	70	75	21.45	12.21	1.17	28.45	206.68	353.43
Section 16	75	80	20.75	11.81	1.21	29.43	206.77	378.40
Section 17	80	85	20.05	11.41	1.21	29.43	199.80	389.61
Section 18	85	90	19.35	11.01	1.24	30.16	197.60	409.04
Section 19	90	95	18.65	10.61	1.24	30.16	190.45	417.10
Section 20	95	100	17.95	10.22	1.26	30.64	186.26	430.27
Section 21	100	105	17.25	9.82	1.26	30.64	179.00	434.97
Section 22	105	110	16.55	9.42	1.26	30.64	171.74	437.93
Section 23	110	115	15.85	9.02	1.26	30.64	164.47	439.14
Section 24	115	120	15.15	8.62	1.31	31.86	163.45	456.02
Section 25	120	125	14.45	8.22	1.31	31.86	155.89	453.65
Section 26	125	130	13.75	7.83	1.31	31.86	148.34	449.48
Section 27	130	135	13.05	7.43	1.31	31.86	140.79	443.49
Section 28	135	140	12.35	7.03	1.36	33.08	138.32	452.32
Section 29	140	145	11.65	6.63	1.36	33.08	130.48	442.34
Section 30	145	150	10.95	6.23	1.36	33.08	122.64	430.48
Section 31	150	155	10.25	5.83	1.36	33.08	114.80	416.74
Sum							5651.17	9702.29

The total moment calculated for scenario B is equal to 9700 k-in. This is 12% larger than the manufacturer's moment calculation of 8768 k-in.